Ligand Substitution Reactions at Inorganic Centers†

David T. Richens*

School of Chemistry, University of St. Andrews, North Haugh, St. Andrews, Scotland, KY16 9ST United Kingdom

Received August 11, 2004

Contents

David Richens is a Senior Lecturer in Chemistry at St. Andrews University in Scotland and has devoted much of his career to the study of the mechanisms of inorganic reactions predominantly from the viewpoint of aqueous solutions. He also retains an interest in macrocyclic metal systems and in metal-promoted oxygen activation and is currently active in studies aimed at generating selective oxygenation (O insertion) catalysts including those that mimic the action of a number of metalloenzymes. His passion however for the study of the mechanisms of reactions at inorganic centers was kindled through his postdoctoral work with Professor Donald Sawyer (University of California, Riverside, 1978–79) and then with Professor Geoffrey Sykes (University of Newcastle, 1979–1983) before moving to Scotland in 1983 and finally to St. Andrews in 1988. He has been interested in developing the aqueous solution chemistry of the 4d and 5d transition metals with an emphasis on the behavior of low symmetry metal centers such as those present in aqueous oxo-bridged cluster species. Following visits in the 1980s to the University of Lausanne, Switzerland with Professor Andre Merbach, he developed the use of ^{17}O NMR spectroscopy to probe the solution structures of and the water exchange dynamics within a range of tri and tetranuclear oxo-bridged aqua clusters including a number of hitherto uncharacterized species. A number of structure/reactivity correlations have been evaluated including a correlation of μ-^{17}O resonance with M-μO bond length. He has also successfully employed M Kedge EXAFS in the elucidation of aqueous solution structures for several of the cluster ions. Dr. Richens is a past chairman of the Royal Society of Chemistry (U.K.) Inorganic Reaction Mechanisms Subject Group of Dalton Division and, in 1997, published the first textbook solely devoted to a discussion of the "Chemistry of the Aqua Ions" covering the entire periodic table with an emphasis on the methods of preparation and with regard to mechanistic studies of the solution chemistry.

1. Introduction

Ligand or group substitution (exchange) comprises one of the most fundamental processes occurring at an inorganic center in the solution phase.[1,2] Extensive reviews of this topic have appeared building upon the basic coverage in the growing number of teaching and research textbooks on inorganic reaction mechanisms from both the past 10−20 years and before. The 1958 book *Mechanisms of Inorganic Reactions* by Basolo and Pearson[3] is considered by most to mark the beginning of the serious and intensive study of inorganic reactions from the viewpoint of the mechanisms involved. The long awaited second edition of this book was published in 1967.[4] This seminal text led onto equally seminal works such as the 1965 book *Ligand Substitution Processes* by Langford and Gray[5] and articles by Eigen and Wilkins[6] and Pearson[7,8] which sought for the first time to systemmise and classify the mechanistic pathways involved. In the

* To whom correspondence should be addressed. Tel.: ++44 1334 463840. Fax: ++44 1334 463808. E-mail: dtr@st-andrews.ac.uk.
† Dedicated to Professor A. E. Merbach on the occasion of his 65th birthday.

10.1021/cr030705u CCC: $53.50
Published on Web 04/13/2005

late 1960s and early 1970s came landmark paperbacks such as *Inorganic Reaction Mechanisms* by Tobe[9] and *Kinetics of Inorganic Reactions* by Sykes.[10] By the end of the 1970s, the field was expanding rapidly[11−14] and reflected in the excellent review series edited by Twigg *Mechanisms of Inorganic and Organometallic Reactions* which covered developments through the 1980s and early 1990s[15] as well as in further texts by Katakis and Gordon,[16] Wilkins,[17] Jordan,[18] Atwood,[19] Henderson,[20] Richens,[21] Hay,[22] and most recently the 1999 updated and expanded version of *Inorganic Reaction Mechanisms* by Burgess and Tobe.[23] The breadth and depth of activity in recent years has been reflected in comprehensive coverage since 1971 in the RSC (U.K.) series of Annual and Specialist Periodical Reports[24] as well as in articles within the 1987 and 2003 volume series *Comprehensive Coordination Chemistry*.[1]

Over the past 20 years or so, the study of inorganic and other reactions under variable high pressure conditions and the construction of volume profiles has contributed enormously to our understanding of the mechanisms of substitution processes at a wide variety of reaction centers. These have been pioneered through the groups of Andre Merbach in Switzerland and Rudi van-Eldik in Germany.[2,25−30] The experimental findings are now being supported by realistic computational modeling at the ab initio SCF level which is now able to simulate transition state structures and increasingly model not only activation energies but also the volume profiles themselves.[27,31] These findings have provided strong support for use of the activation volume as a powerful mechanistic parameter. Density functional theory has been successfully used to model the solvent exchange process on aquated Pd^{II}, Pt^{II},[32,33] and Zn^{II} [33] cations. In the case of aquated Zn^{II}, the theoretically optimized transition state structure clearly demonstrates the dissociative nature of the water exchange reaction, a prediction that has not yet been proven by experiment. The improvement over the past 10 years in the ability to simulate reactions at a wide variety of inorganic centers using quantum mechanical and other approaches has been particularly noteworthy with the routine capability now of meaningful simulation of both transition states and reactive intermediates.

The study of the mechanisms of ligand substitution processes is now a vast topic with relevance to biological processes as well as to the chemistry behind a number of well established industrial homogeneous catalytic processes. Since these topics have been covered extensively elsewhere,[19,34] I have decided to be selective in the choice of coverage here with emphasis given to reactions at cationic transition metal centers specifically involving water ligand exchange and replacement processes wherein distinct trends around the periodic table are emerging both from the data now available experimentally along with support from the increasingly powerful and relevant computational approaches. Recent work is highlighted where relevant.

The review begins with brief coverage of some of the basic experimental and theoretical concepts underpinning the elucidation and classification of ligand substitution mechanisms, the evolution and limitations of the Langford and Gray labels, and a consideration of alternatives. Specific examples are then illustrated according to coordination number with coverage of main group, d-block transition metal and f-block lanthanide elements. The activation volume is highlighted as a powerful mechanistic parameter, a feature echoed throughout the review in chosen examples.

There is particular coverage of cis and trans effects exerted by certain resident donor atoms, including carbon, in relation to the rates and mechanisms of four coordinated square planar and six coordinated octahedral ligand substitution. There is also discussion of the growing experimental data available on centers possessing irregular low symmetry coordination geometries such as found in hybrid organometallic complexes and in metal clusters. In polynuclear oxo-bridged metal aqua clusters, for example, the presence of neighboring oxo and hydroxo groups lead to extreme associative or dissociative behavior in the case of water exchange as illustrated by their position within a plot of log k_{H_2O} versus the measured activation energy for water exchange on a range of mononuclear aqua species. Some interesting conclusions are reached as to the mechanistic behavior of some homoleptic metal aqua ions. It is clear from examples presented in this review that small somewhat subtle changes to the coordination geometry, neighboring ligands, and often marginal steric effects can profoundly affect both the rate and mechanism of ligand substitution, a finding that is of direct relevance to the low symmetry inorganic centers present in biology and in complexes used for medicinal applications.

2. Thermodynamics: Stability Constants for Metal Complex Formation

Stability constants have long been employed as an effective measure of the affinity of a ligand in replacing coordinated water on a metal ion in aqueous solution from the earliest systematic study of transition metal ammonia complexes by Bjerrum in his classic dissertation of 1941 leading on to the work on metal chelates in 1945 by Calvin and Wilson. Since discussions on the practical techniques for the measurement and for the correct formulation of stability constants have appeared now in a number of excellent texts[35] and compilations,[36] there is little need for a further detailed discussion here. Any method that can allow the accurate monitoring of the equilibrium concentration of one of the components in a solution of known analytical composition can in principle be used to measure equilibrium constants. In addition to potentiometry, one can employ spectrophotometry (absorbance measurements of the component at a particular wavelength), as well as others, e.g., NMR, polarography (reduction potentials), ion-exchange, specific ion EMF (ion-selective electrode measurement), colorimetry, and ionic conductivity (see ref 35 for references and other examples). In cases where very high stability constants are relevent for a particular ligand, a number of methods based upon competition between different ligands have also been devised.[37]

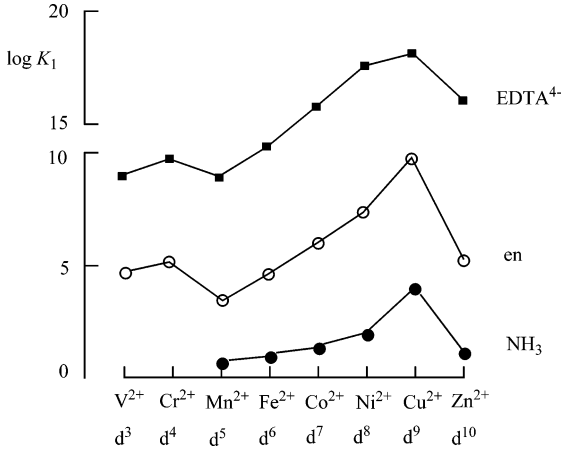

Figure 1. Stability constants (log K_1) for complex formation on the divalent aqua ions of the first row transition metals: the Irving−Williams effect.

Stability constants reflect the affinity of a ligand for a particular metal ion and indeed the type of bonding present. For the alkali, alkaline earth, and lanthanide elements, where the bonding is largely electrostatic (ionic), the strongest complexes formed are those with hard base donors such as F^-, RCO_2^-, RO^-, R_2N^-, etc. Also since ligand field effects are absent or minimal, chelating ligands (e.g., EDTA) or macrocyclic ligands (e.g., cryptands and crown ethers) are required for the highest constants. On the other hand, the constants for many of the transition metal ions, particularly those of the second and third rows, reflect considerable covalency in the bonds with some of the strongest complexes being formed with monodentate ligands, e.g., CN^-. However strong complexation should not be confused with inertness in a kinetic sense. The complex $[Ni(CN)_4]^{2-}$ provides an excellent case in point, its thermodynamic strength reflected by the value of log β_4 (22) but the complex is highly labile ($k = 2.3 \times 10^6$ s^{-1} for exchange with free CN^-; see later). For many first row transition metal ions however, many of the highest constants are still invariably seen for chelate and macrocyclic complexes. One of the most illustrated and understood trends is along the first row from left to right along to Zn^{2+}. For complexation to the first four ligand donors, values of log β_{1-4} increase steadily along the period left to right from V^{2+} to Ni^{2+} paralleling the increasing Z_{eff}, leading to a maximum at Cu^{2+}, the so-called Irving-Williams effect, illustrated for log K_1 in Figure 1.[38]

The maximum at Cu^{2+} arises as a result of the Jahn−Teller distortion of the e_g^3 configuration of the assumed initial octahedral geometry which leads to a strengthening of the ligand field for four donors usually in the equatorial plane at the expense of a weaker field for those axial, usually two or sometimes one (see section 3.4.3.2). A similar maximum although less defined is seen for Cr^{2+} which is also subject to a Jahn−Teller distortion of the e_g^1 level. The sharp drop in log K_1 values from Cr^{2+} to Mn^{2+} and from Cu^{2+} to Zn^{2+} is due to the high spin d^5 and filled d^{10} configurations respectively of the following ions leading to a complete loss in LFSE. These effects

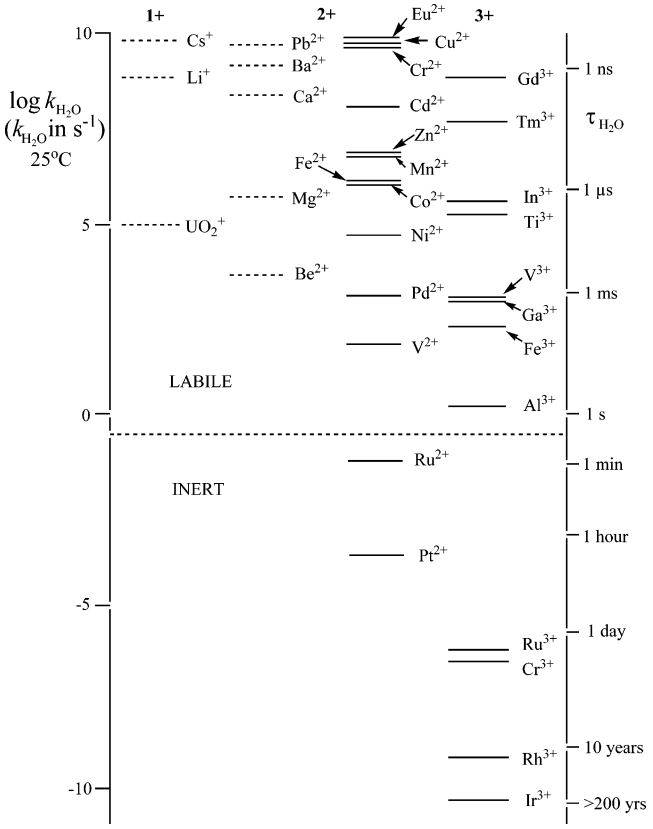

Figure 2. Range of water exchange rate constants (log k_{H_2O}, s^{-1}) and mean lifetime (τ_{H_2O}, s) for primary shell water molecules on aqua metal ions at 25 °C (the dotted line represents Taube's inert/labile boundary [42]).

are also evident in the dynamics of water exchange on the aqua ions (see later).

3. Kinetics and Dynamics

3.1. Survey of Water Ligand Exchange Rates on Metal Aqua Ions

Water exchange between the first coordination sphere and the second coordination sphere (or first solvation sphere) of a hydrated metal ion, or aqua ion, is the simplest of all ligand substitution process in aqueous solution. Remarkably, some 20 orders of magnitude cover the present range of water exchange rates on aqua metal ions from the most labile, Eu^{2+} and Cs^+ (residence time, 25 °C, $\sim 10^{-10}$ s), to the most inert, Ir^{3+} (residence time $\sim 10^{10}$ s), Figure 2.[28,39−41] An understanding of the origins of this huge variation in lability and the accompanying mechanistic variation of the water exchange processes (see later) is fundamental to the interpretation of metal ion complexation and ligand substitution processes in chemical and biological systems, and as such the water exchange process has been the subject of much intense investigation and may be represented for a generic hydrated metal ion, $[M(H_2O)_n]^{m+}$, as is shown in (5) where H_2O^* represents a water from the second solvation shell. The mean lifetime τ_{H_2O} of a particular water molecule, or aqua ligand, in the first coordination sphere is defined as $1/k_{H_2O}$ where k_{H_2O} is the rate constant for the exchange of a single water molecule

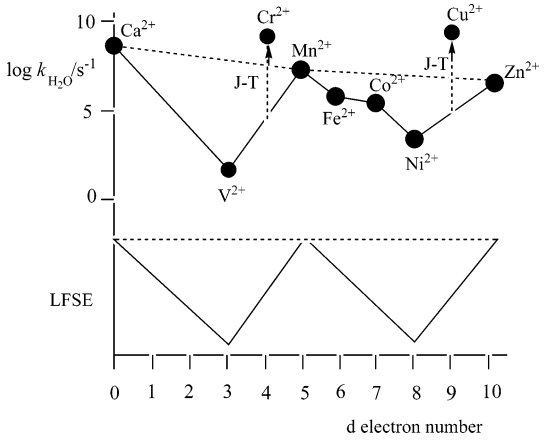

Figure 3. Correlation of log k_{H_2O} (s^{-1}) with LFSE (kJ mol^{-1}) for the first row transition metal $[M(H_2O)_6]^{2+}$ cations. (J−T is the apparent rate acceleration resulting from the Jahn−Teller distortion away from regular octahedral geometry).

from the first coordination sphere. The rate of water exchange on $[M(H_2O)_n]^{m+}$ is given by (6).

$$[M(H_2O)_n]^{m+} + H_2O^* \overset{k_{H_2O}}{\rightleftharpoons} [M(H_2O)_{(n-1)}H_2O^*]^{m+} + H_2O \quad (5)$$

$$\text{rate} = nk_{H_2O}[M(H_2O)_n^{m+}] \quad (6)$$

It is recognized that this remarkable range of rates reflects at the one extreme the size of the metal ion, r_M,[43] and the magnitude of the cationic charge (electrostatic), thus somewhat correlating with the extent of hydration, and at the other extreme the presence of ligand field effects (transition metal cations). The divalent lanthanide $[Eu(H_2O)_7]^{2+}$ is at the fast extreme with τ_{H_2O} (298.2 K) = 2.0×10^{-10} s, a period in which light travels ~6 cm and a water exchange event occurs every ~2.8×10^{-11} s.[44] This is similar to the lability deduced from ligand substitution studies for the largest singly positive ion $[Cs(H_2O)_8]^{+}$ [39] possessing the lowest charge density. On the other hand $[Ir(H_2O)_6]^{3+}$ is at the slow extreme of the lability scale with τ_{H_2O} (298.2 K) = 9.1×10^9 s which corresponds to ~300 years and a water exchange event occurring every ~50 years.[41] Ir^{3+} is a third row low spin t_{2g}^6 transition metal ion with the maximum LFSE for its octahedral field of coordinated waters (−2.4 Δ_o) with Δ_o appreciably large (see below). Hence water exchange has to overcome a relatively large activation barrier with consequences for the adopted mechanism (see section 3.4.4.1). For the first row divalent transition metal ions, log k_{H_2O} correlates very well with the crystal field activation energy as proportional to the LFSE associated with the particular electronic configuration, Figure 3. It may be noted that ~100 kJ mol^{-1} of LFSE amounts to a kinetic effect between $[Ca(H_2O)_8]^{2+}$ (d^0) and $[V(H_2O)_6]^{2+}$ (t_{2g}^3) in excess of 6 orders of magnitude. The relative inertness of $[V(H_2O)_6]^{2+}$ shows how LFSE factors can override charge/size effects apparent elsewhere in the periodic table.

The unusually high lability of $[Cr(H_2O)_6]^{2+}$ and $[Cu(H_2O)_{5/6}]^{2+}$ is due to the well-established Jahn−Teller distortion from regular octahedral geometry leading to weakly bonded axial waters (one or two) in rapid fluctionality with their less labile equatorial counterparts. In the case of relatively inert systems, the transition metal ions, one can easily talk of a discrete primary hydration shell undergoing slow exchange. In the case of large univalent ions such as $[Cs(H_2O)_8]^+$ which possess a primary shell lability comparable to that of the secondary solvation shell, one has difficulty discussing the presence of a discrete primary shell as opposed to the situation of the naked metal cation merely moving through the bulk solvent. In another striking comparison, the oxo groups of ClO_4^- reflect the high M−O bond strength exemplified by extremely long half-life (>100 years) for exchange with bulk water at 25 °C. This may be compared to the diffusion controlled rate ($t_{1/2} < 10^{-10}$ s) for water exchange on the hydrated Cl^- ion. Both acid and base catalyzed pathways for water exchange on oxo anions have been detected.

Three broad categories of exchanging inorganic centers can be distinguished: (i) the main group metal s−p block ions, (ii) the transition metal d-block ions, and (iii) the trivalent lanthanide f-block ions. Within the main group metal ions, the labilities of the alkali metal ions are encompassed by an approximately 1 order of magnitude variation consistent with the increase in lability from Li^+ to Cs^+ being dominated by a decrease in surface charge density and an increase in coordination number which changes from the variously quoted values of 4 and 6 for Li^+ to 9 for Cs^+ and intermediate values for Na^+, K^+, and Rb^+. The alkaline earth metal ions show almost 6 orders of magnitude variation in lability with $[Be(H_2O)_4]^{2+}$ being the least labile whereas $[Ba(H_2O)_8]^{2+}$ is one of the most labile metal ions. The labilities of the d^{10} $[Zn(H_2O)_6]^{2+}$, $[Cd(H_2O)_6]^{2+}$, and $[Hg(H_2O)_6]^{2+}$ ions are at the higher end of the lability scale as anticipated for metal ions of moderate to low surface charge density and span 2 orders of magnitude as a consequence of increasing ionic radius as the group is descended. The lability of trivalent $[Al(H_2O)_6]^{3+}$ falls in the middle of the lability range shown in Figure 2, consistent with the small size and high charge of Al^{3+}. The decrease in surface charge density of the metal center from $[Al(H_2O)_6]^{3+}$ to $[In(H_2O)_6]^{3+}$ results in a 6-fold order of magnitude increase in lability, but the lability of $[Tl(H_2O)_6]^{3+}$ has not been determined. The second category is represented by the transition metal ions, all of which shown in Figure 2 are six coordinate with the exception of square-planar $[Pd(H_2O)_4]^{2+}$ and $[Pt(H_2O)_4]^{2+}$ and possibly five coordinated $[Cu(H_2O)_5]^{2+}$. Their labilities encompass almost 20 orders of magnitude largely as a consequence of their d orbital occupancies influencing their transition state energetics and stereochemistries as are discussed below. The third category are the large and very labile trivalent lanthanide ions whose coordination number decreases from nine in $[Ce(H_2O)_9]^{3+}$ to eight in $[Lu(H_2O)_8]^{3+}$ with the change occurring about halfway along the series around Eu^{3+} and Ga^{3+} as the lanthanide contraction occurs with increasing atomic number coincident with a decrease in lability over 2 orders of magnitude.

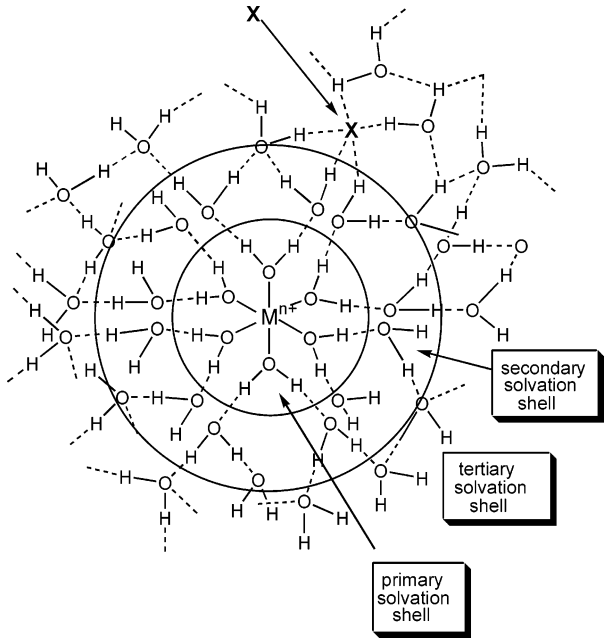

Figure 4. Hydrogen-bonded localized water structure surrounding a metal cation in aqueous solution (here the metal ion is assumed to have a primary hydration number of 6).

As well as the primary shell of water molecules, there exists, depending upon the charge on the metal ion, a well defined second coordination sphere of water molecules, illustrated in Figure 4 for the case of a six-coordinated ion. Generally, information about the number of waters in the second coordination sphere and their corresponding residence times is scarce, and the only reported experimentally determined lifetime of a water molecule exchanging between the second coordination sphere and bulk water is 1.28×10^{-10} s at 298.2 K for $[Cr(H_2O)_6]^{3+}$ which compares with 1.44×10^{-10} s obtained from molecular dynamic calculations.[28,45] Similar calculations show hydrated Nd^{3+}, Sm^{3+}, and Yb^{3+} to have 17.61, 17.13, and 16.74 water molecules in the second-coordination sphere, respectively, with residence times of 1.3×10^{-11}, 1.2×10^{-11} and 1.8×10^{-11} s.[46] These few data are consistent with the exchange of water between the second coordination sphere and the bulk being close to diffusion control as has been generally assumed to be the case in mechanistic models for substitution of water in the first coordination sphere (see discussion later).

3.2. Measurement of the Water Exchange Process

The standard methods involve labeling studies employing the use of the two isotopes of oxygen: ^{17}O and ^{18}O.

3.2.1. ^{18}O Labeling

This method has been pioneered by workers such as Hunt, Plane, and Taube[47] and Murmann and Gamsjager.[48] The technique involves measurement of the oxygen/water exchange by converting the oxygen in the species after a set time into a gaseous form usually CO_2 or O_2 itself and measuring the ^{18}O:^{16}O ratio in a mass spectrometer. Several of these methods have been described.[49] Use of CO_2 makes use of the equilibration reaction 7 for which K is known as a function of temperature, $\log K = 16.6T^{-1} - 0.01569$.

$$K = \frac{[C^{18}O_2]^{1/2}[H_2{}^{16}O]}{[C^{16}O_2]^{1/2}[H_2{}^{18}O]} \qquad (7)$$

Quenching of the reaction can be achieved in a number of ways, e.g., by a pH jump to a region where exchange is much slower or by precipitation of the oxygen-containing compound in the form of a solid derivative. The solid compound is then washed and dried for conversion into a gaseous oxygen form. Similarly, samples of water can be analyzed. Exchange reactions with half-lives as low as 10 s can be followed by use of a multi-mixing stopped-flow apparatus. A disadvantage of the ^{18}O method is the requirement for high enrichment levels. However, the accuracy of the mass spectral determination of the isotope ratio can be around 1 in 10 000 which is by far superior to any other method and somewhat compensates. Furthermore, ^{18}O is much cheaper compared to ^{17}O (around a factor of 10 per atom % enrichment) and to use since mg amounts and enrichments of only $\sim 10\times$ natural abundance can suffice owing to the accuracy of the isotope ratio determination. The main source of experimental error is in sampling, sampling induced exchange and ensuring that the gaseous oxygen form analyzed is pure and representative. Labeling with ^{18}O is the only available method for measuring water exchange on inert paramagnetic species e.g. complexes of Cr^{3+} [47,50,51] and is a convenient method for many slow exchanging oxo anions.[48]

3.2.2. ^{17}O Labeling (NMR)

The ^{17}O NMR method[52,53] however is the only one that can be applied to labile aqua metal ions with half-lives of <10 s and particularly where there are a number of different exchanging oxygen sites (e.g., on polynuclear species). For slow exchanging oxygen sites on diamagnetic metal ions, one can monitor the exchange very simply by conventional means by following the growth or decay to equilibrium of the ^{17}O resonance of the particular oxygen, hydroxide, or water site. It is often good practice to measure the rate both ways as a check. Given a choice following the decay of the peak height (area) of an enriched sample to equilibrium in natural abundance water is to be preferred owing to the presence of more reliable data over the crucial first half-life. The measuring accuracy is however still somewhat inferior to the mass spectral method. Half-lives of around a few seconds can be followed by rapid injection methods of the type pioneered by Merbach and coworkers.[28] Water exchange rates measured by the ^{17}O NMR isotope dilution method include that on $[Ru(H_2O)_6]^{2+}$ (by rapid injection), $[Ru(H_2O)_6]^{3+}$, $[Rh(H_2O)_6]^{3+}$, and $[Pt(H_2O)_4]^{2+}$.

For faster exchanging metal ions with half-lives (25 °C) of <1 s, one can employ a number of linebroadening methods.[53] For diamagnetic metal aqua ions with half-lives of between 1 s and 1 ms, the line width

of the bound water ^{17}O NMR resonance can be measured as a function of various parameters such as temperature and $[H^+]$ at a constant ionic strength. Again Mn^{2+} can act as a convenient relaxation agent for the intense line of free water. The bound water line width can be related to a measure of the transverse relaxation time T_2 (for bound water both T_1 and T_2 are comparable) which is a function of two components, the quadrupolar relaxation time T_{2Q} and the bulk water exchange rate constant k_{H_2O} according to (8).

$$\frac{1}{T_{2obs}} = \frac{1}{T_{2Q}} + k_{H_2O} \tag{8}$$

The temperature dependence of k_{H_2O} is fitted to the normal Eyring expression (9) for the purpose of estimating $\Delta H^{\ddagger}_{H_2O}$ and $\Delta S^{\ddagger}_{H_2O}$, whereas an Arrhenius expression (10) is normally used for T_{2Q}. $1/T_{2Q}$ is proportional to the correlation time relating to the tumbling frequency of the water molecules. This depends on the viscocity of the medium and as such the use of media of low viscocity is preferred for the narrowest lines, reproducibility and the avoidance of medium effects.

$$k_{H_2O} = \frac{k_B T}{h}\exp(-\Delta H^{\ddagger}_{H_2O}/RT + \Delta S^{\ddagger}_{H_2O}/R) \tag{9}$$

$$\frac{1}{T_{2Q}} = \frac{1}{T_{2Q}^{298.2}}\exp\left(\frac{E_Q}{R}\left\{\frac{1}{T} - \frac{1}{298.2}\right\}\right) \tag{10}$$

In terms of noncomplexing anionic media the preferred order appears to be ClO_4^- > BF_4^- > PF_6^- > $CF_3SO_3^-$ ($tfms^-$) > p-$CH_3C_6H_4SO_3^-$ (pts^-).[54] A particularly nice example where two different coordinated water ligands are exchanging on different time domains is that of the incomplete cuboidal Mo^{IV} cluster ion, $[Mo_3S_4(H_2O)_9]^{4+}$ [55] The plot of $\ln(1/T_{2obs})$ as a function of reciprocal absolute temperature is shown in Figure 5. Here the local geometry at Mo is highly distorted due to the M−M interactions, see section 3.4.10.2 later. The c-H_2O ligands, approximately trans to the capping sulfide group, exchange much more slowly than the d-H_2O's, which are approximately trans to the bridging sulfides, the latter also showing an exchange rate acceleration with decreasing $[H^+]$. The c-H_2O's only show the quadrupolar contribution which works to sharpen the lines as the temperature is increased. In contrast, at temperatures depending upon the $[H^+]$, the line width of the d-water resonance goes through a minimum and then increases with temperature due to the chemical exchange. The fit is basically to two intersecting straight lines going in opposite directions with temperature. The $[H^+]$ dependence of the d-H_2O exchange is of the form (11) indicating dominant involvement of $Mo_3S_4(OH)^{3+}$(aq), hydrolysis constant K_{11} (0.18 M), the significance of which suggests that

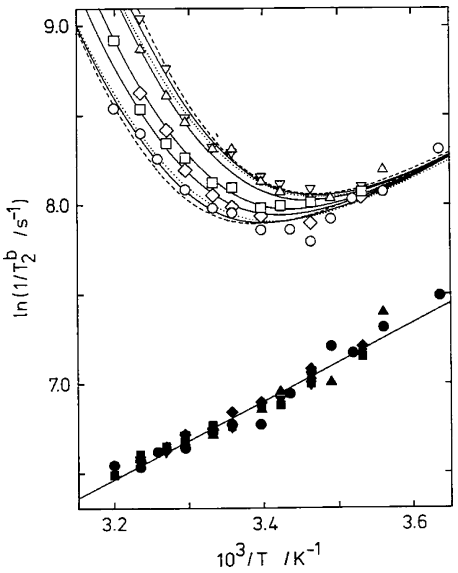

Figure 5. Plot of $\ln(1/T_{2obs})$ (^{17}O) versus $10^3/T$(°K) for the coordinated waters of $[Mo_3(\mu_3\text{-}S)(\mu\text{-}S)_3(c\text{-}H_2O)_3(d\text{-}H_2O)_6]^{4+}$ at $I = 2.00$ M $(Na^+)ClO_4^-$ as a function of $[H^+]$: circles (1.56 M); squares (1.18 M); diamonds (0.945 M); triangles (0.664 M), and inverted triangles (0.545 M); filled symbols (c-H_2O); open symbols (d-H_2O).[55]

the relevant deprotonation occurs at an adjacent water ligand on the same Mo center.

$$k_{H_2O} = \frac{k_{OH}K_{11}}{[H^+] + K_{11}} \tag{11}$$

This is believed to be a rare example of the cis conjugate-base effect (see sections 3.4.4.2 and 3.4.7). At sufficiently high values, the line width of the ^{17}O resonance peak becomes indistinguishable from the baseline and thus immeasurable around a half-life for exchange at 25 °C of ~0.1 ms. This is the situation arising in the case of the more labile aqua Mo^V dimer ion $[Mo_2O_4(H_2O)_6]^{2+}$. The much slower c-H_2O exchange on $Mo_3S_4^{3+}$(aq) can be studied at 25 °C by conventional fast injection isotopic enrichment and interestingly it shows no corresponding $[H^+]$ dependence. Other labile diamagnetic metal ions that have had their water exchange rates measured by the ^{17}O NMR line broadening technique include $[Be(H_2O)_4]^{2+}$, $[Al(H_2O)_6]^{3+}$, $[Ga(H_2O)_6]^{3+}$ and $[Pd(H_2O)_4]^{2+}$.

For faster exchanging metal ions that are paramagnetic, Swift and Connick[53] developed a method based upon an analysis of both the chemical shift and relaxation times for the ^{17}O NMR nuclei of both free and bound water and showed that the former could be used for the measurement of water exchange rates for labile paramagnetic metal ions such as the those of the first row divalent and trivalent transition metals. The relaxation of the ^{17}O nucleus of waters bound to a paramagnetic metal ion has been shown to be due to scalar coupling between the magnetic moment of the ^{17}O nucleus and the unpaired electrons. The line width of the free water ^{17}O resonance can be monitored as a function of temperature over a very wide temperature range owing to its intrinsically longer relaxation time. At sufficiently high temperatures, the line widths eventually decrease

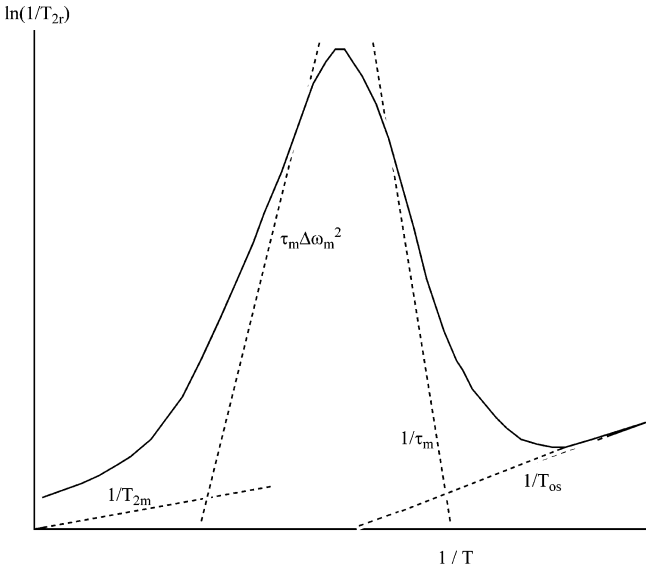

Figure 6. Full Swift-Connick temperature dependence of $\ln(1/T_{2obs})$ for the ^{17}O nucleus of a water molecule in the presence of fast exchanging metal ion. (The dashed lines represent the four regions where predominant relaxation contributions lead to a simplification of eq 8.)[53]

again, Figure 6 in accordance with the full expression (12)

$$\frac{1}{T_{2r}} = \frac{1}{\tau_m}\left[\frac{{T_{2m}}^{-2} + (T_{2m}\tau_m)^{-1} + {\Delta\omega_m}^2}{({T_{2m}}^{-1} + {\tau_m}^{-1})^2 + {\Delta\omega_m}^2}\right] + \frac{1}{T_{2os}} \quad (12)$$

where T_{2r} is the reduced bulk water relaxation time, related to the observed relaxation time T_{2obs} by (13), T_{2m} is the relaxation time for bound waters in the absence of exchange, $\Delta\omega_m$ is the chemical shift between the bulk and bound waters in the absence of exchange, τ_m is the residence time of bound water, and T_{2os} is the contribution due to the simple outer-sphere interaction. In (13)

$$\frac{1}{T_{2r}} = \frac{1}{p_m}\left(\frac{1}{T_{2obs}} - \frac{1}{T_{2s}}\right) \quad (13)$$

T_{2s} is the contribution to the bulk water relaxation from the pure solvent and p_m is the ratio of the number of moles of water bound to the metal to the total moles of water. Finally $\Delta\omega_r$, the reduced chemical shift of the bulk water, is given by (14)

$$\Delta\omega_r = \frac{\Delta\omega_s}{p_m} = \frac{\Delta\omega_m}{(\tau_m/T_{2m} + 1)^2 + {\tau_m}^2\,{\Delta\omega_m}^2} + \Delta\omega_{os} \quad (14)$$

where $\Delta\omega_s$ is the chemical shift of the pure bulk solvent and $\Delta\omega_{os}$ is the chemical shift difference between pure bulk solvent and the solvent in the presence of the paramagnetic metal ion, the correction being due to the simple outer-sphere interaction. The region wherein the diamagnetic metal ions mentioned above undergo exchange is given simply by $1/\tau_m$ termed the "slow" exchange domain. The water exchange rate constant k_{H_2O} is simply given by $1/\tau_m$. Water exchange on the labile paramagnetic metal hexaaqua ions; Mn^{2+}, Fe^{2+}, Co^{2+}, and Ni^{2+} has been investigated using the full Swift-Connick eq 8 in the region of data around the 'maximum' and into the region dominated by the term $T_{2m}\tau_m$ in Figure 6. The Swift-Connick treatment has also been applied successfully for the determination of the water exchange rate constants on the highly labile paramagnetic trivalent lanthanide ions.[29]

Despite the wide range of time scales available for monitoring rates using NMR it is not possible to cover the entire range. Occasionally, the exchange half-life falls in the range that makes it unavailable to study. This is when the rate is too slow and the activation parameters are such that it cannot be brought on to the linebroadening time scale at elevated temperatures while at the same time being too fast for a rapid mixing conventional isotopic dilution approach. This occurs for half-lives (at 25 °C) in the range $\sim 10\ s < t_{1/2} < 10^{-2}$ s. For paramagnetic metal ions, one can simply put an upper limit on the half-life of 10^{-2} s. Unfortunately, paramagnetic $[Mo(H_2O)_6]^{3+}$ is one such metal ion whose rate of water exchange falls within this so-called "blind" region.

3.2.3. Estimates from Complex Formation Rates using Relaxation Methods

Although the ever increasing routine availability of high field NMR instruments is lowering the upper rate limits for monitoring of solvent exchange processes, most of the quoted rate constants for water exchange on the most labile of the diamagnetic metal ions such those of groups 2 and 12 and the heavier members of groups 13−15 are still based largely on extrapolation from rate constants for complex formation reactions. These are available from use of rapid mixing techniques such as stopped-flow spectrophotometry, or if an equilibration reaction is relevant the use of relaxation methods such as temperature jump (if spectroscopic monitoring is possible) or, e.g., ultrasound absorption (if not). This is because of the general observation that the more labile a metal ion is the more insensitive are the observed rates of reaction to the nature of the incoming ligand nucleophile. The result is such that they become largely comparable to, or certainly within an order of magnitude of, the rate constant for water exchange. Many of the estimates from ultrasound absorption have been based on the values of rate constants determined for SO_4^{2-} complexation reactions, such as for the following: Be^{2+}_{aq} ($\sim 10^2\ s^{-1}$), Mg^{2+}_{aq} ($\sim 10^5\ s^{-1}$), Ca^{2+}_{aq} ($\sim 10^8\ s^{-1}$), Zn^{2+}_{aq} ($\sim 10^7\ s^{-1}$), Cd^{2+}_{aq} ($\sim 10^8\ s^{-1}$), Hg^{2+}_{aq} ($\sim 10^8-10^9\ s^{-1}$), and the Ln^{3+}_{aq} ions ($\sim 10^8\ s^{-1}$).[6] Directly measured values now exist for Be^{2+}_{aq} and Mg^{2+}_{aq} and many of the Ln^{3+}_{aq} ions but not for the rest. The ultrasound absorption method has not been without its critics although wherever water exchange rate constants have been determined by other means (e.g., by NMR or T-jump) the values from ultrasound have been largely comparable.[11] Much of the kinetic data on labile metal ions has recently been reviewed by Wilkins.[56] Since Margerum's article in 1978,[11] much of the data and most of the mechanistic conclusions reached have stood the test of time over the past 25 or so years although most of the water exchange kinetic data obtained by NMR prior to 1970

has now been remeasured using more powerful modern instruments, and it therefore should be viewed with caution. Margerum stated in 1978 that "many metal ion substitution reactions seem to be largely insensitive to the nature of the ligands in the second co-ordination sphere" i.e., controlled by the rate of water ligand dissociation.[11] With the exception of a few clear-cut examples, this remains a fairly accurate picture at least of reactions at the most labile of metal centers and for many divalent octahedral species.

3.3. Kinetics of Formation of Metal Complexes in Aqueous Solution

3.3.1. Eigen-Wilkins Reactant Preassociation

Manfred Eigen pioneered the development of rapid mixing and relaxation methods for studying reactions on labile metal ions.[6a] Reactions on $Ni^{2+}(aq)$ were found to fall into the range suitable for stopped-flow monitoring, Figure 2, and rates were measured for a range of different incoming ligands, L^{x-}. Wilkins subsequently reviewed the rate data for different L^{x-} substituting on $[Ni(H_2O)_6]^{2+}$ and noticed that although there existed a large L^{x-} dependence on the observed rate constant no correlation was apparent with a reliable nucleophilicity parameter, namely the respective pK_a value of HL. It was eventually shown in a wider study that the observed variation in rate constant depended mainly on the charge $x-$ and this led on to a realization that the interchange of ligands on a complex such as $[M(H_2O)_n]^{m+}$ takes place within a rapid preformed outer-sphere encounter complex; $[M(H_2O)_n]\cdot L^{(m-x)}$, held together by electrostatics.[6b] This is envisaged as rapid diffusion-controlled entry of L^{x-} into the second coordination sphere of the metal ion complex. The rate-limiting event then occurs through L^{x-}/H_2O interchange within the two coordination spheres within the encounter complex. Only in the case of the most labile metal ions are rates of substitution of a water molecule in the first coordination sphere within an order of magnitude of its entry to the second coordination sphere, and consequently all substitution rate-limiting events occur in the first coordination sphere of $[M(H_2O)_n]^{m+}$. In aqueous solution, the substitution of a ligand, L^{x-}, into the first coordination sphere is always preceded by its entry into the second coordination sphere of water molecules. Although a variety of kinetic methods have been applied to the rate determining steps involving ligand interchange, it is seldom the case that more than one stage of the transfer of a monodentate ligand, L^{x-}, from bulk water to the first coordination sphere is detected other than by the ultrasonic method where up to three steps have been detected.[57] These steps were identified in early studies as shown in (15)

$$\underset{\mathbf{A}}{M^{m+}} + L^{x-} \underset{k_{10}}{\overset{k_{01}}{\rightleftharpoons}} \underset{\mathbf{B}}{M\cdot OH_2\cdot OH_2\cdot L^{(m-x)+}} \overset{k_{12}}{\underset{k_{21}}{\rightleftharpoons}} \underset{\mathbf{C}}{M\cdot OH_2\cdot L^{(m-x)+}} \overset{k_{23}}{\underset{k_{32}}{\rightleftharpoons}} \underset{\mathbf{D}}{ML^{(m-x)+}} \quad (15)$$

where **A** represents M^{m+} and L^{x-} separated by more than two water molecules, **B** represents M^{m+} and L^{x-} separated by two water molecules, **C** represents M^{m+} and L^{x-} separated by one water molecule in the outer-sphere complex, and **D** represents M^{m+} and L^{x-} in contact in the new complex $[M(H_2O)_{(n-1)}L]^{(m-x)}$.[6a] The diffusion-controlled formation of **B** (k_{01}/k_{10}) is followed by the fast formation of **C** (k_{12}/k_{21}), which leads to the slower formation of **D** (k_{23}/k_{32}). In most ligand substitution studies, **B** is not detected and the simplified sequence of the Eigen-Wilkins mechanism (16) is often discussed instead.[6b] The sequential equilibria in (16) are characterized by $K_{12} = k_{12}/k_{21}$ (often denoted as K_{os}) and $K_{23} = k_{23}/k_{32}$, respectively.[58] Usually, it is only possible to characterize the kinetics of the second equilibrium of (16) so that the overall equilibrium is expressed as in (17) irrespective of the intimate mechanism of ligand substitution.

$$\underset{\mathbf{B}}{M^{m+}} + L^{x-} \overset{k_{12}}{\underset{k_{21}}{\rightleftharpoons}} \underset{\mathbf{C}}{M\cdot OH_2\cdot L^{(m-x)+}} \overset{k_{23}}{\underset{k_{32}}{\rightleftharpoons}} \underset{\mathbf{D}}{ML^{(m-x)+}} \quad (16)$$

$$M^{m+} + L^{x-} \overset{k_f}{\underset{k_b}{\rightleftharpoons}} ML^{(m-x)+} \quad (17)$$

The first-order rate constant for the approach to equilibrium, k_{obs}, is given by (18) where the first and second right-hand terms equate to k_f and k_b, respectively in (17), when $[L^{x-}] \gg [M^{m+}]$.

$$k_{obs} = \{(k_I K_{os}[L^{x-}])/(1 + K_{os}[L^{x-}])\} + k_{-I} \quad (18)$$

When $K_{os}[L^{x-}] \ll 1$, $k_{obs} \approx k_I K_{os}[L^{x-}] + k_{-I}$ and when $K_{os}[L^{x-}] \gg 1$, $k_{obs} \approx k_I + k_{-I}$, where k_I and k_{-I} characterize L^{x-} interchange between the first and second coordination spheres. Equivalent expressions apply when $[M^{m+}] \gg [L^{x-}]$. If L^{x-} is uncharged the stability of the outer-sphere complex may be so low that its concentration does not differ significantly from that arising from diffusive collisions. It is within this kinetic framework that the intimate mechanism of the ligand substitution process has to be identified. In the case of $[Ni(H_2O)_6]^{2+}$, it was found that the observed variation in rate constant k_{obs} with different L^{x-} reflected the variation in the encounter complex formation constant K_{os} rather than any variation in k_I. Indeed values of k_I were found to be largely constant and moreover close to k_{H_2O} for $[Ni(H_2O)_6]^{2+}$, 3.6×10^4 s^{-1} (25 °C) implying a process largely controlled by dissociation of a water ligand from the first coordination sphere.

Eigen[6a] and Fuoss[58] developed eqs 19 and 20 for the estimation of K_{os} based on extended Debye–Huckel theory and a hard sphere model for the reacting species.

$$K_{os} = \frac{4\pi N a^3}{3000} \exp\left(\frac{-U}{kT}\right) \quad (19)$$

where

$$U = \frac{z_1 z_2}{\epsilon}\left(\frac{1}{a(1+\kappa a)}\right) \text{ and } \kappa = \sqrt{\frac{8\pi N e^2 I}{1000\epsilon kT}} \quad (20)$$

and N is Avogadro's number (6.022×10^{23}), a is the

distance of closest approach (cm), e is the electron charge, k is the Boltzmann constant, ϵ is the bulk solvent dielectric constant, I is the ionic strength, and z_1 and z_2 are the charges on the respective species. Values of $\sim$1 M^{-1} for a 2+/1- reactant pair and $\sim$2 M^{-1} for a 3+/1- pair at ionic strength 1.0 M seem to be largely in keeping with calculated values. Apparent from (19) and (20) is that K_{os} values increase with the product z^+, z^-, decreasing ionic strength and decreasing dielectric constant. For highly charged reacting pairs, e.g., 2+/2- or greater the value of K_{os} can be large enough to give rise to a nonlinear dependence on $[L^{x-}]$ as $[L^{x-}]$ is increased. A good example of this is shown by the slow complexation of $EDTA^{4-}$ (added as Na_2H_2EDTA) to $[Cr(OH_2)_6]^{3+}$ in the pH range 3.5−5.5, to form $[Cr(EDTA)(H_2O)]^-$ the psuedo first-order rate constant for which is independent of $[H_2EDTA^{2-}]$ at concentrations $\geq$0.1M. The $[H^+]^{-1}$ dependence on the rate moreover shows that the deprotonated 3+/3- reactant pair $[Cr(OH_2)_6]^{3+}$.$HEDTA^{3-}$ is the actual reacting species. This is a commonly used laboratory experiment for illustrating complex formation kinetics and $[H^+]$ effects.

3.3.2. Mechanistic Classification

Systemisation and categorization of reactions occurring at inorganic metal centers only received serious attention through the 1950s and early 1960s through the pioneering work of Taube, Basolo, Pearson, Eigen, Wilkins, Langford, Gray, and others. It is now generally assumed that most interchange reactions between a positively charged metal ion in aqueous solution and incoming ligands L^{x-} proceed through rapid formation of the Eigen−Wilkins encounter species. It is within the interchange step involving the first and second coordination spheres of the encounter complex that mechanistic distinctions are seen between different M^{m+}/L^{x-} combinations throughout the periodic table. Kinetic measurements provide information about the transition state stoichiometry and the enthalpic and entropic changes characterizing the transition state. However, these do not directly provide details of stereochemical changes occurring along the reaction coordinate. Nevertheless, kinetic variations coinciding with changes in M^{m+} size and electronic configuration give some stereochemical clues[6b,29] and the stereoretentive reactions of square-planar Pd^{2+} and Pt^{2+} complexes (see below) give strong insight into stereochemical changes along the reaction coordinate.[59] Most informative however has proved to be the variation of k_I as a function of entering ligand type, leaving ligand type, pH, temperature and pressure where the challenge is one of careful and meaningful interpretation.

3.3.2.1. A, I_A, I, I_D and D Labels. In 1965 Langford and Gray[5] proposed a classification of ligand interchange processes at metal centers as being of three basic types; associative (**A**), dissociative (**D**) and interchange (**I**), as distinct from the already well-established S_N1 or S_N2 labels used for reactions on carbon. These labels, particularly the **I** label, follow from the realization that reactions at M^{m+} centers are always associated with a degree of preassociation with any anion or dipolar nucleophilic incoming ligand molecule as alluded to already above. If one considers substitution of a water ligand on the aqua complex $[M(H_2O)_n]^{m+}$ by L^{x-}, the extreme **A** mechanism involves $[M(H_2O)_n]^{m+}$ and L^{x-} passing through a first transition state to form a reactive intermediate $[M(H_2O)_nL]^{(m-x)+}$ in which the coordination number of M^{m+} is increased by one (21). This intermediate survives several molecular collisions before passing through a second transition state to form the product $[M(H_2O)_{(n-1)}L]^{(m-x)+}$. Thus, the rate determining step (k_1) is the bond making between L^{x-} with M^{m+}. In the back reaction, the rate determining step is characterized by k_{-2}. The rate of approach to equilibrium in the presence of excess $[L^{x-}]$, characterized by k_{obs} in (22) is dependent on the nature of L^{x-}. The full form of the rate law may actually be as in (18) with formation of a reactant pair preceding the formation of $[M(H_2O)_nL]^{(m-x)+}$.

$$[M(H_2O)_n]^{m+} + L^{x-} \underset{k_{-1}}{\overset{k_1}{\rightleftharpoons}} [M(H_2O)_nL]^{(m-x)+} \underset{k_{-2}}{\overset{k_2}{\rightleftharpoons}} [M(H_2O)_{(n-1)}L]^{(m-x)+} + H_2O \quad (21)$$

$$k_{obs} = k_1[L^{x-}] + k_{-2} \quad (22)$$

The dissociative **D** mechanism operates when $[M(H_2O)_n]^{m+}$ passes through a first transition state to form a reactive intermediate, $[M(H_2O)_{(n-1)}]^{m+}$, in which the coordination number of M^{m+} is decreased by one (23). This intermediate also survives several molecular collisions before passing through a second transition state with L^{x-} to form the product $[M(H_2O)_{(n-1)}L]^{(m-x)+}$. Thus, the rate determining step (k_1) involves bond breaking. [An intermediate may defined as a species able to undergo several molecular collisions and therefore an ability to distinguish between different incoming nucleophiles. Within the **D** mechanism the intermediate can be considered as having lost all memory of the departed ligand and thus an ability to treat all ligands held within the secondary shell assemblage as independently reacting species]. In the back reaction, the rate determining step is characterized by k_{-2}. The rate of approach to equilibrium in the presence of excess $[L^{x-}]$, characterized by k_{obs} in (24) and is independent of the nature of L^{x-}. However, as we have seen, the tendency toward forming outer-sphere reactant-pair complexes often prevents the observation of either of the limiting rate laws shown in (22) and (24) but this does not preclude the operation of either an **A** or a **D** mechanism within the preformed outer-sphere complex.

$$[M(H_2O)_n]^{m+} + L^{x-} \underset{k_{-1}}{\overset{k_1}{\rightleftharpoons}} [M(H_2O)_{(n-1)}]^{m+} + L^{x-} \underset{k_{-2}}{\overset{k_2}{\rightleftharpoons}} [M(H_2O)_{(n-1)}L]^{(m-x)+} + H_2O \quad (23)$$

$$k_{obs} = (k_1k_2[L^{x-}] + k_{-1}k_{-2})/(k_{-1} + k_2[L^{x-}] \quad (24)$$

Indeed the rate law in (24) has the same $[L^{x-}]$ dependence as (18) for formation of the reactant-pair and in a number of classical cases (e.g., the case of Rh^{3+}(aq) highlighted below) has led to the wrongful diagnosis of the presence of an extreme **D** process.

Between the **A** and **D** mechanistic extremes there exists a continuum of mechanisms in which the entering and leaving ligands make varying contributions to the transition state energetics. They extend from the associative interchange ($\mathbf{I_A}$) mechanism where bond making is of major importance, through the interchange (**I**) mechanism where bond making and breaking are of similar importance, to the dissociative interchange ($\mathbf{I_D}$) mechanism where bond breaking is of major importance. Within the **I** process, there is no discernible intermediate formed akin to an S_N2 reaction on carbon.

Distinction between the associatively or dissociatively activated mechanisms should be possible through a comparison of the rate of exchange on $[M(H_2O)_n]^{m+}$ and the rate at which L^{x-} substitutes into the first coordination sphere. For the **A** and $\mathbf{I_A}$ mechanisms, the rate of substitution by L^{x-} may vary from being much less than to much greater than the rate of water exchange with corresponding variations in $\Delta H^{\ddagger}$ and $\Delta S^{\ddagger}$. In contrast, for the **D** mechanism, the rate of substitution by L^{x-} cannot be faster than the rate of water exchange and may be significantly slower as a consequence of statistical factors.[60] Also, $\Delta H^{\ddagger}$ should be similar to that for the water exchange process. Correspondingly, the selectivity for L^{x-} is expected to decrease from the $\mathbf{I_A}$ to the $\mathbf{I_D}$ mechanism. These generalizations are subject to the L^{x-} selectivity range being substantially contracted for L^{x-} hard bases substituting on M^{m+} hard acids,[61,62] and L^{x-} selectivity ranges decreasing as the lability of M^{m+} increases to the point at which no selectivity is exhibited when water exchange approaches diffusion controlled rates where $k_{H_2O} \approx 3.6 \times 10^{11}\ s^{-1}$ and the frequency at which encounters between L^{x-} and $[M(H_2O)_n]^{m+}$ occur leads to very high substitution rates.[63] For each mechanism, microscopic reversibility requires that the same reaction coordinate should be traversed from left to right and vice versa so that the same mechanism operates in both directions.

There is growing acceptance that the truly extreme **A** or **D** situation strictly may never be relevant for ligand substitution/exchange reactions at metal centers in aqueous media because the leaving or entering ligand always remains associated to some extent with the assemblage of hydrogen-bonded water molecules in the second and, if relevant, primary coordination spheres, e.g., Figure 4, along the reaction coordinate to the transition state. Thus one might argue that the interchange **I**, $\mathbf{I_A}$, or $\mathbf{I_D}$ labels are the only ones that need to be considered for aqueous reactions as has been suggested by Swaddle[64] and Lay.[65] Swaddle[62,66] in particular has argued that adopting the Langford and Gray labels is highly restrictive since they introduce an interpretation based largely upon the chosen operational criteria, i.e., a classification based upon only one measurable property, i.e., a sensitivity or insensitivity to the nature of the entering ligand. It has been argued that for meaningful mechanistic interpretation a continuous range of phenomena is required that lies in a continuum in the strengths of interactions between central metal and active ligands as one goes along a series of reactions, without necessarily any clear break in behavior. Possible approaches to this are discussed below in section 3.3.2.3.

Clearly it is desirable to have additional criteria through which mechanisms may be assigned. The variation of the magnitude of $\Delta H^{\ddagger}$ and $\Delta S^{\ddagger}$, and the sign of the latter parameter within a series of similar ligand substitution systems can give a guide to mechanistic change. Thus, in similar systems, associatively-activated substitutions tend to have smaller $\Delta H^{\ddagger}$ magnitudes than do dissociatively activated substitutions, and $\Delta S^{\ddagger}$ tends to be negative and positive for associatively and dissociatively activated substitutions, respectively. Even so, it is often difficult to find a series of similar ligand substitutions from which mechanistic deductions may be made solely from $\Delta H^{\ddagger}$ and $\Delta S^{\ddagger}$, and the magnitudes of the contributions to them arising from interactions occurring beyond the first coordination-sphere can be uncertain. Fortunately, the volume of activation, $\Delta V^{\ddagger}$, has proven to be an additional powerful parameter through which water, other solvent exchange, and a range of ligand substitution mechanisms may be assigned and is largely replacing the use of $\Delta S^{\ddagger}$. However as will be seen at the end of the review consideration of the $\Delta S^{\ddagger}$ value alongside $\Delta V^{\ddagger}$ is fundamentally crucial for meaningful diagnosis.

3.3.2.2. Activation Volume, $\Delta V^{\ddagger}$. The activation volume is determined from the pressure dependence of the logarithm of the rate constant for the substitution reaction according to (25) and (26) where $\ln k_0$ is the value at zero pressure.

$$(\delta \ln k/\delta P)_T = -\Delta V^{\ddagger}/RT \quad (25)$$

$$\ln k_P = \ln k_0 - \Delta V^{\ddagger} P/RT + \Delta \beta^{\ddagger} P^2/2RT \quad (26)$$

It is normally expressed in units of $cm^3\ mol^{-1}$. $\Delta\beta^{\ddagger}$ measures the pressure dependence of $\Delta V^{\ddagger}$ itself, and for reactions in aqueous solution, it is more often than not very small and can be neglected. Thus, $\Delta V^{\ddagger}$ can often be evaluated directly from the slope of $\ln k$ vs P. $\Delta V^{\ddagger}$ is a small coefficient meaning that quite high pressures of several kbar (100 MPa) are required for an appreciable effect on the rate to be seen as diagnostic. However, the errors are relatively small (usually <3%) since unlike $\Delta S^{\ddagger}$, which is prone to the large experimental error in extrapolating rate data to infinite temperature, $\Delta V^{\ddagger}$ is determined from a slope. Equipment for spectrophotometric monitoring (even under rapid mixing conditions) and even probes for NMR measurement in solution under pressures of up to 2 kbar and beyond are now in routine use in a growing number of laboratories around the world.[25−30,67]

An associatively activated process is indicated when the application of pressure causes k_{obs} to increase such that $\Delta V^{\ddagger}$ is negative. On this basis, a contracted transition state involves a greater degree of bond making than breaking. Conversely a dissociatively activated process is indicated when the application of pressure causes a decrease in k_{obs} such that $\Delta V^{\ddagger}$ is positive and more expanded transition state is indicated with a greater degree of bond breaking than making.

Table 1. Experimental Volumes of Activation ($cm^3\ mol^{-1}$) Representing Water Exchange (k_{H_2O}) on Mononuclear Aqua Metal Ions

Be^{2+}										
−13.6										
Mg^{2+}										Al^{3+}
+6.7										+5.7
Ca^{2+}	Sc^{3+}	Ti^{3+}	V^{3+}	Cr^{3+}	Mn^{3+}	Fe^{3+}	Co^{3+}			Ga^{3+}
		−12.1	−8.9	−9.6	-	−5.4	-			+5.0
			V^{2+}	Cr^{2+}	Mn^{2+}	Fe^{2+}	Co^{2+}	Ni^{2+}	Cu^{2+}	Zn^{2+}
			−4.1	-	−5.4	+3.8	+6.1	+7.2	+2.0	+7?[c]
Sr^{2+}	Y^{3+}			Mo^{3+}		Ru^{3+}	Rh^{3+}			In^{3+}
-	-			−17?[b]		−8.3	−4.2			-
						Ru^{2+}		Pd^{2+}	Ag^{2+}	Cd^{2+}
						−0.1		−2.2	-	−6?[c]
Ba^{2+}	Ln^{3+}[a]						Ir^{3+}			Tl^{3+}
-	−6						−5.7			-
								Pt^{2+}		Hg^{2+}
								−4.6		-

[a] For the elements Tb^{3+} to Tm^{3+} [b] Based on the activation volume of −11.4 $cm^3\ mol^{-1}$ for the 1:1 complex formation reaction of $[Mo(_{H_2O})_6]^{3+}$ with NCS^-.[71] [c] Based on the activation volumes for 1:1 complexation with 2,2-bipyridine.[72]

Two components compose $\Delta V^{\ddagger}$.[27−29] The intrinsic component, $\Delta V^{\ddagger}_{int}$, arises from changes in the internuclear distances of the reactants during the formation of the transition state and the electrostriction component, $\Delta V^{\ddagger}_{elect}$, arises from changes in the electrostriction of solvent in the second coordination sphere and beyond as charge distribution changes when the transition state forms. When charged reactants are involved, $\Delta V^{\ddagger}_{elect}$, may dominate $\Delta V^{\ddagger}$ so that $\Delta V^{\ddagger}_{int}$, which contains most of the mechanistic information, cannot be readily determined. However, solvent exchange reactions such as water exchange on $[M(H_2O)_n]^{m+}$ involves negligible differences in electrostriction between the reactants and the transition state such that $\Delta V^{\ddagger}_{elect} \approx 0\ cm^3\ mol^{-1}$ and $\Delta V^{\ddagger} \approx \Delta V^{\ddagger}_{int}$. In these cases, the activation volume is particularly powerful and can provide a direct indicator of mechanism through comparison despite the absence of a full rate law and thus a rigorous kinetic treatment. This topic is reviewed separately in this volume and elsewhere.[28] A necessary presumption within this argument is that the volume change within the coordination sphere of the complex itself can be largely neglected allowing the sign of the activation volume to be directly diagnostic of the mechanistic type. This follows the assumption originally made by Stranks[68] that an associatively activated process will have a negative activation volume corresponding to the loss, from the initial state, of what will be the effective partial molar volume of the entering water ligand on forming the transition state. Conversely, a dissociatively activated process will involve the liberation, at the transition state, of the equivalent effective partial molar volume of the leaving group, Figure 7. This presumption has received backing from the calculation of bond length changes occurring on formation of the transition state in several cases.[69,70] For limiting **A** or **D** mechanisms, $\Delta V^{\ddagger}$ should relate directly to the full partial molar volume of the entering/leaving ligand electrostricted within the secondary hydration shell. Interchange $\mathbf{I_D}$ or $\mathbf{I_A}$ processes will have positive or negative $\Delta V^{\ddagger}$ values as required but of a magnitude somewhat less than that corresponding to the full partial molar volume of the electrostricted entering/leaving ligand.

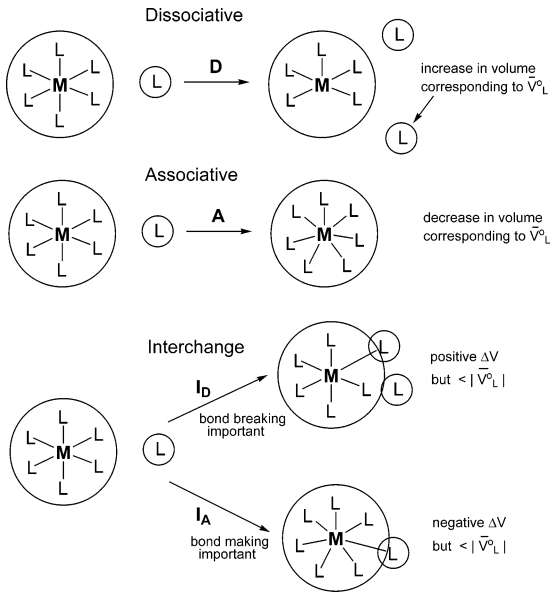

Figure 7. Volume changes accompanying ligand substitution reactions assuming a negligible change in volume of the first coordination sphere of the complex.

Activation volumes have now been measured for water exchange reactions on a wide range of simple mononuclear $M^{m+}(aq)$ ions[67] and some distinct trends have emerged as shown in Table 1.[28] For the first row, octahedral divalent and trivalent metal ions a trend is seen from negative values of $\Delta V^{\ddagger}$ for the early elements (Ti^{3+}, $V^{2+/3+}$, Cr^{3+}, and Fe^{3+}) to positive values for the later ones (Fe^{2+}, Co^{2+}, Ni^{2+}, and Ga^{3+}; see also section 3.4.4.1). Thus, for ions of the same charge, an increase in electron density and a decrease in size correlates with a trend toward more positive values of $\Delta V^{\ddagger}$. Merbach has argued[28,29,52a] that the trend reflects increasing dissociative character in the water exchange reactions, indeed perhaps evidence of a changeover from associative (probably $\mathbf{I_A}$; negative $\Delta V^{\ddagger}$ values) to dissociative (probably $\mathbf{I_D}$; positive $\Delta V^{\ddagger}$ values). Similarly a general trend to more associative **A** or $\mathbf{I_A}$ behavior (more negative $\Delta V^{\ddagger}$ values) seems apparent down a particular group, Table 1. Recent advances in quantum mechanical treatments are now offering a strong theoretical basis for the observed values of $\Delta V^{\ddagger}$ through computation of realistic transition state volumes.

Table 2. Kinetic Data for Ligand Substitution Reactions on Trivalent Hexaaqua Metal Ions at 25 °C

		$[Mo(H_2O)_6]^{3+}$	$[Ti(H_2O)_6]^{3+}$	$[Cr(H_2O)_6]^{3+}$	$[V(H_2O)_6]^{3+}$	$[Fe(H_2O)_6]^{3+}$
water exchange $\Delta V^{\ddagger}$/cm^3 mol^{-1}		−17?	−12.1	−9.6	−8.9	−5.4
incoming ligand	pK_a HL	$10^1 k_f$/M^{-1} s^{-1}	10^{-3} k_f/M^{-1} s^{-1}	10^7 k_f/M^{-1} s^{-1}	10^{-2} k_f/M^{-1} s^{-1}	10^{-1} k_f/M^{-1} s^{-1}
H_2O	−1.74	∼1?	8.6[a]	2.6[a]	0.54[a]	1.73[a]
Cl^-	−2	0.046		0.29	<0.03	0.71[b]
Br^-	−2			0.09	<0.1	0.16
I^-	−2			0.008		
NCS^- (N donor)	−1.84	3.2	8.0	18	1.1	9.5
$HC_2O_4^-$	1.23	4.9	390		1.3	
NO_3^-	−2			7.1		
SO_4^{2-}	1.92			110		
5-nitrosalicylic acid (HX)					0.035	
5-nitrosalicylate(1-)	2.24				12.3	
salicylic acid (HX)					0.049	
salicylate(1-)	2.97				14	
malonate(1-)	2.83		420		38	
methylmalonate(1-)	3.07		320			
4-aminosalicylate(1-)	3.6				70	
acetic acid (HX)			0.97			2.7
acetate(1-)	4.75		1800			
chloroacetic acid (HX)			0.67			
chloroacetate(1-)	2.85		210			1.5
dichloroacetate (1-)	1.48		110			0.12
trichloroacetate(1-)	0.70					0.063
O_2		1800				
$[Co(C_2O_4)_3]^{3-}$		3.4 (redox)				
4-isopropyltropolone (Hipt)						0.5

[a] Second-order rate constant for water exchange = 6 k_{H_2O}/55.56. [b] Average of two values.

For ions of a given charge Swaddle[73] has described an empirical method for calculating partial molar volumes of $[M(H_2O)_n]^{m+}$ ions using (27) where $V°_{abs}$ is the absolute volume relative to $V°_{abs}$ $(H^+) = -5.4$ cm^3 mol^{-1}, r_M is the ionic radius of the metal ion (pm),[43] and Δr is the apparent radius of a coordinated water molecule, determined empirically and 18.07 is the partial molar volume of water in cm^3 mol^{-1}.

$$V°_{abs} = 2.523 \times 10^{-6}(r_M + \Delta r)^3 - 18.07n - \frac{417.5z^2}{r_M + \Delta r} \quad (27)$$

The inclusion of the final term takes into account solvent electrostriction around the charged ion. This approach satisfactorily reproduced experimental partial molar volumes for a range of hydrated metal ions encompassing the first transition series, several $Ln^{3+}{}_{aq}$ ions and those from the s and p blocks. Using appropriately adjusted values of r_M and n, to account for the change in M−L distance with coordination number, Swaddle used (27) to estimate the limiting volume changes for the extreme **A** or **D** water exchange mechanisms. The limiting $\Delta V^{\ddagger}$ values, which are a function of both r_M and $m+$, were typically ∼13.5 cm^3 mol^{-1} for a typical first row M^{3+} ion and 13.1 cm^3 mol^{-1} for typical first row M^{2+} ion. In addition one could argue that as r_M decreases, i.e., toward the right along the first transition metal period, the packing of water around a metal ion could eventually approach the "close-packed" limit and as such a smaller limiting volume change for a limiting dissociatively activated process of ∼ +9 cm^3 mol^{-1} might apply. [It had been earlier noted that in the close packed structure of ice the octahedral interstitial sites were of a cavity size similar to the ionic radius of most first row M^{2+} ions (57 pm). Within such a close-packed structure, the effective radius of a water molecule is ∼9 cm^3 mol^{-1}. Thus, the volume change to the system on the expulsion of a water molecule from a close packing arrangement to that in the free state might be estimated as ∼18 − 9 = ∼9 cm^3 mol^{-1}.[73,74]] For the more expanded situation of an associatively activated process, a similar restriction may not apply and a limiting value of ∼ −13 cm^3 mol^{-1} may still be valid. From Table 1, it is seen that $\Delta V^{\ddagger}$ for water exchange on $[Ti(H_2O)_6]^{3+}$ (−12.1 cm^3 mol^{-1}) is indeed underestimated by the close-packed model and is close to the empirical limit of ∼ −13.5 cm^3 mol^{-1} calculated by (27). On the other hand $\Delta V^{\ddagger}$ for water exchange on $[Ni(H_2O)_6]^{2+}$ is +7.2 cm^3 mol^{-1}, significantly below the +13.1 cm^3 mol^{-1} limiting value but close to that predicted by the close packed model. Indeed +10.0 cm^3 mol^{-1} is the most positive recorded activation volume so far observed for a water exchange process on a transition metal aqua ion species in aqueous media[75] (see section 3.4.4.2). One concludes therefore from the $\Delta V^{\ddagger}$ data that water exchange on $[Ti(H_2O)_6]^{3+}$ is associatively activated, possibly $\mathbf{I_A}$ approaching the **A** limit, whereas that on $[Ni(H_2O)_6]^{2+}$ is dissociatively activated, possibly $\mathbf{I_D}$ on the verge of **D**. The available kinetic data for substitution reactions on these and other ions back up the conclusions from the water exchange activation volume. For example, substitution reactions on $[Ti(H_2O)_6]^{3+}$ cover a wide range of rates for different entering L ligands and moreover correlate with a widely used parameter for measuring incoming ligand nucleophilicity namely the pK_a of HL[18], Table 2. Moreover these rate variations are more than can be accounted for by changes in K_{os} and so the mechanism is clearly strongly associative. Indeed

Table 3. Ratio of Rate Constants for NCS^- Complexation Relative to Cl^- and Activation Volumes for Water Exchange on $[ML_5(H_2O)]^{z+}$ Ions[77]

$[ML_5(H_2O)]^{z+}$	R^a	$\Delta V^{\ddagger}_{H_2O}$/cm^3 mol^{-1}
$[Mo(H_2O)_6]^{3+}$	62	not available
$[V(H_2O)_6]^{3+}$	≥36	−8.9
$[Cr(H_2O)_6]^{3+}$	55	−9.6
$[Co(H_2O)_6]^{3+}$	≥43	not available
$[Fe(H_2O)_6]^{3+}$	14	−5.4
$[Cr(NH_3)_5(H_2O)]^{3+}$	6	−5.8
$[Co(H_2O)_5OH]^{2+}$	2	not available
$[Cr(H_2O)_5OH]^{2+}$	1	+2.7
$[Rh(NH_3)_5(H_2O)]^{3+}$	0.6	−4.1
$[Fe(H_2O)_5OH]^{2+}$	0.6	+7.0
$[Co(NH_3)_5(H_2O)]^{3+}$	0.5	+1.2
others		
$[Mo_3S_4(H_2O)_9]^{4+}$	1.2	not available
$[Mo_3S_4(H_2O)_8OH]^{3+}$	1.4	not available

[a] Ratio of second-order rate constants, M^{-1} s^{-1}, at 25 °C.

some stable seven coordinated Ti^{III} complexes are known such as $[Ti(C_2O_4)_3(H_2O)]^{3-}$.[76] A similar correlation is apparent for the d^2 ion $[V(H_2O)_6]^{3+}$ but the situation is less clear in other examples in Table 2 despite the presence of highly negative water exchange activation volumes. Table 2 would be assisted by further examples. Nonetheless, in the case of $[Fe(H_2O)_6]^{3+}$, the lessening degree of selectivity appears to reflect the less negative activation volume and more interchange ($\mathbf{I_A}$) character.

The Langford and Gray labels continue to be widely employed and will be referred to frequently in this review in discussing specific examples. However a number of alternatives to their use for mechanistic classification have been suggested and some of these are discussed below.

3.3.2.3. Metal Center Selectivity Scales. As an alternative to the rigid Langford and Gray classifications, there have been a number of attempts to come up with a measure of the selectivity of a metal ion center (the substrate) for a range of different entering group nucleophiles. These would seek to measure the relative importance of bond making with the entering group along the reaction coordinate to the transition state. In 1975 Sasaki and Sykes[77] proposed a scale based upon the ratio of rate constants (R) for complexation with the ligands NCS^- and Cl^-, these two chosen largely because of available rate data for a wide range of metal ions (e.g., in Table 2 above) and because they are viewed as being sufficiently different in their nucleophilicity so as to give a meaningful measure of an entering group selectivity. It was concluded that associatively activated reactions would be indicated if $R \geq 10$, whereas dissociatively activated reactions would be indicated by values around unity. Some of the data is compiled in Table 3. Values well in excess of 10 are seen for Mo^{3+}, V^{3+}, Cr^{3+}, and Fe^{3+} which are in keeping with the conclusion of associatively activated reactions on these metal ions whereas hydroxo aqua complexes and the aquapentammine complexes of Rh^{III} and Co^{III} fall as expected into the dissociative category. $[Cr(NH_3)_5(H_2O)]^{3+}$ appears to be somewhat borderline. The behavior of $[Co(H_2O)_6]^{3+}$ is however somewhat exceptional and not in keeping with the general behavior of low spin t_{2g}^6 metal ions. $[Co(H_2O)_5OH]^{2+}$, on the other hand, duly falls into the dissociative category as expected. The absence (thus far) of measurable activation volumes for water exchange on $[Mo(H_2O)_6]^{3+}$ [71] and on both $[Co(H_2O)_6]^{3+}$ and $[Co(H_2O)_5OH]^{2+}$ is a pity. Critics of this approach argue the deficiency of a mechanistic prediction based upon the relative affinities for only these two somewhat comparable ligands. Nonetheless the values in Table 3 are in keeping with conclusions reached elsewhere.

Table 4. Selectivity Parameter S, Relative to $[Cr(H_2O)_6]^{3+}$, for the Reaction of Some Cationic Substrates with Mononegative Anions in Aqueous Solution[63,64] [a]

substrate	S^b
$[Mo(H_2O)_6]^{3+}$	1.1[c]
$[Cr(H_2O)_6]^{3+}$	1.0
$[Fe(H_2O)_6]^{3+}$	0.7
$[Cr(H_2O)_5OH]^{2+}$	0.4
$[Cr(NH_3)_5(H_2O)]^{3+}$	0.3
$[Fe(H_2O)_5OH]^{2+}$	0.1
$[Co(NH_3)_5(H_2O)]^{3+}$	−0.1

[a] Source: refs 50, 63, 77, and 79. [b] ±0.1, rate constants have dimensions M^{-1} s^{-1}. [c] Only two data points.

Swaddle[63,64] has proposed a selectivity scale based upon parameter S (28) which relates the behavior of different metal ions toward a much wider range of ligands. S measures the selectivity of a substrate A (a metal ion complex) relative to another B.

$$S = (\mathrm{d} \ln k^{\mathrm{A}})/(\mathrm{d} \ln k^{\mathrm{B}}) \qquad (28)$$

"d ln k" represents the change in ln(rate constant) as the incoming ligand (of similar charge) is varied. Since S is a relative quantity, it was decided that a suitable reference compound B might be $[Cr(H_2O)_6]^{3+}$, Table 4. The reason not more metal ions appear in this table is due to a lack of kinetic data on a wide enough range of mononegative ligands. The choice of mononegative nucleophiles is moreover limited to those with negligible Bronsted basicity because of the "proton ambiguity" problem.[18,78] This arises because reaction of $[M(H_2O)_6]^{3+}$ with L cannot be separated, by kinetic evaluation, from reaction of $[M(H_2O)_5OH]^{2+}$with HL because of rapid proton transfer. The result is the product of constants for the two reactant pair reactions that cannot be separated unless some assumptions are made. Furthermore, for meaningful comparisons, rate constants in (25) and (26) should be first order k_I's to allow for any reactant-pair preassociation. Here lies an additional problem. Accurate and reliable resolution of k_{obs} values into k_I and K_{os} is only rarely possible for aqueous reactions and calculated K_{os} values as mentioned above are prone to uncertainty since they are based on "hard sphere" models.[58] However, provided one confines the comparison to ions of similar charge type, second order k's can be used as in the comparison in Table 3.

What Tables 2−4 show is that it is unhelpful often to draw a line rigidly defining the substrates as having associative or dissociative tendency but to picture them along a continuous scale of relative affinities. Only at the extreme ends can one talk confidently of an associative or dissociative mecha-

nism as being important based solely on the properties of the metal center. One goal of future research should be to expand the list of substrates in Tables 2−4 to include as many examples as possible. Here perhaps lies the definitive scale of comparison for different metal aqua complexes.

3.3.2.4. Ligand Nucleophilicity Scales. A degree of confidence would arise from an independent measuring scale for incoming ligand nucleophilicity on a metal ion center. One measure of L^{x-} nucleophilicity is its relative affinity for the simplest of all cations namely the proton H^+ as measured by the Bronsted basicity or simply the pK_a of H_xL.[18] Thus, it is seen that a correlation of rate exists with pK_a of H_xL for substitution on $[Ti(H_2O)_6]^{3+}$ (associative) but not on $[Ni(H_2O)_6]^{2+}$ (dissociative). Other factors affecting nucleophilicity are oxidizability (a more easily oxidizable ligand being more willing to give up its electrons as measured by the standard reduction potential), polarizability, and solvation energy (a more highly solvated ligand will be a poorer nucleophile and will require solvation changes to accompany metal complex formation).

3.3.2.5. Hard and Soft Acids and Bases. This idea of separating metal ions into hard (a) and soft (b) categories was first put forward by Chatt and Ahrland in 1958[80] and 10 years later Pearson expanded the idea to a discussion of hard and soft acids (M^{m+}) and bases (L^{x-}).[8] The basic principal was that the strongest interaction, which could be measurable by a rate of complex formation or the magnitude of a stability constant, section 1.4.1, would be found for a hard acid with a hard base and likewise for a soft−soft matching pair. This theory remains attractive as one of the few to treat metal centers and ligands largely as independent reacting entities without the necessity to define the type of interaction. One of the problems with the hard−soft acid−base theory is that it is largely qualitative. With this in mind, Pearson has since attempted to establish a quantitative scale of "hardness" and "softness" based on ionization potentials (I) and electron affinities (A).[7,61] The absolute hardness is defined as $h = (I - A)/2$ and softness $s = 1/n$. Table 5 lists Pearson's estimates for absolute hardness along with the absolute electronegativity using Mulliken's scale ($c = (I + A)/2$). The strength of the Lewis-acid−Lewis-base interaction were assumed to be related to the fractional electron transfer given by $\Delta N = (c_1 - c_2)/2(h_1 + h_2)$.

A number of other scales have been proposed but few have received universal acceptance by inorganic chemists. It seems there is no alternative but to treat each inorganic center individually.

Table 5. Pearson's Quantification of Absolute "Hardness"[7,61]

acid	h	c	base	h	c
Ca^{2+}	19.52	31.39	H_2O	9.5	3.1
Fe^{3+}	12.08	42.73	NH_3	8.2	2.6
Zn^{2+}	10.88	28.84	Me_2O	8.0	2.0
Ru^{3+}	10.7	39.2	CH_3CN	7.5	4.7
Cr^{3+}	9.1	40.0	F^-	7.01	10.41
Mn^{2+}	9.02	24.66	Me_3N	6.3	1.5
Co^{3+}	8.9	42.4	Me_3P	5.9	2.8
Co^{2+}	8.22	25.28	Me_2NCHO	5.8	3.4
Pt^{2+}	8.0	27.2	OH^-	5.67	7.5
Os^{3+}	7.5	35.2	pyridine	5.0	4.4
Fe^{2+}	7.24	23.42	Cl^-	4.7	8.31
Cr^{2+}	7.23	23.73	Br^-	4.24	7.6
Pd^{2+}	6.75	26.18	I^-	3.7	6.76

general categorization as previously quoted in text books	
hard acids:	H^+, Li^+, Mg^{2+}, Cr^{3+}, Co^{3+}, Fe^{3+}
soft acids	Cu^+, Ag^+, Pd^{2+}, Pt^{2+}, Hg^{2+}, Tl^{3+}
borderline:	Mn^{2+}, Fe^{2+}, Zn^{2+}, Pb^{2+}
hard bases:	F^-, Cl^-, H_2O, NH_3, OH^-, $CH_3CO_2^-$
soft bases:	I^-, CO, PPh_3, C_2H_4, RSH
borderline:	N_3^-, pyridine, NO_2^-, Br^-, SO_3^{2-}

3.4. Survey of Coordination Numbers

3.4.1. Coordination Number 4 (Tetrahedral)

3.4.1.1. Beryllium(II). The most extensively studied tetrahedral center outside carbon and silicon is the small group 2 metal ion Be^{2+}. The earliest estimate of the water ligand replacement rate on $[Be(H_2O)_4]^{2+}$ was obtained from ultrasound absorption monitoring of complexation by SO_4^{2-}.[81] The water ligand residence time at 25 °C was estimated to be around 2−10 ms thus well within the range of monitoring by normal linebroadening NMR methods. At the time of the early measurements the $[Be(H_2O)_4]^{2+}$ exchange process attracted much interest as the first example of a measured proton exchange ($k_H = 8.0 \times 10^4$ s^{-1}, determined using ^{1}H NMR[82]), which was faster than water exchange (determined using ^{17}O NMR[83,84]). The variable pressure ^{17}O NMR water exchange study by Merbach et al.[84] is probably the most reliable. The $\Delta V^{\ddagger}$ of −13.6 cm^3 mol^{-1} is the most negative value so far obtained for a water exchange process on an aqua metal ion and thus it is concluded that water exchange on $[Be(H_2O)_4]^{2+}$, because of the hydration number of four and small size of water, may offer a rare definitive example of the limiting **A** process. Indeed using Swaddle's empirical approach (19), the expected limiting $\Delta V^{\ddagger}$ value assuming the **A** process has been calculated from the difference between the partial molar volume for the aqua ion of increased coordination number and that of the aqua ion $[Be(H_2O)_4]^{2+}$ in its initial state. Using Shannon's values[43] for the radii of Be^{2+} (45 pm for five coordination) and H_2O (238.7 pm) the limiting $\Delta V^{\ddagger}$ value for an **A** process on Be^{2+} is calculated as −12.9 cm^3 mol^{-1}.[73a] The agreement between experiment and calculation is gratifying especially since no detectable 5-coordinated intermediate has been found to support the **A** assignment. Further support for the associative nature of the reaction comes from the negative $\Delta V^{\ddagger}$ and $\Delta S^{\ddagger}$ values and small $\Delta H^{\ddagger}$ value from kinetic data for the 1:1 complex forming reaction with 4-isopropyltropolone (Hipt), Table 6.[87] Likewise kinetic data for the reaction of $[Be(H_2O)_4]^{2+}$ with F^-/HF support associative activation with a second-order rate constant faster than the equivalent value for water exchange.[86] A scarcity of complex formation kinetic data on Be^{2+} limits further confirmation of a strong entering ligand dependence and further studies are needed given the lack of data generally on tetrahedral species.

Table 6. Water Exchange and Complex Formation Kinetic Data for $[Be(H_2O)_4]^{2+}$ at 25 °C[a]

incoming ligand	k_f,[a] M^{-1} s^{-1}	$\Delta H_f^{\ddagger}$, kJ mol^{-1}	$\Delta S_f^{\ddagger}$, J K^{-1} mol^{-1}	$\Delta V_f^{\ddagger}$, cm^3 mol^{-1}
H_2O [84]	52.77[c]	59.2 ± 1.5	+8.4 ± 4.5	−13.6 ± 0.5
HF [86]	73.0			
F^- [86]	720			
Hipt [87]	58.1 ± 0.5	38.1 ± 0.4	-83.5 ± 1.3	−7.1 ± 0.2
	k_b,[b] M^{-1} s^{-1}	$\Delta H^{\ddagger}$,[c] kJ mol^{-1}	$\Delta S^{\ddagger}$,[c] J K^{-1} mol^{-1}	$\Delta V^{\ddagger}$,[c] cm^3 mol^{-1}
Hipt [87]	49.8 ± 0.5	35.7 ± 0.4	−92.7 ± 1.2	−12.4 ± 0.2

[a] Hipt, 4-isopropyltropolone. [b] k_f and k_b are the forward and reverse second-order rate constants, respectively. [c] Second-order rate constant for water exchange evaluated as 4 k_{H_2O}/55.56.

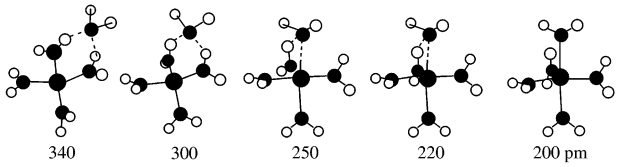

Figure 8. Formation of the trigonal bipyramidal pentahydrated transition state from approach of a second shell water molecule as a function of Be−O distance (pm) to the incoming water.[88]

A number of theoretical studies have probed the associative mechanism further. Winter et al.[88] have used Hartree−Fock level ab initio calculations to compute optimum geometries for $[Be(H_2O)_4]^{2+}$ and $[Be(H_2O)_5]^{2+}$ in an attempt to model the activation parameters $\Delta H^{\ddagger}$ and $\Delta V^{\ddagger}$ for the A process. The intermediate structures, Figure 8, were determined by optimizing all degrees of freedom for the pentahydrated complex except the Be−O distance for the incoming water molecule. The final geometry was constrained to trigonal bipyramidal with both axial bonds equal (Be−O = 200 pm) while optimizing all other degrees of freedom. With only one water molecule within the secondary shell, they reproduced the experimental $\Delta H^{\ddagger}$ value very closely (calculated value 62.6 kJ mol^{-1}). However, the calculated $\Delta V^{\ddagger}$ was ∼0 cm^3 mol^{-1}. This discrepancy was assigned to the effects of the restricted secondary shell which was viewed as unable to confine the leaving water. Including a continuum model for the solvent however was not found to improve the agreement. Bock and Glusker[89] have used ab initio methods to look at a range of $Be^{2+}\cdot H_2O$ clusters and showed that the next most favorable energy situation for Be^{2+}(aq) was not a water cluster with primary hydration number >4 but the 3(+3) cluster, "$Be(H_2O)_3^{2+}\cdot 3H_2O$", which interestingly models the dissociative situation. With this in mind, and since size and electrostriction are key factors for Be^{2+}, it was no surprise to find for more sterically demanding $[BeL_4]^{2+}$ complexes, e.g., with L = trimethyl phosphate, a solvent exchange process independent of the solvent concentration[90] and for L = tetramethylurea a $\Delta V^{\ddagger}$ value of +10.0 cm^3 mol^{-1} [84] implying an activation process now dominated by resident ligand bond breaking. As one increases the steric bulk of the entering ligand, it is not inconceivable therefore that a point will be reached when the only activation process open to $[BeL_4]^{2+}$ is one largely dissociative in character. Indeed a number of three coordinated Be^{2+} compounds are known such as BeF_3^- and Be{O(2,4,6-$Bu^t_3C_6H_2$)}$_2$(OEt_2) even if they are somewhat special cases.[91] Thus, although the water exchange process itself appears close to what we might term the "associative limit", it is clear that the properties of both entering and leaving ligand play a dominant role in defining the mechanisms governing ligand replacement reactions at small, highly electrostricted, metal ions such as Be^{2+}. This is no surprise given the well-established S_N1 and S_N2 mechanisms on tetrahedral carbon in which either trigonal carbocation intermediates (S_N1) or five coordinated transition states (S_N2) are well established and indeed probably occur in parallel.

3.4.1.2. Silver(I). EXAFS studies of Ag^+(aq) in nitrate aqueous solutions up to 9 M show evidence of coordination of one nitrate ion in the tetrahedral coordination sphere. Similar coordination of one ClO_4^- was also found but only at the highest anion concentrations ∼9.0 M. Complexation reactions on $[Ag(OH_2)_4]^+$ are fast with typical rate constants ∼10^6 M^{-1} s^{-1}.[92]

3.4.1.3. Silicon(IV). Substitution reactions on tetrahedral silicon are more associative than those on carbon due to the larger size and availability of low lying 3d orbitals. Intermediates akin to carbocations for Si such as R_3Si^+ have not been found.[93] The stereochemistry of the product, retention, or inversion largely depends on the nature of the entering or leaving group as for S_N2 reactions on carbon. Soft nucleophiles tend to attack apically in relation to the tbp intermediate species (29) to give inversion products whereas hard ones attack equatorially to give retention. The presence of good leaving groups X

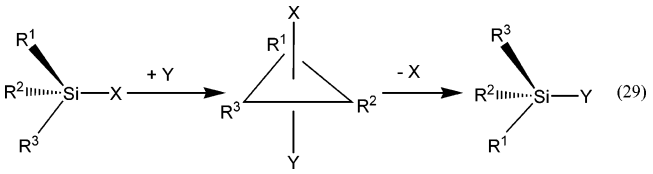

(29)

however invariably give inversion products. The product observed also depends on the solvent with strongly coordinating ones such as DMF or DMSO often attacking first to form 5-coordinated species which is then displaced by the incoming nucleophile. In all cases the product formed ultimately depends on the position at which the nucleophile attacks either remote from, or adjacent to, the leaving group.

3.4.1.4. Phosphorus(V). Tetrahedral phosphorus exhibits every kind of substitution mechanism from **D** through to **I** to **A** depending upon the nature of the entering and leaving group although the dominant mechanism is associative. As with Si, strongly electronegative entering groups such as OH^- in the hydrolysis of chlorophosphinoxides lead invariably to the inversion phosphinic acid product via apical attack in a S_N2 type process (30). In other cases, the

Table 7. Kinetic Parameters for Cyanide Exchange on $[M(CN)_4]^{2-}$ Complexes at 25 °C[94,95]

complex	k_{CN-},[a] M^{-1} s^{-1}	$\Delta H^{\ddagger}$, kJ mol^{-1}	$\Delta S^{\ddagger}$, J K^{-1} mol^{-1}	$\Delta V^{\ddagger}$, cm^3 mol^{-1}
$[Ni(CN)_4]^{2-}$ [b,c]	2.3×10^6	21.6	−51	−19
$[Pd(CN)_4]^{2-}$ [c]	82	23.5	−129	−22
$[Pt(CN)_4]^{2-}$	11	25.1	−142	−27
$[Au(CN)_4]^{-}$	6.2×10^3	40	−38	+2

[a] For the second-order pathway for reaction with CN^-. [b] For formation of $[Ni(CN)_5]^{3-}$. [c] More complex behavior, involving protonated (HCN) species, is seen at lower pH's.

sterochemistry is retained suggesting equatorial attack.

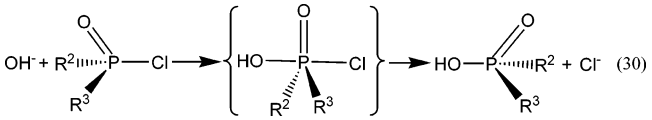

3.4.2. Coordination Number 4 (Square-Planar)

There have been many excellent reviews of ligand substitution reactions at square-planar centers,[59] and the mechanisms involved are reasonably well understood. Square-planar four coordination occurs most commonly for d^8 transition metals, commonly observed for Pd^{II}, Pt^{II}, Au^{III}, Ni^{II} (occasionally), Rh^{I}, and Ir^{I} (in organometallic derivatives) as a consequence of favorable ligand field effect. The antitumor activity of cis-platin (*cis*-$Pt(NH_3)_2Cl_2$) and second generation analogues has stimulated much of the research over the past 30 or so years. A comparison between four of the elements is possible in the case of high field tetracyano complexes $[M(CN)_4]^{n-}$, Table 7.[94,95] In particular the extreme lability of $[Ni(CN)_4]^{2-}$ contrasts with its high thermodynamic stability ($\log \beta_4 = 22$), a classic text book example of lability and instability being not necessarily connected. Given four coordination, it is not surprising to find that the substitution mechanism is predominantly associative in nature[59] with the nature of the entering ligand frequently exhibiting a significant effect on the rate although other factors have influence. However, it is not exclusively so (see later). Ligand substitution usually occurs with stereoretention and the lability of the leaving ligand, X, is strongly affected by the ligand trans to it. This is consistent with an **A** or an $\mathbf{I_A}$ mechanism occurring through a trigonal bipyramidal transition state or reactive intermediate where the trans directing ligand and the entering and leaving ligands share the equatorial plane (see later). Reactions of the general type (31):

$$ML_3X + Y \rightarrow ML_3Y + X \qquad (31)$$

wherein Y replaces the one ligand X commonly obey the well-established two term rate law (32):

$$-d[ML_3X]/dt = (k_S + k_Y [Y])\,[ML_3X] \qquad (32)$$

where k_S represents a solvation path if the solvent has coordinating properties and k_Y is the path directly dependent upon Y. The effect of solvent is nicely illustrated in the classic 1968 text book example of Odell et al.[96] of the reaction of $NHEt_2$ with

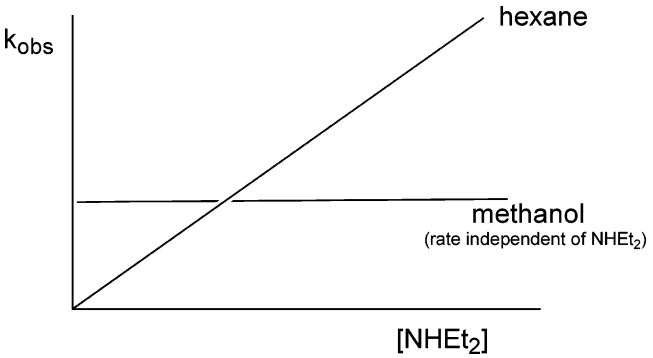

Figure 9. Dependence of k_{obs} on $[NHEt_2]$ for the reaction of *trans*-$[Pt(PPr^i_3)(NHEt_2)Cl_2]$ with $NHEt_2$ in hexane and methanol.[96]

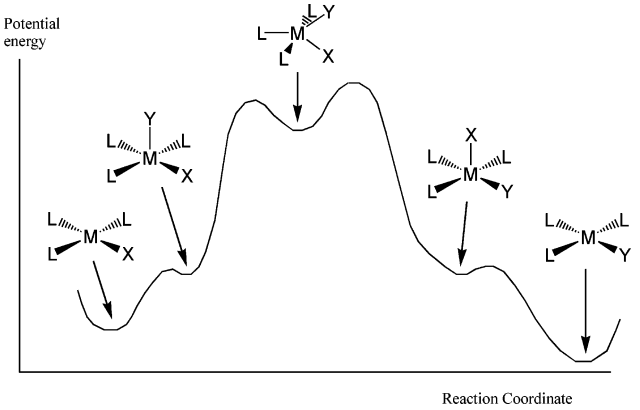

Figure 10. Potential energy profile for a typical square-planar substitution reaction.

trans-$[Pt(NHEt_2)(PPr^i_3)Cl_2]$ in hexane and methanol, Figure 9. In hexane, the Y dependent path, k_Y, dominates. In methanol, the solvent path k_S dominates, now an effective competing nucleophile and, more importantly, in vast excess. Since the solvation path, when dominant, comprises the slow step, this implies in the example shown that the methanol solvated complex (one Cl^- replaced) is more reactive than its chloro counterpart. Five-coordinate complexes of Pt^{2+} and other d^8 metal ions have stereochemistries approximating to both a trigonal bipyramid and a square pyramid, and the energy differences between the two stereochemistries is small.[2b,59] Accordingly, it is thought that stereoretentive associatively activated ligand substitution on square-planar complexes, such as $[ML_3X]$, occurs through a series of five-coordinate transition states and reactive intermediates for substitution by Y as shown schematically in the potential energy profile shown in Figure 10 with participation from both square-pyramidal and trigonal bipyramidal species. These species are assumed to be able to distinguish between different nucleophiles in solution. Involvement of the trigonal bipyramidal intermediates is required for ligand interchange to occur and is important in the explanation of well-known strong trans effects resulting from certain resident ligands L.

In the solvent-assisted pathway, k_S, a similar set of reactions 33 and 34 as in Figure 10 results in the solvent S initially displacing X and then replaced

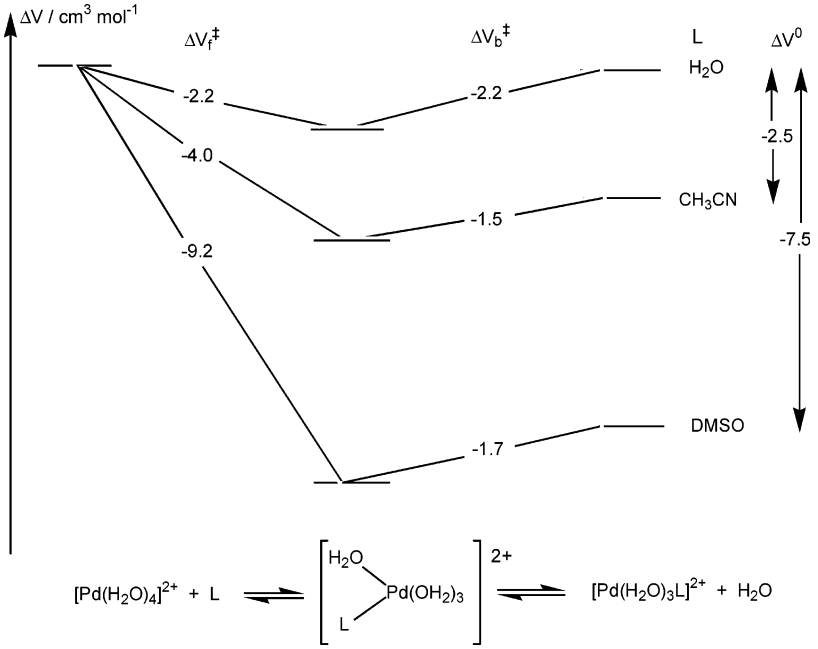

Figure 11. Volume profile for the reversible formation and aquation of $[Pd(H_2O)_3L]^{2+}$ from $[Pd(OH_2)_4]^{2+}$.

Table 8. Kinetic Parameters for Water Exchange on $[Pd(H_2O)_4]^{2+}$ and $[Pt(H_2O)_4]^{2+}$ at 25 °C[97–99]

complex	k_{H_2O}[a]/ s^{-1}	$\Delta H^{\ddagger}$/ kJ mol^{-1}	$\Delta S^{\ddagger}$/ J K^{-1} mol^{-1}	$\Delta V^{\ddagger}$/ cm^3 mol^{-1}
$[Pd(H_2O)_4]^{2+}$	5.6×10^2	49.5 ± 1.9	-26 ± 6	-2.2 ± 0.2
$[Pt(H_2O)_4]^{2+}$	3.9×10^{-4}	89.7 ± 2.4	-9 ± 8	-4.6 ± 0.2

[a] Studied by ^{17}O NMR.[98]

Table 9. Rate Constants for 1:1 Complex Forming Reactions on $[Pd(H_2O)_4]^{2+}$ and $[Pt(H_2O)_4]^{2+}$ [97–107]

incoming ligand	k_{Pd}/ M^{-1} s^{-1}	k_{Pt}/ M^{-1} s^{-1}	k_{Pd}/k_{Pt}	ref
H_2O	40.3 [a]	2.8×10^{-5} [a]	1.5×10^6	97,98
Cl^-	1.8×10^4	2.66×10^{-2}	6.8×10^5	100,101
Br^-	9.2×10^4	2.11×10^{-1}	4.4×10^5	100,101
I^-	1.14×10^6	7.7	1.4×10^5	102
SCN^-	4.4×10^5	1.33	3.3×10^5	101,103
$(CH_3)_2SO$	2.45	8.4×10^{-5}	2.9×10^4	104,105
CH_3CN	3.09×10^2			106
Me_2S	1.51×10^5	3.6	4.2×10^4	107
$(NH_2)_2CS$	9.6×10^5	13.9	6.9×10^4	103

[a] Rate constant converted to second-order units ($4\,k_{H_2O}/55.56$).

itself rapidly by Y in another set of reactions as in Figure 10.

$$ML_3X + S \xrightarrow{\text{slow}} ML_3S + X \quad (33)$$

$$ML_3S + Y \xrightarrow{\text{fast}} ML_3Y + S \quad (34)$$

3.4.2.1. Palladium(II) and Platinum(II). The associative nature of the complex forming reactions on these square-planar centers is reflected in negative activation volumes for both water exchange and substitution on the respective tetraaqua species (35), Tables 8 and 9 and a strong dependence on the nature of the entering ligand.

$$[M(H_2O)_4]^{2+} + Y^{x-} \underset{k_b}{\overset{k_f}{\rightleftharpoons}} [M(H_2O)_3Y]^{(2-x)+} + H_2O\ (M^{2+} = Pd^{2+}\ \text{or}\ Pt^{2+}) \quad (35)$$

Here the ligand substitution rate constant, k_f, for $[Pd(H_2O)_4]^{2+}$ and $[Pt(H_2O)_4]^{2+}$ varies from 1.8×10^4 to 1.14×10^6 dm^3 mol^{-1} s^{-1} for $Y^{x-} = Cl^-$ and I^- when $M^{2+} = Pd^{2+}$ and from 2.66×10^{-2} to 7.7 dm^3 mol^{-1} s^{-1} when $M^{2+} = Pt^{2+}$. Large variations in k_f are also seen for other substituting ligands, which is evidence for the operation of an associatively activated mechanism.[2a,102] In each case k_f for the Cl^- and I^- is greater than k_f for water exchange ($k_f = 4k_{H_2O}/55.5 = 40.3$ and 2.8×10^{-5} dm^3 mol^{-1} s^{-1} respectively for $[Pd(H_2O)_4]^{2+}$ and $[Pt(H_2O)_4]^{2+}$).

Rates for substitution on $[Pt(H_2O)_4]^{2+}$ are significantly lower (factor of 10^6) than those on $[Pd(H_2O)_4]^{2+}$ reflecting an ~18 kJ mol^{-1} larger $\Delta H^{\ddagger}$ typically for Pt^{2+}. The slower rates of ligand exchange are key to the antitumor activity of Pt^{II} complexes, e.g., *cis*-$[PtCl_2(NH_3)_2]$ since they allow the cytoactive compound to arrive in the cell intact leading to effective binding to the cellular DNA rather than to extracellular binding sites such as sulfur. The largest rates are found for incoming soft ligands with the ratio k_{Pd}/k_{Pt} increasing with increasing hardness showing that Pt^{2+} is more sensitive than Pd^{2+} to the nature of the entering ligand reflective of its softer nature.[2a] These trends also reflect higher covalence in the Pt−L bonds. Both exchanges are characterized by small negative $\Delta V^{\ddagger}$ values consistent with associative mechanisms operating.[72b,97] The relatively small values of $\Delta V^{\ddagger}$ are however a long way from the associative limit. This has been interpreted in two ways. First consider the following observations on the $[M(H_2O)_4]^{2+}$ ions. When $M^{2+} = Pd^{2+}$ and $Y^{x-} = H_2O$, CH_3CN, and DMSO, $\Delta V_f^{\ddagger} = -2.2$, -4.0, and -9.2 cm^3 mol^{-1}, respectively, and $\Delta V_b^{\ddagger} = -2.2$, -1.5, and -1.7 cm^3 mol^{-1}.[104,106] These values are illustrated in the volume profile shown in Figure 11.[2a] A contraction occurs on formation of the transition state ($\Delta V_f^{\ddagger}$) as DMSO substitutes for H_2O, a smaller one as CH_3CN substitutes, and a yet smaller one as water substitutes. A contraction also occurs for the reverse

reaction but here the three negative $\Delta V_b^{\ddagger}$ values are identical within experimental error consistent with the volume difference between the transition state and the reactants being independent of the leaving ligand when the entering ligand is water. Release of either DMSO or CH_3CN into bulk solution would be expected to produce a large expansion. This suggests that each of these ligands remain tightly bound to the Pd^{2+} center in the T−S and it follows that an extreme **A** mechanism probably operates despite the small $\Delta V_b^{\ddagger}$ values. Similar findings are apparent with regard to the same reaction on Pt^{2+}. Thus, with square-planar complexes in aqueous solution, it is probable that a very weakly interacting water lies close to the metal ion center on either side of the square plane and that the volume change occurring on formation of the five-coordinate transition state is minimized as a consequence. Second a significant degree of bond lengthening of the M−L bonds within the tbp transition state could lead to an increase in the volume somewhat offsetting the decrease resulting from the take up of the entering ligand.[97,98] In the case of aqua complexes, this could conceivably result from increased π-bonding to water (trigonal bound O) or from a significantly large contribution from $\Delta V_{solv}^{\ddagger}$.

Much larger negative activation volumes result from other reactions wherein M−L bond expansion is less likely. For example solvolysis of $[PtCl_4]^-$ and $[Pt(NH_3)Cl_3]^-$ in water is characterized by activation volumes of -17 cm^3 mol^{-1} and -14 cm^3 mol^{-1} respectively. Similarly replacement of Cl^- by Br^- on *trans*-$[Pt(PEt_3)_2Cl_2]$ in methanol or methanol water have substantially negative activation volumes of -28 and -27 cm^3 mol^{-1} respectively for the k_S and k_Y pathways.

3.4.2.1.1. Entering Group and the n°_{Pt} Scale. Extensive studies have been carried out particularly on Pt^{II} complexes partly because of conveniently slow rates and because it better distinguishes nucleophiles and partly because of the importance of *cis*-platin and its analogues in treating cancer. This has led to the defining of an effective nucleophilicity scale for various incoming ligands, termed n_{Pt}°. This is defined according to $\log(k_Y/k_S)$. All other things being equal, it was found that the order of nucleophilicity is (i) $I^- > Br^- > Cl^- \gg F^-$, (ii) phosphines > arsines > stibines ≫ amines, and (iii) S-donors > O-donors. It is important to note that this order does not correlate with other commonly used indicators such as basicity and redox potential. The best nucleophiles are highly polarizable and soft ($I^- > Br^-$; S > O, etc.). This has been rationalized in terms of soft ligands such as I^-, with S-donors being best able to cope with the e^- density present already in the z direction from the filled M nd_{z^2} orbital as they bind to the low lying M $n + 1p_z$ orbital to form the initial square-pyramidal species, Figure 12.

3.4.2.1.2. Leaving Group Effect. Extensive studies of substitution reactions on $[Pt(dien)X]^{n+}$ **1** (replacement of X) have led to the following generally accepted order of ease of displacement: $H_2O \gg Cl^- > Br^- > I^- > N_3^- > SCN^- > NO_2^- > CN^-$. Here the strength of M−X appears to directly correlate with

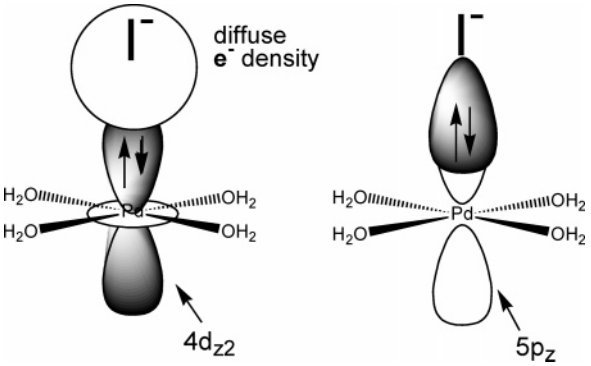

Figure 12. Interaction of the soft, polarizable I^- ion along the z direction of square planar $[Pd(H_2O)_4]^{2+}$.

the rate of displacement. The relatively small $\Delta H^{\ddagger}$ (36−80 kJ mol^{-1}) and significantly negative $\Delta S^{\ddagger}$ (−50 to −130 J K^{-1} mol^{-1}) and negative $\Delta V^{\ddagger}$ values characteristic of these reactions is further evidence of the associative nature of the mechanism.

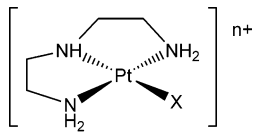

1

3.4.2.1.3. trans Directing Effect. The trans effect is well established in substitution reactions on square-planar complexes and can defined as "the effect of a resident ligand upon the rate of substitution of a ligand trans to it". Although this effect (and related cis effect) is seen in relation to substitution reactions on some higher coordination number species (see later), it is most widely evident in square-planar systems. The classic example is the enhanced lability of the Cl^- ligand trans to the ethene group in Zeise's salt $[Pt(CH_2{=}CH_2)Cl_3]^-$. Recent advances in low-temperature fast reaction kinetic studies of these and similar cases have established without doubt that despite the lability observed the reactions are associative in nature exhibiting the expected two term rate law. The extensive studies on Pt^{II} complexes carried out subsequently have led to the following qualitative trans-directing sequence: C_2H_4, CO, $CN^- > PR_3$, $H^- > CH_3^-$, thiourea > $C_6H_5^-$, NO_2^-, $SCN^- > I^- > Br^-$, Cl^- > pyridine, NH_3, OH^-, H_2O.[59] The trans-directing effect requires rationalization within the associative mechanism. The lack of a theoretical basis for the effect despite clear experimental evidence for it has been highlighted by Tobe[9] as one of the "holy grails" of inorganic mechanisms. The principal difficulty is the lack of direct information about the nature of the transition state. Ground state trans effects manifest themselves in structural data with the detection of some bond lengthening to the ligand opposite, but this is not always found and moreover fails to correlate with the rate order above and difficult to rationalize in the context of the associative mechanism. Indeed the bond weakening effect may at its extreme be a reflection of the operation of an alternative dissociative path (see below). It can be seen from the rate order above that the most effective trans-directing ligands (T) are good π-acceptors (tran-

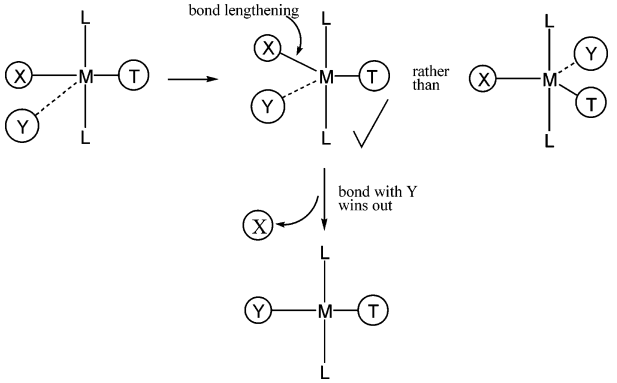

Figure 13. trans directing effect rationalized within the general accepted associative process on square-planar complexes.

sition state effect) and strong σ donors (ground-state bond weakening effect). The trans-directing order for π acceptors is: C_2H_4, CO > CN^- > NO_2^- > SCN^- > I^- > Br^- > Cl^- > NH_3 > OH^- and for σ donors it is H^- > PR_3 > SCN^- > I^- > CH_3^- > CO > CN^- > Br^- > Cl^- > NH_3 > OH^- giving rise to the overall qualitative sequence above. By definition both of these would be expected to possess relatively short bonds to M with build up of significant e^- density on the donor atom of T. This has led to a mechanism for rationalizing the effect involving a five coordinated trigonal bipyramidal intermediate, shown in Figure 13. Here approach of the entering group Y is restricted by the electronic (high e^- density on T) and steric repulsion (short M−T bond) from T to a trigonal bipyramidal intermediate with Y on the same side as X. Then it becomes a question of which bond is retained to give the final product. As M−Y wins over M−X preferential substitution occurs at X opposite to T. The strong trans direction shown by π acceptors has been rationalized within the five coordinated intermediate species above whereas the effectiveness of σ donors such as H^- and CH_3^- is less clear and must reflect a contribution from significant ground-state M−X bond weakening.

The trans-directing effect described above is a kinetic phenomenon and should not be confused with trans influence, which is purely a thermodynamic phenomenon. This is when certain ligands influence the ground state properties of groups to which they are trans. Such properties include metal−ligand bond lengths, vibration frequency or force constants and NMR coupling constants. The trans influence series based on structural data, has been given as $R^- \sim H^- \geq PR_3 >$ CO ~ C=C ~ Cl^- ~ NH_3 .

3.4.2.1.4. Dissociative Pathway. The normal mechanism for substitution within square-planar d^8 metal complexes is associative. Density functional theory calculations indeed show associative activation to be energetically favored over dissociative activation for water exchange on $[M(H_2O)_4]^{2+}$ ions (M = Pd and Pt) and on *trans*-$[PtCl_2(OH_2)_2]$.[32] Activation energies computed for dissociative water exchange on $[Pd(H_2O)_4]^{2+}$ were 142 kJ mol^{-1} larger than for associative water exchange involving an axially elongated trigonal bipyramidal transition state. Modeling the latter case led to remarkably good agreement between calculated and experimental $\Delta H^{\ddagger}$ values for the above three complexes. The presence however of bulky cis-oriented resident groups, such as *o*-tolyl or mesityl, or strong σ donors, such as CH_3^- and $C_6H_5^-$, lead to extremely slow substitution rates for Pt^{II} complexes and, in the case of complexes with cis Pt−C bonds, positive activation volumes indicating a changeover in mechanism from associative to dissociative.[108−110] Substitution on the *N*-methylated complex $[Pd(Me_5dien)X]^{n+}$ **2** by Y^{x-} ($X = Cl^-$, Br^-; $Y^{x-} = Br^-$, I^-, SCN^-, NO_2^-, N_3^-) for example obeys the rate law; rate = k $[Pd(Me_5dien)X^{n+}]$ − with no apparent k_Y term (32). For $X = Cl^-$, the rate of

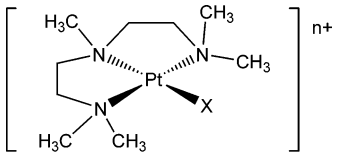

2

substitution is ~400 times slower than the corresponding reaction on $[Pd(dien)X]^{n+}$, a fact that was initially interpreted as due to suppression of the associative process by the bulky Me_5dien. However, in cases such as this, it appears the reaction remains associative as confirmed by the significantly negative activation volumes for water exchange; −2.8, −7.2, and −7.7 cm^3 mol^{-1} respectively on $[Pd(dien)H_2O]^{2+}$, $[Pd(Me_5dien)H_2O]^{2+}$, and $[Pd(Et_5dien)H_2O]^{2+}$, despite the decrease in k_{H_2O} (25 °C); respectively 5100, 187, and 2.9 s^{-1}.[111] It can be assumed that the absence of the k_Y term for Y^{x-} substitution on $[Pd(Me_5dien)X]^{n+}$ arises from rate determining formation of a reactive solvento species (k_S path). Indeed use of powerful π-accepting S-nucleophiles such as $SC(NH_2)_2$ (thiourea) and $S_2O_3^{2-}$ leads to reactions on $[Pd(Me_5dien)Cl]^+$ following a bimolecular relationship (k_Y path). A further example is provided by phosphine exchange at the extremely bulky complex *trans*-$[Pt(SnPh_3)_2(PMe_2Ph)_2]$ which follows a second-order rate law with $\Delta S^{\ddagger} = -131$ J K^{-1} mol^{-1}. The situation may however be different in the case of good σ-donors particularly M−C bonded species. For example in *trans*-$[Pt(PEt_3)_2RCl]$ (R = *o*-tolyl, mesityl), the dissociative pathway for Cl^- replacement appears to operate even with good S-nucleophiles such as SCN^-, PhS^-, and $S_2O_3^{2-}$.[108−110] This is believed to be due to a combination of the extreme steric hindrance provide by the ortho substituents on R combined with a significant ground-state M−X bond weakening effect. Activation volumes for solvent exchange on *cis*-$[PtPh_2(Me_2SO)_2]$, *cis*-$[PtPh_2(Me_2S)_2]$, and *cis*-$[PtMe_2(Me_2SO)_2]$ have values respectively of +4.7, +5.5, and +4.9 cm^3 mol^{-1}.[108] Similarly the isomerization of *cis*- to *trans*-$[PtR(PEt_3)_2(MeOH)]^+$ has activation volumes between +16 and +20 cm^3 mol^{-1} reflecting the dissociative nature of these reactions. In the latter, dissociative loss of MeOH is assumed to occur to give a three coordinated species. Finally, the reaction of *cis*-$[PtMe_2(Me_2SO)_2]$ with pyridine in toluene exhibits two stages with the first having parallel associative ($\Delta V^{\ddagger} = -11.4$ cm^3 mol^{-1}) and dissociative processes (established by the respective incoming and leaving ligand concentrations on the rate) with the second

stage predominantly dissociative ($\Delta S^{\ddagger} = +86$ J K^{-1} mol^{-1}).[112]

3.4.2.2. Gold(III). Substitution at 5d^8 Au^{III} is hindered for many ligands by redox processes involving reduction of Au^{III} to Au^{I} or Au^{0}. Therefore, the range of ligands studiable in detail is limited. The pathway adopted appears to be almost exclusively associative with convincing evidence for higher coordination number intermediates. Reactions are typically 10^2-10^3 times faster than equivalent ones on Pt^{II} and sometimes faster than reactions on Pd^{II}. Ligand substitution by each of H_2O, Cl^-, Br^-, I^-, and SCN^- on $[AuCl_4]^-$, $[AuBr_4]^-$, and $[Au(NH_3)_4]^{3+}$ all show good linear correlations of $\Delta G^{\ddagger}$ with ΔG° indicating associative character. The chloride exchange reaction on $[AuCl_4]^-$ obeys the typical second order rate law with significantly negative $\Delta S^{\ddagger}$ (-31 J K^{-1} mol^{-1}) and $\Delta V^{\ddagger}$ (-14 cm^3 mol^{-1}) values.[95] Reaction rates are extremely sensitive to the nature of the entering ligand with the dependence of the nature of the leaving ligand diminishing as the entering ligand nucleophilicity increases. Both the cis- and trans-directing effect have been noted and appear to be more important than for Pd^{II} and Pt^{II}. The order is for trans-directing: $CN^- > NH_3 > Br^- \geq Cl^-$ and for cis-directing: $R_3P \sim SCN^- > Br^- > Cl^- > NH_3$. This order, as different from that relevant to reactions on Pt^{II}, is explained by exclusive formation of square-pyramidal intermediates rather than rearrangenent to tbp forms as in the case of the reaction of $[AuCl_4]^-$ with SCN^-. The reaction of $[AuCl_4]^-$ with I^- to give $[AuCl_3I]^-$ is however strongly catalyzed by chloride and obeys the rate law (36) with suggestions of rapid preequilibrium formation of octahedral $[AuCl_6]^{3-}$ followed by rate determining substitution by I^- to give $[AuCl_5I]^{3-}$ which then rapidly loses chloride.[113] Redox reactions accompanying such substitutions are however a reoccurring problem and the above conclusions have not been substantiated in later studies.[114]

$$-\mathrm{d}[AuCl_4^-]/\mathrm{d}t = k[AuCl_4^-][I^-][Cl^-]^2 \quad (36)$$

A six-coordinated intermediate species has also been proposed for the reactions of $[AuX_2(bipy)]^+$ with X^- (= Cl^- or Br^-). In many of the redox reactions, such as the reactions of $[AuCl_4]^-$ with malonate and chloromalonate, the kinetics are consistent with rate determining substitution of the ligand into the Au^{III} coordination sphere prior to the redox step.

3.4.2.3. Rhodium(I) and Iridium(I). The involvement of a number of these species as effective catalysts for industrial scale hydrogenation, hydroformylation, and other carbonylation reactions has been extensively discussed and reviewed. Five-coordinated Rh^{I} and Ir^{I} species are readily formed and play an important role as intermediate species in the catalytic processes. As expected therefore ligand substitution reactions are strongly associatively activated. Exchange with CO on the Monsanto (Cativa)-type active species *cis*-$[M(CO)_2X_2]^-$ (M = Rh, Ir; X = Cl^-, Br^- or I^-) is as expected strongly associatively activated[115] with highly negative $\Delta V^{\ddagger}$ and $\Delta S^{\ddagger}$ values. The value for X = Cl^- are typical; $\Delta V^{\ddagger} = -17.2$ (Rh), -20.9 (Ir) cm^3 mol^{-1}; $\Delta S^{\ddagger} = -125$ (Rh), -135 (Ir) J K^{-1} mol^{-1}. More negative values are relevant for Ir vs Rh and $\Delta S^{\ddagger}$ gets progressively more negative from X = I^- to Cl^-. Formation of $[M(CO)_3X_2]^-$ as a discrete intermediate may be invoked here. The associatively activated oxidative addition reaction, central to action of these species as catalysts, is of course a type of inner-sphere redox process involving formation of an octahedral trivalent metal species and as such lies outside the scope of this review.

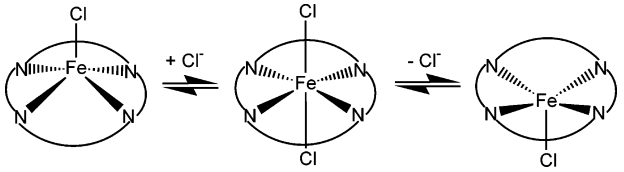

Figure 14. Cl^- promoted inversion of square-pyramidal [FeCl(porphyrin)] complexes.

3.4.2.4. Substitution Reactions at Other Square-Planar Centers. Reaction of Ni^{2+}_{aq} and Cu^{2+}_{aq} with tetrazamacrocycles and porphyrins gives rise to square-planar M^{II} complexes in both cases at least in nonaqueous media. The kinetics of formation and dissociation of these complexes has been extensively reviewed and will be discussed in section 3.4.5.

3.4.3. Coordination Number 5

In five-coordinated complexes, both associative and dissociative substitution pathways are possible in principle as can occur on other coordination geometries. Five coordination however involves two limiting stereochemistries, trigonal bipyramidal and square-pyramidal, which normally have similar energies. Many square-pyramidal complexes have "sitting atop" structures in which the central metal ion sits out of the plane of the four equatorial donors. One of the most important examples of this stereochemistry is deoxyhemoglobin in which the proximal histidine bound Fe^{II} ion sits out of the plane of the protoporphyrin ring.

3.4.3.1. Iron(III). In the square-pyramidal Fe^{III} complex [FeCl(porphyrin)], added Cl^- promotes inversion through a presumed six-coordinated transition state species, Figure 14; the inversion rate increasing as the basicity and ligand field strength of the porphyrin ring decrease, i.e., as the tendency toward adding an extra axial ligand increases.

3.4.3.2. Copper(II). The enhanced lability of d^9 Cu^{2+}_{aq} has long been discussed in terms of a dynamic Jahn–Teller effect whereby a tetragonal distortion of $[Cu(H_2O)_6]^{2+}$, Figure 15a, randomly reorientates or inverts about the *x*, *y*, and *z* axes very rapidly so that the lifetime of a given distortion, $\tau_i = 5.1 \times 10^{-12}$ s is much less than the lifetime of water molecule, $\tau_{H_2O} = 2.3 \times 10^{-10}$ s at 298.2 K. $[Cu(CH_3OH)_6]^{2+}$ has been rationalized similarly with $\tau_i = 1.2 \times 10^{-11}$ s much less than $\tau_{H_2O} = 3.2 \times 10^{-8}$ s.[116–118] Thus, each coordinated water and methanol molecule experiences 45 and 2700 inversions, respectively, prior to exchanging. Countless examples of tetragonally distorted six coordinated complexes of Cu^{II} have been structurally characterized adding weight to the presence of this solvent exchange mechanism. However subsequently more detailed neutron diffraction and

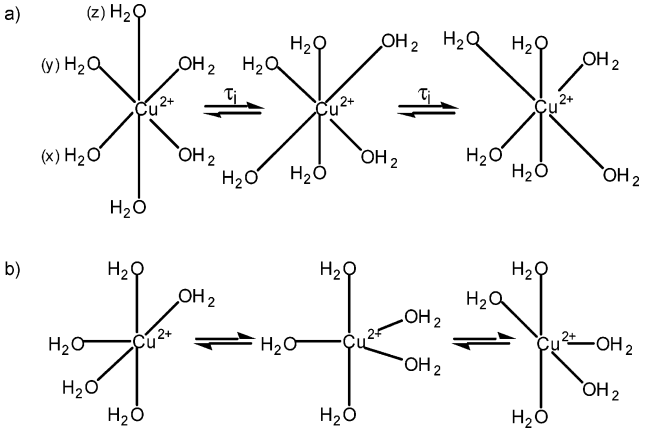

Figure 15. (a) Inversion of the tetragonal distortion in $[Cu(H_2O)_6]^{2+}$ whereby each coordinated water experiences a bond elongation. (b) The Berry twist mechanism in $[Cu(H_2O)_5]^{2+}$ whereby each apical coordinated water in the square pyramid may exchange with a water in the square plane via a trigonal bipyramidal intermediate.

molecular dynamics studies on $Cu^{2+}{}_{aq}$ have been interpreted through an alternative mechanism involving a five coordinated $[Cu(H_2O)_5]^{2+}$ aqua ion which rapidly interconverts between square pyramidal and trigonal bipyramidal stereochemistries of similar energy, Figure 15b, with a recalculated lifetime of 1.9×10^{-10} s.[119] The small positive activation volume ($+2.0$ cm^3 mol^{-1}) for water exchange on $Cu^{2+}{}_{aq}$ indicates as expected considerable transition-state like behavior in the rapidly fluxionating ground-state species.[117,118]

Five coordinated Cu^{II} is in fact well-established such as in trigonal bipyramidal $[Cu(bipy)_2Cl]^+$, $[Cu(tren)(H_2O)]^{2+}$ (tren = **4**),[120] and $[Cu(terpy)(H_2O)_2]^{2+}$ (terpy = **5**)[121] and square-pyrimidal $[Cu(tet\ b)(H_2O)]^{2+}$ (tet b = **3**)[122] and $[CuL(H_2O)]^{2+}$ (L = *N*,*N*′-bis-(2-pyridylmethylene)-1,3-diamino-2,2-dicarboxypropane).[123] Detailed substitution studies involving replacement of the coordinated waters have been carried out on $[Cu(tren)(H_2O)]^{2+}$, $[Cu(terpy)(H_2O)_2]^{2+}$, and $[Cu(tet\ b)(H_2O)]^{2+}$. These complexes substitute via associatively activated processes. For $[Cu(tet\ b)(H_2O)]^{2+}$ a wide variation of rate constants with different X^{n-} ligands (37) coupled with negative activation entropies, a sensitivity of k_f but an insensitivity of k_{aq} to the nature of X^{n-} provide strong indicators of an associative mode of activation.[122]

$$[Cu(tet\ b)(H_2O)]^{2+} + X^{n-} \underset{k_{aq}}{\overset{k_f}{\rightleftharpoons}} [Cu(tet\ b)X]^{(2-n)+} + H_2O \quad (37)$$

Since no six-coordinated species has been detected spectroscopically, the reaction is believed to occur via an Eigen−Wilkins preassociation $\mathbf{I_A}$ mechanism. Significantly negative values of $\Delta V^{\ddagger}$ for both water exchange and pyridine substitution on $[Cu(tren)(H_2O)]^{2+}$ (ranging from -4.7 to -10 cm^3 mol^{-1}) also indicate associative activation. Here it is believed that imposition of the rigid trigonal bipyramidal stereochemistry restricting rotation provides a significant ligand field activation barrier toward operation of the normal Jahn−Teller activated dissociative process.[120] Water exchange on $[Cu(tren)(H_2O)]^{2+}$ is

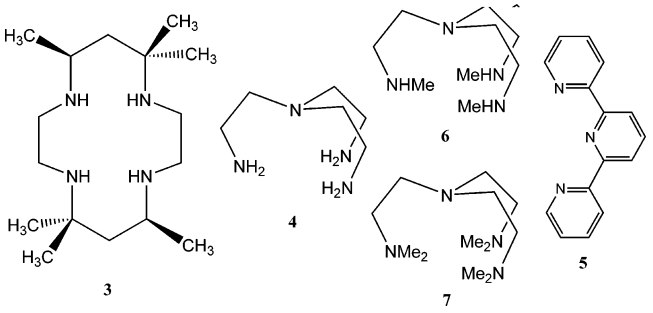

therefore $\sim 10^4\times$ slower than on the highly labile fluxional $Cu^{2+}{}_{aq}$. Activation volumes for the replacement of water on $[Cu(Me_3tren)(H_2O)]^{2+}$ (Me_3tren = **6**) by pyridine and vice versa are respectively -8.7 and -6.2 cm^3 mol^{-1} indicate retention of the associative pathway ($\mathbf{I_A}$) although here rates are $\sim 10^2\times$ slower than on the tren complex due to the steric hindrance of the three Me groups. Water exchange on $[Cu(Me_3tren)(H_2O)]^{2+}$ in acidic aqueous solution has $\Delta S^{\ddagger}$ and $\Delta V^{\ddagger}$ values respectively of -6 J K^{-1} mol^{-1} and $+0.3$ cm^3 mol^{-1}. The small near zero values here are suggested to reflect an interchange mechanism wherein one ligand arm dissociates as the incoming water molecule binds to Cu^{2+}. The incorporation of six methyl groups into the tren ligand however causes sufficient steric crowding for substitution on $[Cu(Me_6tren)(H_2O)]^{2+}$ (Me_6tren = **7**) to proceed dissociatively[120,124,125] accompanied by a further reduction in rate (by $10^5\times$ vs tren). Here substitution rates are now some $10^{10}\times$ slower than on $Cu^{2+}{}_{aq}$; the retardation is explained in terms of a strong ligand field effect from the rigidly imposed trigonal bipyramidal stereochemistry. The substitution mechanism is complex and like the Me_3tren complex is believed to involve Cu−N bond rupture and de-chelation of the tren ligand, accompanied by further coordination of water prior to the dissociative substitution. It is clear that steric effects and perhaps electronic effects from N-alkyl substituents can significantly increase the degree of dissociativeness as observed already in the cases of small Be^{2+}, square-planar complexes of Pd^{2+} and Pt^{2+}, and to be discussed below in reactions on inert low spin Co^{III}. The mer coordinating tridentate ligand terpy **5** is of interest since the Jahn−Teller distortion prevents two of the ligands from coordinating to Cu^{2+} in a regular octahedral fashion. The monoterpy complex $[Cu(terpy)(H_2O)_2]^{2+}$ is moreover five-coordinated and forms rapidly (k_f(25 °C) = $1.2 \pm 0.1 \times 10^7$ M^{-1} s^{-1}) from $Cu^{2+}{}_{aq}$. A trigonal bipyramidal structure with both waters equatorial has been assumed cf. $[Cu(terpy)Cl_2]$. In contrast to $[Cu(tren)(H_2O)]^{2+}$ above, water exchange on $[Cu(terpy)(H_2O)_2]^{2+}$ is rapid and comparable to that on $Cu^{2+}{}_{aq}$ suggesting some degree of rapid fluxionality (k_{H_2O}(25 °C) = $6.6 \pm 0.9 \times 10^8$ s^{-1}, $\Delta H^{\ddagger} = 20.7 \pm 2$ kJ mol^{-1}, $\Delta S^{\ddagger} = -6.6 \pm 6$ J K^{-1} mol^{-1}, and $\Delta V^{\ddagger} = 0.0 \pm 0.2$ cm^3 ‡mol^{-1})[121] which may involve the terpy ligand readily flipping between tridentate and bipy-like bidentate coordination modes (see section 3.4.5).

3.4.4. Coordination Number 6 (Octahedral)

This group comprises the largest set of species for which kinetic data of ligand substitution reactions has been gathered. These species have formed the bedrock around which the mechanistic classification of ligand substitution reactions has been drawn up as well as defining trends and comparisons within the periodic table. For the purpose of this review, it has been decided to subdivide the survey under the following headings; ligand substitution on hexaaqua metal ions, reactions of hydroxy-aqua species and base hydrolysis, and finally reactions involving ligand chelation.

3.4.4.1. Ligand Replacement on Hexaaqua Ions. For the divalent 3d metals, the lability toward water exchange and ligand substitution generally increases in the sequence: $Cu^{2+} \approx Cr^{2+} > Zn^{2+} \approx Mn^{2+} > Fe^{2+} > Co^{2+} > Ni^{2+} > V^{2+}$ as a consequence of the variations of the electronic occupancy of their d orbitals. This sequence qualitatively coincides with the expectations arising from ligand field activation energies (LFAEs) as is also the case for the trivalent metal ions with the same electronic configurations.[126−128] High-spin d^3 and d^8 metal ions have substantial LFAE contributing to their $\Delta H^{\ddagger}$ with the consequence that V^{2+}, Ni^{2+}, and Cr^{3+} are much less labile than the other di- and trivalent first-row transition metal ions. Similar conclusions have arisen from molecular orbital calculations.[129] The rate and activation energy itself however gives little mechanistic information, the most powerful probe being the activation volume. Here distinct trends show up both across and down the periodic table. Along the 3d period from left to right, there is a clear change from negative activation volumes for water exchange on $[M(H_2O)_6]^{2+}$ for the more expanded early ions when $M^{2+} = V^{2+}$ (−4.1) and Mn^{2+} (−5.4) to increasingly positive values for the later ions when $M^{2+} = Fe^{2+}$ (+3.8), Co^{2+} (+6.1) and Ni^{2+} (+7.2 $cm^3\ mol^{-1}$) indicate a changeover in mechanism from associative activation for the first two to dissociative activation for the rest as was discussed earlier, Table 1.[28] In agreement with these conclusions, density function calculations show that water exchange on $[Zn(H_2O)_6]^{2+}$ occurs through a **D** mechanism[130] as predicted earlier by the activation volume (+7.1 $cm^3\ mol^{-1}$) for complexation by 2,2- bipyridine.[72] A similar trend is seen for 3d trivalent metals with water exchange activation volumes for $[M(H_2O)_6]^{3+}$ ions ranging from d^1 Ti^{3+} (−12.1), d^3 Cr^{3+} (−9.6), d^5 Fe^{3+} (−5.4), across to d^{10} Ga^{3+} (+5.0 $cm^3\ mol^{-1}$). Qualitatively, the change from associative to dissociative activation as d orbital electronic occupancy increases may be explained through an increasing repulsion between an entering water molecule approaching a face of the octahedral $[M(H_2O)_6]^{3+/2+}$ and the t_{2g} electrons disfavoring the increase in coordination number required by an **A** activated transition so that a **D** activated transition state is favored as atomic number increases. Ab initio calculations at the Hartree−Fock level for water exchange on the d^0 to d^{10} first row hexaaqua transition metal ions ranging from Sc^{3+} to Zn^{2+} predict this change from associative to dissociative activation so that only **A** mechanisms are possible for Sc^{3+}, Ti^{3+}, and V^{3+}, only **D** mechanisms are possible for Ni^{2+}, Cu^{2+}, and Zn^{2+}, whereas a gradual change from associative to dissociative activation is predicted for other first row transition metal ions with d^2 to d^7 electronic configurations.[69,70,131]

Table 10. Invariant Calculated Values of $V^{\ddagger}$ for the Transition State Involved in Water Exchange on Selected Metal Ion Perchlorates[132]

	V°_{abs}, $cm^3\ mol^{-1}$	$\Delta V^{\ddagger}$, $cm^3\ mol^{-1}$	$V^{\ddagger}$, $cm^3\ mol^{-1}$
$[M(H_2O)_6]^{2+}$			
Mn	-17.4	-5.4	-22.8
Fe	-25.3	+3.8	-21.5
Co	-25.4	+6.1	-19.3
Ni	-28.4	+7.2	-21.2
$[M(NH_3)_5(H_2O)]^{3+}$			
Co	54.9	+1.2	56.1
Rh	61.2	-4.1	57.1
Ir	61.2	-3.2	58.0
Ru	63.2	-4.0	59.2
Cr	65.3	-5.8	59.5

Ab initio calculations have proved effective for calculating realistic energies for both transition state and intermediate species and are now being modified to give realistic volume profile calculations (see later). Swaddle[132] has observed a clear correlation between the ground-state absolute partial molar volume V°_{abs} and the observed $\Delta V^{\ddagger}$ value for water exchange for several 3d $[M(H_2O)_6]^{2+}$ and 3d/4d/5d $[M(NH_3)_5(H_2O)]^{3+}$ complexes, Table 10. The larger the V°_{abs}, the more negative is the observed value of $\Delta V^{\ddagger}$, implying an essentially invariant value of the volume of the transition state, $V^{\ddagger}$, in each case. This was interpreted as the transition states involving cooperative movement of the entire assemblage of primary and secondary hydration shells so as to become essentially insensitive to the nature of the metal center whereas the molar volume of the static ground state system directly reflects the properties of that system. Thus, not unsurprisingly, those metal aqua ions and complexes with the larger V°_{abs} values are more expanded and thus likely to allow a greater penetration of the entering ligand nucleophile along the reaction coordinate to the transition state. This is now believed to be especially relevant to the negative activation volumes seen for the larger 4d and 5d transition metal centers with filled t_{2g}^6 configurations such as Rh^{3+} and Ir^{3+} (see below).

Rate data particularly as a function of the nature of the entering or leaving ligands can in some cases provide useful data although care is needed. As seen in Table 2 a correlation with k_{obs} is sometimes seen e.g. for $[Ti(H_2O)_6]^{3+}$ and $[V(H_2O)_6]^{3+}$ with a reliable incoming ligand L nucleophilicity parameter, e.g., the Bronsted basicity (i.e., pK_a value for HL) and not simply charge. For $[Ti(H_2O)_6]^{3+}$ the variation in k_{obs} is greater than that accounted for by Eigen−Wilkins preassociation, and so an associative mechanism is concluded, probably close to the **A** limit as suggested by the activation volume for water ex-

change (-12.1cm^3 mol^{-1}). Similarly for $[Co(H_2O)_6]^{2+}$ ($+6.1$) and $[Ni\text{-}(H_2O)_6]^{2+}$ ($+7.2$ cm^3 mol^{-1}) the variation here is accounted for by K_{os} (18) with little variation seen in k_I with the nature of the entering ligand consistent with a dissociative mechanism, $\mathbf{I_D}$ or **D**.

In aqueous media however it is actually difficult to be sure whether the mechanism is $\mathbf{I_{D(A)}}$ or extreme **D(A)** for reasons given earlier. For example the extreme **D** process (24) gives rise to a rate expression with a nonlinear dependence on the concentration of the entering ligand seemingly identical to the Eigen−Wilkins preassociation situation (18) as highlighted earlier. The **D** mechanism might be indicated if an Eigen−Wilkins analysis of the kinetic data fails to give a reasonable value for K_{os} for the reactant pair in question. However, this could not be used as sufficient proof on its own and other indicators are required. For example an extreme **D** process would be expected to have a rate constant for the water dissociation step matching that of water exchange. Any discrepancy, i.e., a smaller value, even within a factor of 2 or 3 of that for water exchange, would imply that the putative five coordinated intermediate cannot be long-lived on the time scale of the relaxation of the coordination sphere. This is exactly the situation for $[Co(CN)_5(H_2O)]^{2-}$, a species long believed to be the archetypal example of the **D** process,[133] but now believed to be in the interchange category[134] admittedly with a strong leaving group (H_2O) dependence. The activation volume for water exchange is $+7$ cm^3 mol^{-1}, identical to the value for $[Ni(H_2O)_6]^{2+}$. A better archetypal example is probably that of substitution on *trans*-$[Co^{III}(tmpyp)(H_2O)_2]^{5+}$ (tmpyp = tetra-4-*N*-methylpyridylporphyrin), e.g., by NCS^- for which $\Delta V^{\ddagger} = +14$ cm^3 mol^{-1} and a degree of curvature in plots of k_{obs} vs [NCS^-] far less than expected for a 5+/1− ion pair.[135] $\Delta V^{\ddagger}$ is reasonable for the loss of one water molecule in the activated complex.[136] Extreme **D** mechanisms are also believed to be relevant to water exchange on a range of substituted porphyrin complexes *trans*-$[Fe(porph)(H_2O)_2]^{3+}$ ($\Delta V^{\ddagger} = +7$ to $+12$ cm^3 mol^{-1}; $\Delta S^{\ddagger} = +60$ to $+100$ J K^{-1} mol^{-1})[137] and to ammoniation of $[Fe^{II}(CN)_5(H_2O)]^{3-}$ ($\Delta V^{\ddagger} = +14$ cm^3 mol^{-1}; $\Delta S^{\ddagger} = +70$ J K^{-1} mol^{-1} for both forward and reverse steps).[138] With regard to the former, a number of five-coordinated Fe^{III} porphyrin complexes are well characterized such as $[FeCl(porphyrin)]^{2+}$ (above, section 3.4.3).

With regard to the **D** mechanism, the heavier group 9 ions $[Rh(H_2O)_6]^{3+}$ and $[Ir(H_2O)_6]^{3+}$ are worthy of some discussion at this point. Water ligand substitution on these low spin t_{2g}^6 species were believed to be prime candidates for the **D** process. Indeed early kinetic studies of water exchange and 1:1 Cl^-, Br^- substitution on Rh^{3+}(aq) by Harris and co-workers were interpreted in that way. The nonlinear "curvature" observed in plots of the first-order rate constant k_{obs} versus [X^-] at [H^+] ≥ 0.5 M was rationalized by steps (38) through (40) within a presumed **D** process involving a discrete pentaaqua intermediate.[139]

$$[Rh(OH_2)_6]^{3+} \underset{k_{-1}}{\overset{k_1}{\rightleftharpoons}} [Rh(OH_2)_5]^{3+} + H_2O \quad (38)$$

$$[Rh(OH_2)_5]^{3+} + L \xrightarrow{k_2} [Rh(OH_2)_5L]^{3+} \quad (39)$$

$$k_{obs} = \frac{k_1 k_2 [L]}{k_{-1} + k_2 [L]} \quad (40)$$

when $k_2[L] \gg k_{-1}$, k_{obs} becomes independant of [L]

Virtually identical rate constants for L = Cl^- and Br^- close to the water exchange rate constant at 25 °C supported the proposal. However, these findings, at least with regard to $[Rh(H_2O)_6]^{3+}$, appear to be at odds with the small and distinctly negative activation volume relevant to the water exchange process (-4.2 cm^3 mol^{-1}).[140] Harris et al. did detect the contribution from small amounts of the distinctly more labile hydroxopentaaqua species ($pK_a \sim 4.0$) which was believed to promote further the **D** process through OH^- ligand assisted labilization, the so-called conjugate base effect (see below). Here a reactive hydroxotetraqua intermediate was assumed to form. A recent reexamination of the Br^- anation reaction on Rh^{3+}(aq) over a wider [H^+] range and under variable high pressure has however provided clear evidence for an Eigen−Wilkins ion-pair interchange process associatively activated on $[Rh(H_2O)_6]^{3+}$ ($\Delta V^{\ddagger} = -3.3$ cm^3 mol^{-1}) but dissociatively activated on $[Rh(H_2O)_5OH]^{2+}$ ($+7.7$ cm^3 mol^{-1}).[141] If substitution at both $[Rh(H_2O)_6]^{3+}$ and $[Rh(H_2O)_5OH]^{2+}$ followed a **D** path akin to (38) through (40) nonlinear curvature of rate with [Br^-] should have been seen over all [H^+] values studied but lowering the acidity below that employed by Harris et al. led to linear plots of k_{obs} with [Br^-] over the entire range of [Br^-] studied. The lack of curvature is consistent with a reactant pair interchange process with a lower value of K_{os} relevant for the lower charged hydroxo ion in the [Br^-] range employed. These results clearly show that the more expanded ground state 4d and 5d 3+ charged species allow significant penetration of the entering ligand into the first coordination sphere at the transition state even in the case when a filled t_{2g}^6 set is relevant. The lack of a discrimination shown by $Rh^{3+}{}_{aq}$ toward Cl^- and Br^- is merely a reflection of this metal center and cannot be used in mechanistic diagnosis. Water exchange on $[Ir(H_2O)_6]^{3+}$ is concluded to operate by a similar $\mathbf{I_A}$ mechanism ($\Delta V^{\ddagger} = -5.7$ cm^3 mol^{-1}),[41] and reference to Table 1 shows that activation volumes for water exchange and substitution on homoleptic species become steadily more negative as one descends a group as further testament to the more expanded ground-state nature of the 4d and 5d reacting species. The strong resident Rh−O and Ir−O bonds in the respective t_{2g}^6 hexaaqua ions is now believed to disfavor the expected **D** process to the extent that the lowest energy pathway available is **I**. These conclusion have been backed up by recent ab initio calculations of both the activation energy

Table 11. Water Exchange Rate Constants on Some Aqua Ions and Their Monohydroxo-aqua Forms at 25 °C

$M^{n+}(aq)$	$k(M^{n+}_{aq})/s^{-1}$	$k(MOH^{(n-1)+}_{aq})/s^{-1}$	$(MOH^{(n-1)+}_{aq}/k\ (M^{n+}_{aq})$	pK_{11}
$[Mo_3S_4(H_2O)_9]^{4+}$	<1	7.5×10^3	>7500	0.66
$[Rh(H_2O)_6]^{3+}$	2.2×10^{-9}	4.2×10^{-5}	19 100	3.5
$[Ir(H_2O)_6]^{3+}$	1.1×10^{-10}	4.0×10^{-7}	3600	4.45
$[Fe(H_2O)_6]^{3+}$	1.6×10^2	1.2×10^5	750	2.19
$[Ga(H_2O)_6]^{3+}$	4.0×10^2	1.1×10^5	275	3.9
$[Ru(H_2O)_6]^{3+}$	3.5×10^{-6}	5.9×10^{-4}	170	2.7
$[Cr(H_2O)_6]^{3+}$	2.4×10^{-6}	1.8×10^{-4}	75	4.0

and volume profile for the water exchange process at the Hartree−Fock (SCF) level which predicts $\mathbf{I_A}$ mechanisms for both ions.[31,142] The extremely slow rates of ligand substitution on $[Ir(H_2O)_6]^{3+}$ are in part due to the hydroxopentaaqua species being only $10^3\times$ more labile than the hexaaqua ion and there is less of it present in the acid solutions employed (pK_a = 4.45).[41] Experimentally, difficulties also arise since $[Ir(H_2O)_6]^{3+}$ is mildly reducing especially at higher temperatures due to water reduction and oxidation to labile and complex Ir^{IV}_{aq} containing solutions.[143] The kinetics of complexation by oxalate/oxalic acid to a mixture of $[Ir(C_2O_4)_3]^{3-}$ and *cis/trans*-$[Ir(C_2O_4)_2(H_2O)_2]^-$ remains one of the few ligand substitution reactions to be studied in detail on $[Ir(H_2O)_6]^{3+}$ although here the mechanism is not a metal-based ligand interchange but one involving metal-bound water (or OH^- ion) attack on the carboxylate ligand (see section 3.4.9).[144]

The situation however is different for anionic Rh^{III} complexes. Water and chloride ligand replacement on chlororhodium(III) anions such as $[RhCl_n(H_2O)_{6-n}]^{(3-n)-}$ ($n \geq 4$) have distinctly positive activation volumes (e.g., $\Delta V^{\ddagger} = +15.7$ cm^3 mol^{-1} for Cl^- replacing water and +14.4 cm^3 mol^{-1} for water replacing Cl^- on $[RhCl_5(H_2O)]^{2-}$) and are strong candidates for the extreme **D** process.[145] Here the observed $\Delta V^{\ddagger}$ is close to the $V°$ for the electrostricted leaving ligand.[63,73] The **D** process here is promoted through a mixture of strong σ-bonded ground-state bond labilization and significant steric hindrance from the resident Cl^- ligands. The electronic labilizing effect from OH^- may have a similar origin (see below). For example $[H^+]$ dependent water exchange studies on the much more labile Ir^{III} ion $[Ir(OH)_6]^{3-}$ show that the exchange proceeds exclusively through a labile pentahydroxoaqua species[146] involving dissociative loss of water.

3.4.4.2. Lability of Hydroxoaqua Ions: The "Conjugate Base" Effect. It is now well established[4,17] that the rates of water ligand exchange and substitution reactions on monodeprotonated aqua metal ions (41) are more often than not faster than equivalent substitution rates on the fully protonated species.

$$[M(OH_2)_n]^{x+} \overset{pK_{11}}{\rightleftharpoons} [M(OH_2)_{n-1}OH]^{(x-1)+} + H^+ \quad (41)$$

Reference to the data below in Table 11 shows that the rate acceleration can amount to >4 orders of magnitude. It has been argued that this largely amounts to a charge neutralization effect and the lower charge on the hydroxo complex explains the lability. Volumes of activation for water exchange moreover tend to be much more positive for the hydroxo aqua ions, Table 12, suggesting that reactions on the monodeprotonated aqua ions are more dissociative in character. Although this behavior would be largely in keeping with reactions of essentially lower charge dipositive ions (see below), one cannot rule out the alternative explanation of a specific electronic effect from the OH^- ligand termed the "conjugate base" labilizing effect. Here the OH^- ligand promotes dissociative loss of a water ligand via stabilization of the trigonal bipyramidal "$[M(H_2O)_4OH]^{2+}$" intermediate, Figure 16 through effective σ

Table 12. Activation Enthalpies and Volumes for Water Exchange on $[M(H_2O)_6]^{3+}$ and on $[M(H_2O)_5OH]^{2+}$

	reaction on $[M(H_2O)_6]^{3+}$		reaction on $[M(H_2O)_5OH]^{2+}$	
M	$\Delta H^{\ddagger}$, kJ mol^{-1}	$\Delta V^{\ddagger}$, cm^3 mol^{-1}	$\Delta H^{\ddagger}$, kJ mol^{-1}	$\Delta V^{\ddagger}$, cm^3 mol^{-1}
Cr	108.6	−9.6	110	+2.7
Ru	89.8	−8.3	95.8	+0.9
Ir	138.5	−5.7		+1.3
Fe	63.9	−5.4	42.5	+7.0
Rh	131	−4.2	103	+1.5
Ga	67.1	+5.0	58.9	+6.2

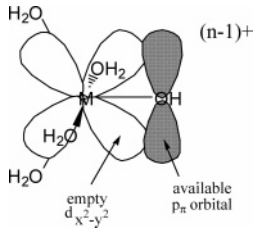

Figure 16. Stabilization of a trigonal bipyramidal $[M(H_2O)_4OH]^{2+}$ intermediate by π donation from OH.

donation into a M σ acceptor orbital such as the $d_{x^2-y^2}$. Such a species however probably has only a fleeting existence in aqueous solution and moreover its formation is not easy to substantiate since it will remain strongly associated with the assemblage of hydrogen-bonded waters surrounding it. The water ligand dissociating could conceivably be cis or trans to the OH group, a fact not easy to establish on mononuclear hydroxopentaaqua complexes because of the rapid proton exchange occurring within the first coordination sphere. However cis conjugate base effects have been detected in several cases such as in the hydroxo ligand-promoted water exchange at the d-H_2O ligands on the trinuclear cluster family $[Mo_3(\mu_3\text{-}X)(\mu\text{-}X)_3(c\text{-}H_2O)_3(d\text{-}H_2O)_6]^{4+}$ (X = O or S) (see section 3.4.10.2).[147]

Support for the conjugate-base effect as being electronic rather than due merely to charge reduction

comes from several other key observations. First, Baldwin[148] found that within the series of chromium complexes $[Cr^{III}(H_2O)_5X]^{2+}$ (X = various monoanionic ligands) one of the water molecules is more labile than the other four, a result that cannot be explained by a mere charge reduction effect. Second, the water exchange rate constant (25 °C) for the 2+ charged triangular acetato-bridged complex $[Mo^{IV}_3(\mu_3\text{-}O)_2(\mu\text{-}O_2CCH_3)_6(H_2O)_3]^{2+}$ is 1.8×10^{-6} s^{-1} [149] which is 4 orders of magnitude smaller than that for the slow exchanging c-H_2O on $[Mo^{IV}_3(\mu_3\text{-}O)(\mu\text{-}O)_3(c\text{-}H_2O)_3(d\text{-}H_2O)_6]^{4+}$ and nearly 8 order of magnitude slower than exchange of the d-H_2O on the same species which is activated through the *cis*-monohydroxo ion.[147] Finally, in the case of the hydroxo-bridged aqua dimers, $[M^{III}_2(\mu\text{-}OH)_2(H_2O)_8]^{4+}$ (M = Cr or Rh), one has defined water ligand positions cis and trans to a bridging OH^- group. Labilization is seen although it is less than the effect from a terminal OH^- ligand. In the Rh^{III} dimer, the waters cis and trans exchange at the same rate (k_{H_2O}(25 °C) = ca. 5×10^{-7} s^{-1}) with activation volumes of ca. +9 to +10 cm^3 mol^{-1}, indicating a strongly dissociative mechanism. These activation volumes are the most positive so far observed on an aqua ion species and may be representative of a limiting **D** process.[75] Further to this the equivalence of rates seen for the cis and trans waters could be as a result of a rapid Berry twist of the five coordinated intermediate (42).

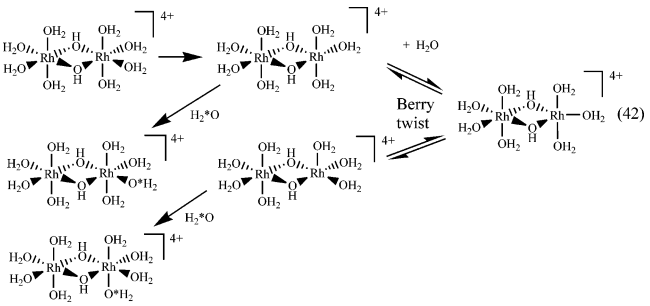

3.4.4.3. Reactions on Co^{III} Amine Complexes. Ligand substitution reactions on low spin diamagnetic t_{2g}^6 Co^{III} systems have been extensively studied over the past four decades partly because they occur at conveniently slow rates and the complexes are more often than not both kinetic and thermodynamically stable allowing study where the stereochemistry is defined and the stereochemistry of the products can be analyzed. The large number of available compounds stemming from the pioneering work of Werner has allowed mechanistic studies to stem systematically investigate variations in leaving group, entering group, spectator ligands and defined stereochemistry. Furthermore, an NMR handle is available. Each of these factors stem from the low spin t_{2g}^6 configuration of the small Co^{III} center which imparts both stability and kinetic inertness. Much initial attention was given to kinetic studies of ligand substitution reactions on the family of so-called acidopentammine complexes $[(NH_3)_5Co^{III}X]^{2+}$ wherein the strong X^- ligand dependence of the rate constant (k_{aq}) for aquation (replacement of X^- by water) coupled with the X^- ligand independence on the rate constant (k_{an}) for the reverse anation reaction (43)

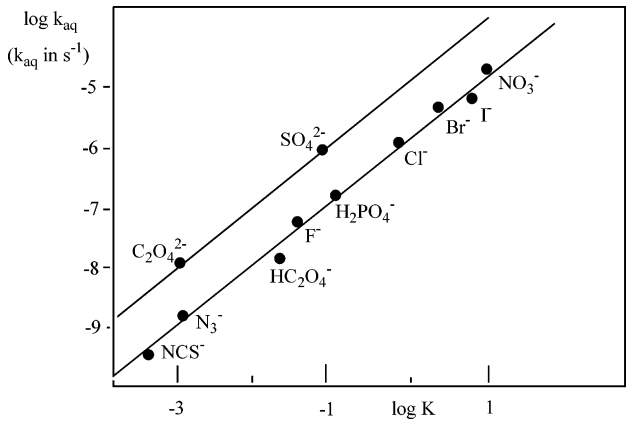

Figure 17. Linear plot (slope = 1) of log k_{aq} versus log K for aquation and correspondinganation of $[(NH_3)_5Co^{III}X]^{n+}$ complexes (X^- = monoanionic ligands shown or water).[150]

reflected the strongly dissociative nature of these reactions, an exception to the general rule for trivalent d-block transition metal centers.

$$[Co(NH_3)_5X]^{(3-n)+} + H_2O \underset{k_{an}}{\overset{k_{aq}}{\rightleftharpoons}} [Co(NH_3)_5H_2O]^{3+} + X^{n-} \quad (43)$$

The resulting linear plot of log k_h versus log K ($K = k_{aq}/k_{an}$) as a function of the nature of X^- with slope = unity provides the classic text book illustration, Figure 17.[150] This is an example of a linear free energy relationship (LFER) since log $k_{an} \propto \Delta G^{\ddagger}$ and log $K \propto \Delta G°$. The unit slope in both cases indicates that the activated complex and product closely resemble each other, i.e., that in the activated complex X^{n-} has departed and the reaction is strongly dissociative in both directions. When X^{n-} is the anion derived from a weak acid (acido group, e.g., N_3^-, CN^-, F^-, NO_2^-, SO_4^{2-}, HPO_4^{2-}, $C_2O_4^{2-}$, malonate^{2-}, CO_3^{2-}, and various acetates), the backward anation reaction is also subject to acid catalysis wherein initial rapid protonation of the leaving group facilitates its dissociation. For example, the reaction with $X^{n-} = F^-$ is faster in D_2O than in H_2O consistent with D_3O^+ being a stronger acid than H_3O^+. The isotope effect confirms that protonation is rapid since the opposite solvent effect would be seen with the reaction slower in D_2O if protonation was rate determining. The effect of increased charge separation in the aquation reaction is seen with the negative values for $\Delta S^{\ddagger}$ and $\Delta V^{\ddagger}$ reflecting the extra solvation of the outgoing X^{n-} group. The work of Tobe[9,13,151] and others using chelated 1,2-diaminoethane and other chelated ligands to replace four of the ammonia ligands began the process of established some of the stereochemical rules for these reactions. The detection of *cis*-aqua products, Table 13, following the aquation of various *trans*-$[Co(en)_2AX]^{n+}$ complexes (A = Cl^-, OH^-, Br^-, NCS^-, $CH_3CO_2^-$) gave the earliest indication of not just the formation of a transition state but the existence of an intermediate that had time to rearrange from the initial square-pyramidal species to a trigonal bipyramidal form close in energy; this rearrangement providing further evidence of the strongly dissociative nature of the reactions. Reactions proceeding with essentially retention of configuration

Table 13: Stereochemistry of Products of the Aquation of Various *trans*-[$CoL_4AX]^{n+}$ Complexes

L_4	A	X	% cis	% trans
$(NH_3)_4$	Cl^-	Cl^-	55	45
en_2	OH^-	Cl^-	75	25
en_2	Cl^-	Cl^-	35	65
en_2	Br^-	Br^-	30	70
en_2	NCS^-	Cl^-	45	55
en_2	$CH_3CO_2^-$	Cl^-	75	25
S,S-trien **8**[a]	Cl	Cl	100 (β-cis)	
R,R-2,3,2-tet **9**	Cl	Cl	50 (β-cis)	50
R,S-2,3,2-tet **9**	Cl	Cl	0	100
S,S-3,2,3-tet **10**	Cl	Cl	0	100
cyclam **11**	Cl	Cl	0	100
tet a **12**	Cl	Cl	0	100
tet b **3**	Cl	Cl	0	100

[a] The labels R and S refer to the absolute configuration of the secondary nitrogen when coordinated.

such as those of *trans*-$[Co(cyclam)Cl_2]^+$ are believed to involve only a square-pyramidal intermediate and possess negative values of $\Delta S^{\ddagger}$ consistent with solvation of the departing X^{n-}. However, those reactions in which substantial stereochemical change is observed in the products are frequently characterized by positive values of $\Delta S^{\ddagger}$. Here a trigonal bipyramidal intermediate is invoked which may be less well solvated than the corresponding square-pyramidal species, thus counteracting the increased solvation of the departing X^{n-}.

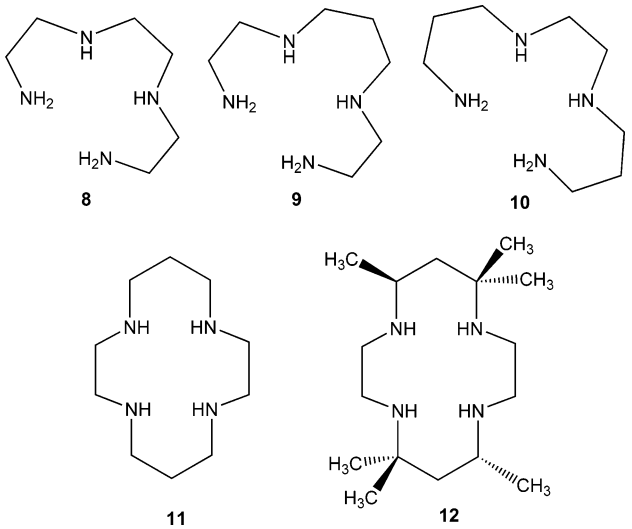

3.4.4.4. Base Hydrolysis and the S_N1_{CB} or D_{CB} Mechanism. It is well established[152] from a multitude of studies that the rates of substitution of various X^{n-} ligands by OH^- on low spin d^6 Co^{III} complexes such as $[L_4(NHR_2)Co^{III}X]^{n+}$ possessing at least one N−H bond are unusually fast compared to substitution of X^{n-} by other ligands, including spontaneous aquation by water.[153] Despite the second-order rate law and clear dependence of rate on $[OH^-]$, the reactions remain strongly dissociative in nature on the small t_{2g}^6 Co^{III} center. In these base-catalyzed reactions, direct attack of the OH^- nucleophile at the Co^{III} center is not relevant but instead OH^- acts as a base[154] removing one of the ligand N−H protons forming an "amido" complex which promotes dissociative loss of X^{n-} ($\mathbf{D_{CB}}$ mechanism) by stabilizing the resulting trigonal bipyramidal intermediate via π-donation, similar to the effect of OH^- in the hydroxopentaaqua ions discussed above. The deprotonation also facilitates loss of the anionic leaving group because of diminished charge separation problems. In the case of certain chelated Co^{III} amine complexes, however, the conjugate base rate enhancement here can be huge (up to 8 orders of magnitude). The $\mathbf{S_N1_{CB}}$ or $\mathbf{D_{CB}}$ mechanism was first proposed in 1937 by Garrick[155] and later revised by Basolo and Pearson[3,4,156] to include the step involving the five coordinated intermediate (44).

$$L_4M(NHR_2)X]^{n+} + OH^- \underset{k_{-1}}{\overset{k_1}{\rightleftharpoons}} L_4M(NR_2)X]^{(n-1)+} + H_2O$$

$$L_4M(NR_2)X]^{(n-1)+} \xrightarrow{k_2} L_4M(NR_2)]^{n+} + X^-$$

$$L_4M(NR_2)]^{n+} + H_2O \xrightarrow{\text{fast}} L_4M(NHR_2)(OH)]^{n+} \quad (44)$$

The final fast step involves aquation with solvent water (not OH^-) with the five coordinated conjugate base, a fact that has been established from oxygen labeling experiments.[157] If both k_1 and k_{-1} are large compared to k_2, as is usually but not always the case, then the rate law (45) is relevant wherein $K_1 = k_1/k_{-1}$.

$$k_{obs} = k_2K_1[OH^-]/(1 + K_1[OH^-]) = k_2K_1[OH^-] \quad (\text{if } K_1 \text{ is small}) \quad (45)$$

$$= k_{OH}\,[OH^-]$$

Since K_1 is usually small (typically 0.1 or less), the simple second order rate law tends to apply in most cases. It has been suggested that OH^- might "ion-pair" with the metal complex prior to the deprotonation step to the conjugate base.[158] Additional compelling evidence for the $\mathbf{D_{CB}}$ mechanism is provided in the few examples when deprotonation is rate determining ($k_2 > k_1,k_{-1}$) such as in the case of substitution on *cis*-$[CoCl_2(cyclam)]^+$. Whatever the steps are prior to its formation however, there is clear consensus that the conjugate base is the reactive species.[152] The magnitude of k_2 is therefore the process of particular interest, and within the origins of its high magnitude lie the reasons for the remarkably fast rates of substitution. However, evaluation of k_2 requires knowledge of K_1, and this is not straightforward since it is k_{OH} that is usually measured experimentally, e.g., from (45).

Since the basic steps in the mechanism were established, there has been much interest and effort to compare the reactivity of different Co^{III} amine complexes toward base hydrolysis in order to establish the particular stereochemical factors governing the reactivity of the conjugate base. Are some conjugate bases complexes more reactive than others? Alkyl substitution for H at the amine nitrogen does increase the rate significantly, e.g., the reaction of OH^- with $[Co(NH_2CH_3)_5Cl]^{2+}$ ($k_{OH}(25\ °C) = 3.2 \times 10^3\ M^{-1}\ s^{-1}$) versus $[Co(NH_3)_5Cl]^{2+}$ ($k_{OH}(25\ °C) = 0.23\ M^{-1}\ s^{-1}$).[67,159] This has been interpreted as being due to

increased σ donation from the N ligands favoring the dissociative loss of Cl^-. However, in a seminal paper by Henderson and Tobe,[160] they established that Co^{III} complexes with chelated polyamines are particularly reactive toward base hydrolysis when at least one *mer*-NH proton is present which when deprotonated would occupy an equatorial position in the trigonal bipyramidal intermediate (or TS). Nordmeyer[161] first showed that the amide group when formed was most effective when cis to the leaving group and this was also corroborated in the case of active *mer*-NH. Much of the work since has largely corroborated these conclusions with some particularly reactive examples being *mer*-$[Co(dien)(tn)Cl]^{2+}$ [162] and *mer*-$[Co(dien)(dapo)Cl]^{2+}$ **13** (46).[163,164] Since then even more reactive pentamine complexes have been found, most notably with pyridine substituents, some of which show remarkable differences in the value of k_{OH} even for very subtle changes in structure such as **14** compared to **15**. In **15** only a single *fac*-NH center is present wherein there is evidence of a competing pseudo-aminate mechanism involving deprotonation rather of the α-CH_2 group of the 2-pyridylmethylene arm confirmed by similar reactivity shown by the $N-CH_3$ derivative of **15**.[152]

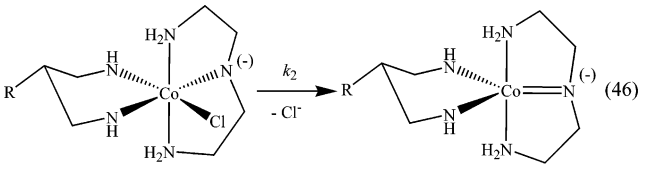

13 R = H (tn), R = OH (dapo)

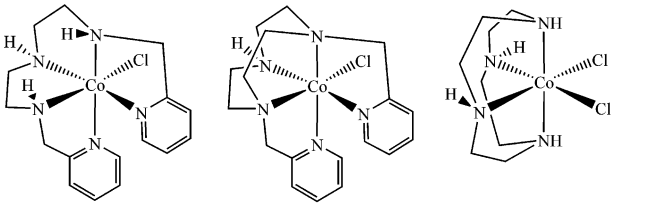

14 $k_{OH} = 2 \times 10^7\ M^{-1}\ s^{-1}$ **15** $k_{OH} = 0.04\ M^{-1}\ s^{-1}$ **16** $k_{OH} = 2.1 \times 10^7\ M^{-1}\ s^{-1}$

The high reactivity toward base hydrolysis of the syn−anti dichlorocyclen complex **16** (the fastest for any dichlorocobalt(III) complex) confirms that the *fac*-NH-*mer*-NH adjacent arrangement, present also in **14,** reflects some of the highest rates yet seen. Another striking comparison of the effect of introducing chelate rings through alkyl linkages is seen between the reactivity of **17** compared to **18**.[165]

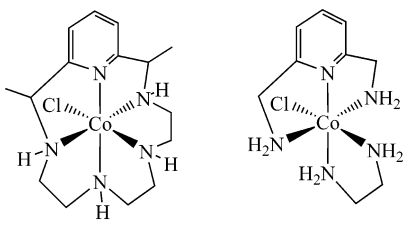

17 $k_{OH} \sim 10^7\ M^{-1}\ s^{-1}$ **18** $k_{OH} = 480\ M^{-1}\ s^{-1}$

Here formation of the favored trigonal bipyramidal intermediate akin to **13** would require the amine-py-amine moiety to be *fac*, a sterically demanding process. Nonetheless the presence of the *mer*-NH in **17** leads to remarkably fast base hydrolysis when compared to when only primary NH_2 groups are present as in **18**.

3.4.4.4.1. Question of the Five-Coordinated "Intermediate". The dissociative nature of these reactions is not in question. Values of k_{OH} for a wide range of Co^{III} amine complexes with various X leaving groups are characterized by large positive values of $\Delta V^{\ddagger}$ (typically +13 to +33 $cm^3\ mol^{-1}$) along with large values of $\Delta H^{\ddagger}$ (typically 60−130 kJ mol^{-1}) and significantly positive values of $\Delta S^{\ddagger}$ (typically +30 to +177 J $K^{-1}\ mol^{-1}$).[166] The remarkably fast rates of base hydrolysis seen in the above examples have been discussed in terms of stabilization of a particular trigonal bipyramidal intermediate with the deprotonated NH group placed in an equatorial position. This has been rationalized as being due to effective Npπ donation into the empty $d_{x^2-y^2}$ of the low spin Co^{III} center. In practice, the intermediates are of a sufficiently short lifetime so as to be unobservable. Therefore, in principle, we do not really know if this idea is correct. In some cases, varying the nature of X^{n-} and observing the distribution of products when several isomers are possible can lead to some informed extrapolations. Anion effects (seen in competition) on the distribution of products and isomers has been a popular approach in recent times used as evidence by those probing the existence of a discrete intermediate which has lost all memory of its departed ligand. A popular competitive ligand has been N_3^-.[167] A powerful probe of the existence of a common intermediate is when it can be formed from various sources and the reactions lead to a consistent distribution of products in competition. One such set of stereochemically defined complexes are the *syn*- and anti isomers of *mer*-$[Co(dien)(diamine)X]^{n+}$.[164,168,169] Using 2-aminomethylpyridine (ampy) as the diamine a total of four isomers can be defined depending upon the linkage position of ampy in relation to Cl^- and the stereochemistry, syn or anti, of the dien NH protons. Base hydrolysis of each isomer in competition with azide leads to the same distribution of hydroxo and azido products indicating that the common intermediate is **19**. The observed product dis-

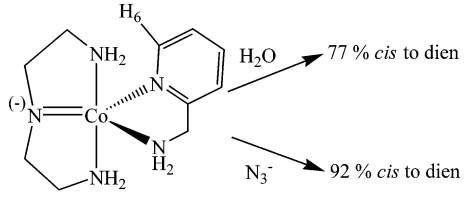

19

tribution (77%) for H_2O, (92%) for N_3^- and cis to the *mer*-NH is moreover consistent with blocking of one of the three equatorial faces of **19** by the ampy ligand while the py H-6 blocks attack at the position leading to the trans product. This contrasts with the favored equilibrium species which is trans for hydroxo (92%) and anti N−H rather than syn but cis for azido (86%) and again largely anti. Both are consistent with the intermediate **19**. These findings provide convincing

Table 14. Main Features of Base Hydrolysis at M^{III} Acido−Amine Complexes[171]

	labilizing effect of amido group		position of the labilizing amido group vs leaving group		steric course	
	weak	strong	cis	trans	stereo-change	retention
Co^{III}		X	X		X	
Cr^{III}	X		X		X	X
Rh^{III}	X			X	X	X
Ru^{III}		X		X		X

support[152] for the importance of intermediates such as **19** with a deprotonated *mer*-NH group cis to the leaving group for facile base hydrolysis although further experimental surprises coupled with the continuing inability to actually observe directly the short-lived intermediates will no doubt keep the mechanistic debate on these processes alive for some time to come.

3.4.4.4.2. Base Hydrolysis at Other Metal Centers. **Cr^{III}.** Base hydrolysis of the Cr^{III} complexes is, like those on Ru^{III} , less well developed, mainly due to the lack of an NMR handle on the reactions and also the difficulty of obtaining stereoisomers of sufficient purity. Cr^{III} complexes are generally less susceptible to base hydrolysis than their Co^{III} counterparts.[22] This has been attributed to a combination of lower acidity in the amine protons and weaker pπ-bonding from the amido species to the Cr^{III} center. Ion-pairing with OH^- has been proposed for the initial step in base hydrolysis of a number of cis/trans macrocyclic complexes $[CrL(H_2O)X]^{2+}$ (L = **3** or **12**; $X^- = NCS^-$, N_3^-, Cl^-).[170]

Ru^{III}. Sufficient kinetic studies on a wide range of Ru^{III} complexes have now been carried out for some informed conclusions to be made. Again studies on polyamine complexes are to the fore. Here whereas anation and acid catalyzed aquation are believed to possess some degree of associativeness base hydrolysis is undoubtedly dissociative as judged by the extremely positive $\Delta S^{\ddagger}$ values (>+140 J K^{-1} mol^{-1}) seen in typically reactions e.g. on *trans*-$[Ru(en)_2Cl_2]^+$ and *trans*-[Ru(cyclam **11**)$Cl_2]^+$.[171] Accelerations up to 8 orders of magnitude versus spontaneous aquation are seen in some cases, e.g., *trans*-[Ru(2,3,2-tet **9**)-$Cl_2]^+$. Interestingly substitution takes place invariably with retention of configuration and more effectively when the amine group is trans to the leaving group rather than when it is cis. Both of these observations would seem to suggest a square-pyramidal intermediate. Although paramagnetic, NMR studies on Ru^{III} are possible since the complexes are relatively inert and exchange broadening is somewhat suppressed. Further work in this area is thus encouraged and may provide further insights into the corresponding Co^{III} chemistry. A comparisons of the main features of base hydrolysis reactions at different metal centers is illustrated in Table 14.

3.4.5. Reactions Involving Chelate Ring Formation and Dissociation

The kinetics of formation of chelate and macrocyclic ligand complexes and their dissociation kinetics have been extensively studied and much is known about the mechanisms involved. In most cases the rate determining step is monodentate ligand formation (to one donor) (k_1) followed by more rapid ring closure (k_2) (47). In such cases, the observed rate is similar

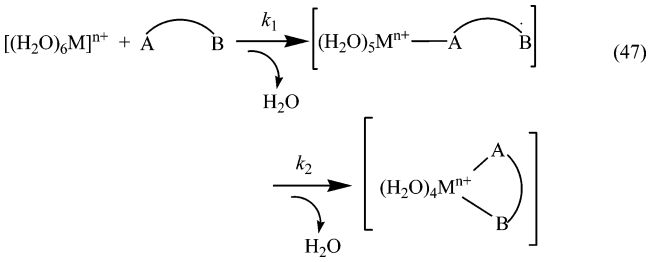

(47)

to the formation of the corresponding monodentate ligand with the same donor on the given metal. If $k_2 \gg k_1$, a single kinetic process characterizes the appearance of the chelated product. If however $k_2 > k_1$ but only by an order of magnitude or so, the kinetics monitored with excess ligand L can be biphasic with the initial fast step (depending upon which species is being monitored) actually corresponding to the ring closure step (rate independent of [L]) followed by a slower step (monodentate ligand formation − rate dependent upon [L]). However, it is not always the case that first bond formation is rate determining especially with regard to labile metal centers. It has been shown from extensive studies of complex formation with Ni^{II} and Cu^{II} with bidentate ligands such as α- and β-amino acids that a shift to rate determining ring closure is determined by the size of the chelate ring formed and by steric factors affecting the flexibility of A−B in (47). The multiplicity of steps involved with complexing multidentate ligands A−B−C−D increases the difficulty in predicting the rate determining step in that one of the steps succeeding first bond formation could become rate determining as steric and conformational constraints imparted as the ligand attaches becomes important. Indeed SCS effects are known to decrease markedly in the order $Cu^{2+} \gg Co^{2+} \gg Ni^{2+}$.

The high equilibrium constants associated with the formation of chelated complexes is usually attributed to slow dissociation rates involving the complex. This is well documented for the group 1 cations wherein the solvent effects on K for various cryptands and crown ethers are due to the dissociation rates being somewhat solvent sensitive covering 9 orders of magnitude.[172] The formation rates are much less sensitive to solvent type covering only 3 orders of magnitude. The thermodynamic chelate "effect" has long been assumed to be largely entropic in nature although recent theoretical modeling in the gas phase shows this not to be the case with both enthalpic and entropic contributions playing a role which varies from one system to another.[173]

The kinetics of complex formation and dissociation of flexible tetraaza macrocycle cyclam-type ligands

and more rigid azaporphyrin ligands have been recently reviewed by Elias[174] and Stuzhin,[175] respectively. Compared with linear tetradentate ligands cyclic tetradentate ligands are different in that the more rigid structure leads to a number of predefined conformations each with their own energy and associated solvation, the disturbance of which during complexation can define which step is rate determining. With cyclic ligands second bond formation could be cis or trans to the first (48) and, depending upon the conformational changes required, could lead to it being rate determining as has been proposed in a number of cases.[176,177]

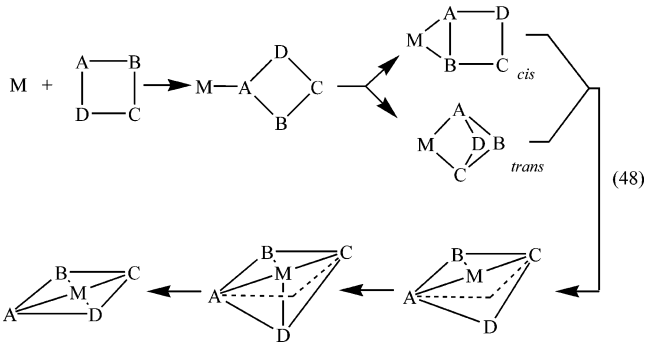

(48)

Mechanistic interpretation in neutral aqueous solution is often hampered by ligand protonation. As a result, many complex formation studies have been carried out on the free ligand in basic media or in nonaqueous solvents. Hay and Hassan[177] have reported on the kinetics of complexation of a range of tetrazamacrocycles in basic media with the hydroxycuprate species: $Cu(OH)_3^-{}_{aq}$ and $Cu(OH)_4^{2-}{}_{aq}$. After the initial encounter, rapid Cu−N bond formation occurs axially to the hydroxy ligands followed by formation of the first chelate ring and then rapid further chelation to the final complex. The rate determining step was assigned to the first chelate ring forming process (second bond formation). The faster rate of complexation in all cases is with $Cu(OH)_3^-{}_{aq}$ conceivably because an equatorial water is replaced in the slow step above rather than an equatorial OH^- ligand. The cyclam reaction has also been investigated by Moore[178] in a detailed study over an extended wavelength range. This showed that two first-order processes contributed to the slow step attributed to isomerization to the stable ligand conformation observed in the solid state structure of the final complex. Ligand conformation is an important consideration in polydentate and macrocyclic complex forming processes. In certain cases, particularly the complexation of crown ethers and cryptands with labile metal centers, rate determining ligand conformation changes can become relevant and this has led to an extension of the Eigen−Wilkins mechanism, known as the Eigen−Winkler mechanism, which correlates the rate of complex formation with that of solvent exchange at the metal ion.[179] Here fast initial bond formation is followed by a number of slow stepwise chelation steps, the rate and thus observability of which are affected by ligand flexibility/rigidity.

Most early complex formation studies on porphyrins were restricted by solubility to nonaqueous solvents such as DMSO. The various steps involve initial association of metal solvate and protonated porphyrin followed by loss of solvent and eventual formation of the so-called "sitting atop" (SAT) complex in which the metal sits above the ring bound to two nitrogens (49). This then collapses rapidly with

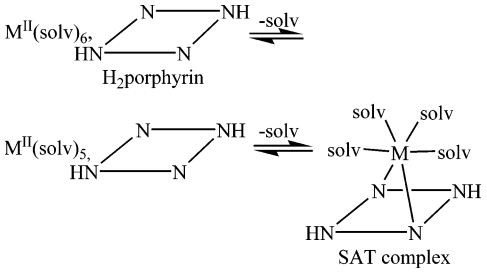

(49)

the concerted release of the two protons to give the final "in plane" complex. Since loss of solvent plays a crucial role, it is no surprise that the rates for the formation largely parallel those for solvent exchange at the metal. The development of sulfonated water-soluble porphyrin and azaporphyrin derivatives have extended complex formation studies to aqueous solution. In azaporphyrins, the change to an N atom as the link between the five-membered pyrrole rings has a significant impact on the porphyrin reaction center decreasing the effective dimension of the coordination cavity and increasing the acidity of the N−H protons.[175] The overall reactivity toward metal salts is affected strongly by solvation. Reactivity is increased in coordinating solvents such as pyridine when the azaporphyrins have a more delocalized structure. This effect is however nullified in protic media when strong hydrogen bonding localizes the structure.

The ligand terpy **5** has been extensively used as a building block in supramolecular coordination structures for number of years now, and as a result, there has been a resurgence of interest in understanding better the steps and intermediates involved in metal complex forming reactions. Extensive studies with terpy and a range of C-substituted terpy ligands have been recently reported by Moore et al.[121] The kinetics are complex and involve terpy behaving as both a bidentate (bipy-like) and *mer* tridentate ligand. The complex formation with Co^{II}, Ni^{II}, and Zn^{II} (studied in excess) involves two stages attributed to formation of a bidentate bipy-like mono(terpy) complex followed by a final chelate ring closure step to the *mer* tridentate derivative (50). In some cases, e.g. with

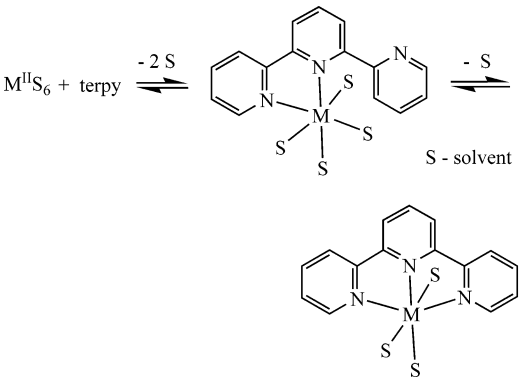

(50)

Zn^{II}, the bidentate mono(terpy) complex has measurable stability. With Cu^{II} only a single rapid stage is seen to give a highly labile aqua complex possibly involving rapid fluxionality between bidentate and *mer* tridentate terpy coordination modes.[121] Protonation of the departing ligand donors particularly when N or O can promote chelate ring dissociation as well as inducing conformational changes to the remaining ligand chelate system promoting complete dissociation. A recent example of this is provided by an extensive study of the formation and dissociation kinetics of a number of octahedral Fe^{III} siderophore model complexes consisting of tren-derived tripodal hexadentate $(O,O)_3$ or $(O,N)_3$ chelates.[180] This study revealed four distinct stages to the $[H^+]$ promoted dissociation of the hexadentate chelate ligand. Dissociation of the first chelated arm is fast followed by two further monitorable stages (slower) involving changes in conformational induced by protonation. The final stage involves dissociation of the remaining four donors. Protonation at a departing N atom aided by Cl^- coordination first to the labile axial site and then to an equatorial site is believed to be relevant to the mechanism of dissociation of L in the square-pyramidal aqua complex $[Cu^{II}L(H_2O)]^{2+}$ (L = *N*,*N*′-bis(2-pyridylmethylene)-1,3-diamino-2,2-dicarboxyethyl)propane) in aqueous HCl media.[123]

3.4.6. Coordination Number 7

Putative seven coordinated aqua ions include $[Sc(H_2O)_7]^{3+}$, $[Eu(H_2O)_7]^{2+}$, and *trans*-$[UO_2(H_2O)_5]^{2+}$ although none have yet been characterized by crystallography. A number of hepta coordinated μ-hydroxo-bridged dimers have been structurally characterized however in the case of *trans*-UO_2^{2+} [182] and Sc^{3+}.[183] The inertness of the *trans*-U=O groups of *trans*-$[UO_2(H_2O)_5]^{2+}$ ($k_{H_2O}(25\ °C) = 9.9 \times 10^{-9}\ s^{-1}$) contrasts with the lability of the five equatorial waters ($k_{H_2O}(25\ °C) = 7.6 \times 10^5\ s^{-1}$) and cannot influence their exchange[181] cf. VO^{2+} (below). Rapid interconversion between $[Sc(H_2O)_7]^{3+}$ and other coordination forms is probably relevant to the extremely rapid substitution reactions ($k_f \sim 10^7\ M^{-1}\ s^{-1}$) on this ion requiring relaxation techniques such as ultrasound.[184] Increasing ligand bulk in the coordination sphere however quickly results in the formation of six-coordinated species such as $[ScCl(H_2O)_5]^{2+}$ (in 4.0 M HCl), $[ScCl_2(H_2O)_4]^+$ (7.0 M HCl), and $[ScCl_4(H_2O)_2]^-$ (11.5 M HCl).[185] The ready accessibility of the higher coordination number species is reflected in the associative nature of many substitution/exchange reactions of archetypal six-coordinated complexes of Sc^{3+} such as TMP exchange on $[Sc(TMP)_6]^{3+}$ (TMP = trimethyl phosphate) studied by ^{45}Sc NMR ($\Delta S^‡ = -60\ J\ K^{-1}\ mol^{-1}$; $\Delta V^‡ = -20\ cm^3\ mol^{-1}$)[186] and exchange of 2,4-pentanedione (acacH) on $[Sc(acac)_3]$ ($\Delta S^‡ = -105\ J\ K^{-1}\ mol^{-1}$).[187] Similarly, an equilibrium between the two divalent species $[Eu(H_2O)_7]^{2+}$ and $[Eu(H_2O)_8]^{2+}$ seems relevant to the extremely fast rates of substitution on Eu^{2+}_{aq}. As a result of the ready accessibility of the higher coordination number species, the water exchange process on $[Eu(H_2O)_7]^{2+}$ ($r_{M2+} = 120$ pm) is the fastest so far measured by NMR on a homoleptic paramagnetic metal ion ($k_{H_2O}(25\ °C) = 5 \times 10^9\ s^{-1}$) and is strongly associatively activated close to the **A** limit ($\Delta V^‡ = -11.3\ cm^3\ mol^{-1}$.[44]

3.4.7. Coordination Numbers 8 and 9.

3.4.7.1. Lanthanide Ln^{3+} Ions. A recent thematic issue of *Chemical Reviews* was devoted to lanthanide chemistry[188] with one chapter devoted to complex formation and ring inversion in macrocyclic complexes.[189] The 15 trivalent lanthanides or f block ions La^{3+}, Ce^{3+}, Pr^{3+}, Nd^{3+}, Pm^{3+}, Sm^{3+}, Eu^{3+}, Gd^{3+}, Tb^{3+}, Dy^{3+}, Ho^{3+}, Er^{3+}, Tm^{3+}, Yb^{3+}, and Lu^{3+} are the most extended range of similar species and are often collectively denoted Ln^{3+}. The sequential electronic filling of the 4f orbitals and increase in nuclear charge results in the lanthanide contraction and a smooth decrease in r_M from 121.6 to 103.2 pm for nine-coordinate La^{3+} to Lu^{3+} and from 116.0 to 97.7 pm for eight-coordinate La^{3+} to Lu^{3+}.[43] Ligand field effects are small because of the diffuseness of the 4f electron cloud and the shielding by the 5s and 5p electrons. Generally, Ln^{3+} behave as large low surface charge density metal ions that exhibit significant variations in their coordination numbers with change of ligand type and in the solid state with co-crystallizing anion. For $[Ln(H_2O)_n]^{3+}$ in aqueous solution $n = 9$ for La^{3+} to Nd^{3+}, $n = 8$ for Gd^{3+} to Lu^{3+} and an equilibrium exists between $[Ln(H_2O)_8]^{3+}$ and $[Ln(H_2O)_9]^{3+}$ for Pm^{3+} to Eu^{3+}.[2b,29,63,73,190,191] Lower coordination numbers are however relevant when considering other ligands, for example, the larger ligands DMF and tetramethylurea lead to eight-coordinated $[Ln(DMF)_8]^{3+}$ and six-coordinated $[Ln(TMU)_6]^{3+}$ complexes, respectively.[192,193] $[Ln(DMF)_8]^{3+}$ is the dominant species when $Ln^{3+} = Ce^{3+}$ to Nd^{3+} and is the only species present when $Ln^{3+} = Tb^{3+}$ to Lu^{3+}.[192] A change from nine to eight coordination is frequently relevant for water ligand substitution on the early Ln^{3+} ions (see below).

The $[Ln(H_2O)_n]^{3+}$ ions are highly labile, with first order rate constants of typically $10^8\ s^{-1}$, with the earliest indication of trends along the series coming from ultrasound studies of sulfate complexation.[194] Complexation reactions have been analyzed by an Eigen-Wilkins approach (51) with estimation of the outer sphere ion-pair association constant K_{os}, coming from the electrostatic models of Bjerrum[195] or Fuoss[58] allowing values of k_I to be compared with the water exchange rate constant. In a few cases, values of K_{os}

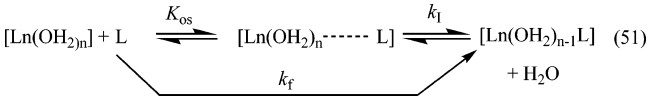

(51)

have been measured experimentally.[196] The studies showed that substitution occurred most rapidly for Sm^{3+}, Eu^{3+}, and Gd^{3+} and decreases systematically as the atomic number decreases or increases to either side,[194] Figure 18. The k_I values for sulfate substitution are similar to k_{H_2O} determined more recently by ^{17}O NMR showing again a decrease either side of the region around Gd^{3+}. After Gd^{3+}, the water exchange rate on the eight coordinated ion decreases with the lanthanide contraction and both $\Delta S^‡$ and $\Delta V^‡$ are negative, Table 15 with the latter being much less

Table 15. Rate Constants and Activation Parameters for the Water Exchange Process on the Eight-Coordinated $[Ln(H_2O)_8]^{3+}$ Ions, Ln = Pr − Yb[197−200]

Ln^{3+}	$10^{-7}\ k_{H_2O}$[b]	$\Delta H^{\ddagger}$, kJ mol^{-1}	$\Delta S^{\ddagger}$, J K^{-1} mol^{-1}	$\Delta V^{\ddagger}$,[a] cm^3 mol^{-1}	$10^2\ \Delta\beta^{\ddagger}$,[a] cm^3 mol^{-1} MPa^{1-}
Gd	83.0 ± 1.0	12.0 ± 1.3	−30.9 ± 4.1	−3.3 ± 0.2	not quoted
Tb	55.8 ± 1.3	12.1 ± 0.5	−36.9 ± 1.6	−5.7 ± 0.5	+0.3 ± 1.6
Dy	43.4 ± 1.0	16.6 ± 0.5	−24.0 ± 1.5	−6.0 ± 0.4	−0.4 ± 1.4
Ho	21.4 ± 0.4	16.4 ± 0.4	−30.5 ± 1.3	−6.6 ± 0.4	−0.6 ± 1.3
Er	13.3 ± 0.2	18.4 ± 0.3	−27.8 ± 1.1	−6.9 ± 0.4	+0.3 ± 1.2
Tm	9.1 ± 0.2	22.7 ± 0.6	−16.4 ± 1.9	−6.0 ± 0.8	+1.2 ± 3.0
Yb	4.7 ± 0.2	23.3 ± 0.9	−21.0 ± 3.3		

[a] Values of $\Delta V^{\ddagger}$ and $\Delta\beta^{\ddagger}$ were determined at the following temperatures, Gd (298.2K), Tb (269.1K), Dy (268.5K), Ho (268.8K), Er (268.8K), and Tm (269.1K). [b] Rate constants are reported at 298 K.

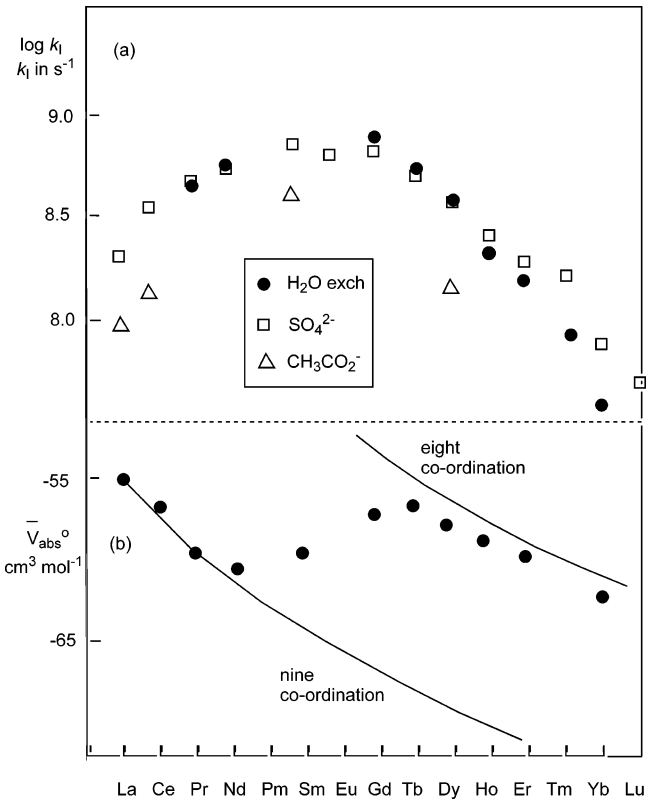

Figure 18. (a) Interchange rate constants for complex formation on Ln^{3+}_{aq} ions[194] and comparison with k_{H_2}.[197,198] (b) Absolute partial molar volumes for Ln^{3+}_{aq} in aqueous $LnCl_3$ compared with calculated values of V^0_{abs} respectively for $[Ln(H_2O)_8]^{3+}$ (upper line) and $[Ln(H_2O)_9]^{3+}$ (lower line).[63,73]

negative than either the $\Delta V^{\ddagger} = -12.9$ cm^3 mol^{-1} calculated for an **A** mechanism for water exchange or the volume change of −10.9 cm^3 mol^{-1} determined for $[Ce(H_2O)_8]^{3+}$ adding a water to form $[Ce(H_2O)_9]^{3+}$ (52).[197,198]

$$[Ce(OH_2)_8]^{3+} + H_2O \overset{\Delta V^{o} = -10.9\ cm^3\ mol^{-1}}{\rightleftharpoons} [Ce(OH_2)_9]^{3+} \quad (52)$$

Thus, an $\mathbf{I_A}$ mechanism is assigned to water exchange on these $[Ln(H_2O)_8]^{3+}$and the decrease in k_{H_2O} and the increase in $\Delta H^{\ddagger}$ with decrease in r_M is attributable to exchange increasing steric crowding in the transition state. As the lighter Ln^{3+} exist as either $[Ln(H_2O)_9]^{3+}$ or an equilibrium mixture of $[Ln(H_2O)_8]^{3+}$ and $[Ln(H_2O)_9]^{3+}$ in water it is proposed that the $\mathbf{I_A}$ water exchange on the heavier $[Ln(H_2O)_8]^{3+}$ occurs through a tricapped trigonal prismatic $[Ln(H_2O)_9]^{3+}$ transition state and that the ground state is an equilibrium mixture of dodecahedral, square prismatic, and cubic $[Ln(H_2O)_8]^{3+}$ as shown in Figure 19. Attempts to directly determine k_{H_2O} (298.2 K) for $[Pr(H_2O)_9]^{3+}$ and $[Nd(H_2O)_9]^{3+}$ using ultrahigh field NMR techniques at 14.1 T only produced lower limit estimates of 5×10^8 and 4×10^8 s^{-1}, respectively, Figure 18.[200] Overall, the directly determined k_{H_2O} data are consistent with the most labile lanthanide centers being Pm^{3+}, Sm^{3+}, Eu^{3+}, and Gd^{3+} for which the energies of $[Ln(H_2O)_8]^{3+}$ and $[Ln(H_2O)_9]^{3+}$ are most similar.

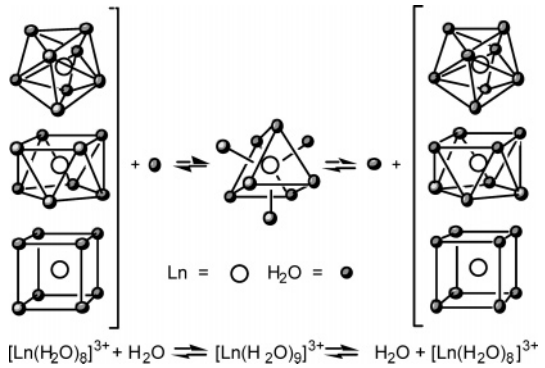

Figure 19. Mechanism for water exchange on $[Ln(H_2O)_8]^{3+}$.

Monte Carlo modeling predicts associatively and dissociatively activated water exchange respectively on $[Ln(H_2O)_8]^{3+}$ and $[Ln(H_2O)_9]^{3+}$.[201] Molecular dynamic simulations of water exchange on $[Nd(H_2O)_9]^{3+}$ and $[Yb(H_2O)_8]^{3+}$ indicate the operation of $\mathbf{I_D}$ and $\mathbf{I_A}$ mechanism, respectively, but the equilibrium between $[Sm(H_2O)_9]^{3+}$ and $[Sm(H_2O)_8]^{3+}$ is maintained by a ninth water molecule that exchanges rapidly between the first coordination sphere and the bulk in an alternation of addition and elimination reactions that does not readily fit into the associative and dissociative activation classifications.[202]

The transformation of $[Nd(DMF)_8]^{3+}$ into its equilibrium partner $[Nd(DMF)_9]^{3+}$ is characterized by $\Delta V^0 = -9.8$ cm^3 mol^{-1}, which is small by comparison with the molar volume of DMF (72 cm^3 mol^{-1}) and is attributed to lengthening of the other eight Nd^{3+}-DMF bonds when $[Nd(DMF)_9]^{3+}$ is formed.[186] Knowledge of this ΔV^0 aids in the interpretation of DMF exchange data for $[Ln(DMF)_8]^{3+}$ when $Ln^{3+} = Tb^{3+}$ to Yb^{3+} where $\Delta V^{\ddagger}$ changes systematically from +5.2 to +11.8 cm^3 mol^{-1} as atomic number increases consistent with the mechanism changing from $\mathbf{I_D}$ to

D as the lanthanide contraction occurs and crowding of the transition state increases.

^{139}La NMR has been used to study ligand complexation/interactions on La^{3+}_{aq}. Merbach and co-workers employed ^{139}La NMR to study the aquation of $[LaL(aq)]^+$ (L = 2,6-dicarboxy-4-hydroxy-pyridine).[203] Kinetic data obtained were k_{aq} (25 °C) = (207 ± 51) s^{-1}, $\Delta H^{\ddagger}$ = 38.3 ± 3.1 kJ mol^{-1}, and $\Delta S^{\ddagger}$ = −72 ± 8 J K^{-1} mol^{-1}. An associative mechanism was inferred. However, this is not always found. A ^{139}La NMR study of La^{3+} complexation with acethydroxamate shows that the reaction appears to proceed dissociatively with significantly positive values of $\Delta S^{\ddagger}$; +108 J K^{-1} mol^{-1} for complexation with the neutral acid form and +68 J $K^{-1}mol^{-1}$ for the hydroxamate anion.[204] Reaction with the anion occurs $10^4\times$ faster ($k = 1.6 \times 10^{10}$ M^{-1} s^{-1}). This dissociative behavior is also seen in the reaction with Fe^{3+}_{aq}. Measurement of the activation volume would be useful here. The vast majority of complex formation and kinetic data has however been accumulated with regard to Ln^{III} polyaminocarboxylate complexes because of the effectiveness of a number of complexes, particularly when Ln = Gd, as contrast agents in magnetic resonance imaging (MRI).[205−207] The kinetics of formation of La^{3+} with *trans*-1,2-diaminocyclohexane-*N*,*N*,*N*′,*N*′-tetraacetic acid have been studied[208] as have complexes of cyclen with two and three CH_2CO_2H pendent arms.[209] The rate-determining step appears to involve rearrangement of an intermediate species following carboxylate deprotonation. Complex formation rate constants increase from Ce^{3+} along to Yb^{3+}. A study of complex formation with tetra-substituted cyclen derivatives on Gd^{3+} has revealed slower rates of complex formation with the acid forms of **21** and **22** compared with the tetracarboxylic acid ligand DOTA **20**.[210] Again deprotonation followed by a rearrangement involving an intermediate species is kinetically relevant.

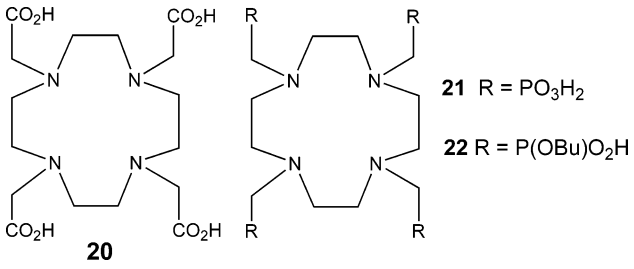

20

Dissociation of the ligands **20**−**22** from the Gd^{3+} center has also been studied. Protonated species are again important.[210] The lower charge on **22** is one factor making the Gd^{3+} complex a viable contrast agent for MRI. Incorporation of a cyclohexyl group into the backbone of **20** slows the rate of ligand dissociation by a factor of 2.[211] This is explained by the extra rigidity imposed by the cyclohexyl group preventing the N-inversion processes that facilitate polyaminocarboxylate ligand dissociation.

Because of the relevance to MRI much emphasis has surrounded ^{1}H NMR relaxation and exchange and substitution kinetics of the coordinated water ligands.[189] In active complexes, the coordinated waters interact (exchange) with the varying water levels in tissue to give the effect. Substitution by polyaminocarboxylate ligands frequently change the coordination number at the Ln^{3+} center and affect the lability of coordinated water and the mechanism of exchange. A good example is that of nine coordinated $[Gd(DOTA^{4-})H_2O]^-$ for which k_{H_2O} (298.2 K) = 4.1 × 10^6 s^{-1}, $\Delta H^{\ddagger}$ = 49.8 kJ mol^{-1}, $\Delta S^{\ddagger}$ = +48.5 J K^{-1} mol^{-1}, and $\Delta V^{\ddagger}$ = +10.5 cm^3 mol^{-1} and the water exchange mechanism is now believed to be **D**.[189,212] This compares with the 200× faster $\mathbf{I_A}$ process relevant on eight coordinated $[Gd(H_2O)_8]^{3+}$. Increasing steric compression by replacing one ethylene bridge of $DOTA^{4-}$ by a propylene bridge ($TRITA^{4-}$) has been shown to further accelerate the water exchange rate by 2 orders of magnitude, Table 16.[213] Similar effects have been observed with Gd^{3+} complexes of diethylenetriamine-*N*,*N*′,*N*″-pentaacetic acid (H_5DTPA).[214]

Table 16. Water Exchange Parameters Obtained for $[GdL(H_2O)]^-$ Complexes from ^{17}O NMR

ligand L	TRITA 15	TRITA-bz-NO_2 16	DOTA 12
10^{-6} k_{H_2O} (298.2 K)/s^{-1}	270 ± 40	120 ± 20	4.1
$\Delta H^{\ddagger}$/kJ mol^{-1}	17.5 ± 1.8	35.5 ± 1.9	49.8
$\Delta S^{\ddagger}$/ J K^{-1} mol^{-1}	−24 ± 9	+21 ± 5	+48.5

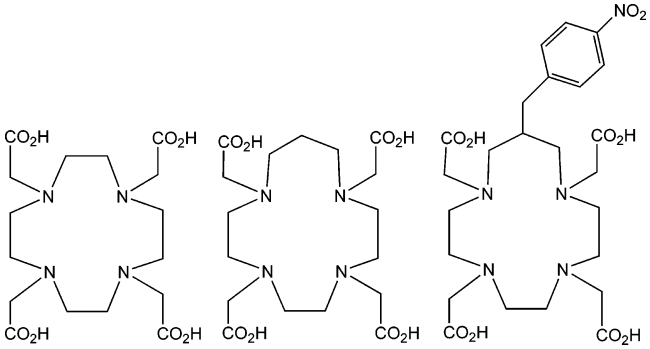

The rate increase can be seen to be primarily enthalpic, a reduction in $\Delta H^{\ddagger}$ through increased incoming ligand participation as exemplified by the increasingly more negative $\Delta S^{\ddagger}$ value. Barriers to stereochemical change are seen to have considerable influence on the kinetics of formation and dissociation. Possible transition states for isomer interconversions in tetraazacarboxylate complexes of La^{3+} and of Y^{3+} have been explored by a combination of computational methods, NMR, and X-ray diffraction. The latter two techniques have revealed two accessible geometrical isomers in solution and in the solid state.[189] A further recent development has been the discovery that the presence of different anions in the aqueous medium affects significantly the dissociative water exchange rate on various $[Gd^{III}L(H_2O)]^{n-}$ (L as in Table 16).[189,] In solid-state structures, different anions affect the Ln-OH_2 bond length as a result of promotion or otherwise of H-bond donation of the coordinated water with the secondary solvation shell. It is believed that this effect is retained in solution through different anion effects on the hydrogen-bonded structure of the secondary solvation shell. A number of Ln^{3+} tetraamide derivatives of DOTA have also been studied in regard to their water

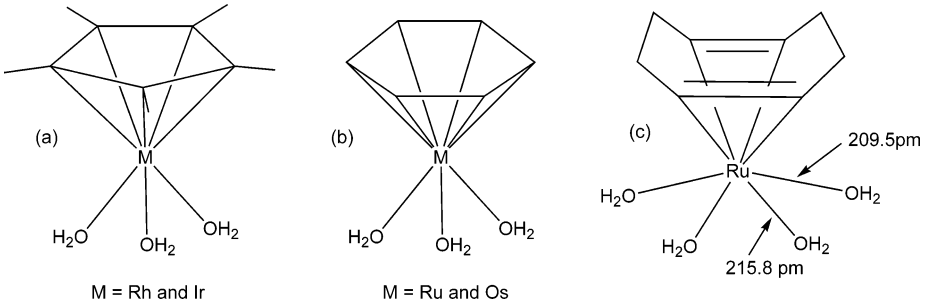

Figure 20. (a) Structures of the hybrid organoaqua complexes (a) $[\pi\text{-Cp*M}(H_2O)_3]^{2+}$ (M = Rh and Ir), (b) $[\pi\text{-}C_6H_6M(H_2O)_3]^{2+}$ (M = Ru and Os), and (c) $[(\pi\text{-COD})Ru(H_2O)_3]^{2+}$ (π-COD = π-1,5-cyclooctadiene).

Table 17. Kinetic Parameters for Water Exchange on the π-Arene Ions $[\eta^6\text{-}C_6H_6M(H_2O)_3]^{2+}$ (M = Ru or Os)[226]

	k_{H_2O}(25 °C)/s^{-1}	$\Delta H^{\ddagger}$/kJ mol^{-1}	$\Delta S^{\ddagger}$/J K^{-1} mol^{-1}	$\Delta V^{\ddagger}$/cm^3 mol^{-1}
M = Ru	11.5 ± 3.1	75.9 ± 3.8	+29.9 ± 10.6	+1.5 ± 0.4
M = Os	11.8 ± 2.0	65.5 ± 2.2	−4.8 ± 6.1	+2.9 ± 0.6
$[Ru(H_2O)_6]^{2+}$	0.018	88 ± 4	+16 ± 15	−0.4 ± 0.7

exchange behavior.[215] In one series of such compounds, the water exchange rate maximized at Eu^{2+} but fell sharply on either side with ionic radius, the fall being unusual sharp. [216] These effects on the water exchange rate have direct implications for the effectiveness of these Ln^{3+} complexes as MRI contrast agents.

3.4.8. Substitution at Water on Species $[M(R)(H_2O)_n]^{m+}$ (n = 1–5)

Certain nonexchanging resident ligands R can exert a significant kinetic effect on the lability of replaceable ligands e.g water cis or trans to them in octahedral and other complexes. Coe and Glenwright recently provided an extensive review of trans effects in octahedral transition metal complexes.[217] Two classes of ligand types were identified: σ donors and σ-donor−π-acceptors similar to those identified for square-planar four coordinated systems. Sometimes a retardation effect is seen, and in others, a labilization occurs. Examples of both situations are highlighted in the selection of examples to follow. In particular the various different effects have been demonstrated clearly in an extensive study of octahedral Ru^{2+} species.

3.4.8.1. R = HS^- or H_2S. In the Cr^{III} aqua ion $[Cr(SH)(H_2O)_5]^{2+}$,[218,219] a labilizing effect from the SH^- ligand has been detected with regard to the rates of substitution at the five remaining water ligands akin to the behavior of OH^- in $[Cr(OH)(H_2O)_5]^{2+}$. The rate constant (25 °C) for 1:1 NCS^- complexation is 8.6×10^{-4} M^{-1} s^{-1} which may be compared with 4.9×10^{-5} M^{-1} s^{-1} for reaction on $CrOH^{2+}_{aq}$. The protonated form $[Cr(H_2S)(H_2O)_5]^{3+}$ is relevant as a transient.[219,220] A ratio $>10^3$ is relevant between corresponding reactions on $[Cr(H_2S)(H_2O)_5]^{3+}$ and $[Cr(H_2O)_6]^{3+}$. A similar labilizing effect on the remaining waters is apparent in a range of compounds of the general formula $[Cr(SR)(H_2O)_5]^{2+}$ (R = alkyl or aryl).[221]

3.4.8.2. R = σ-Bonded Alkyl. A number of interesting organometallic−aqua hybrid compounds have been characterized and studied. These compounds are of interest concerning the feasibility of carrying out organometallic transformations in aqueous media. The water ligands of σ-bonded alkylpentaaqua Cr^{III} species show significant labilization.[222] The lability versus $[Cr(H_2O)_6]^{3+}$ is illustrated by the following half-lives respectively (25 °C) for 1:1 complexation with NCS^-, 42s (R = CH_2Cl), 128s (R = $CHCl_2$), and 9.3×10^6s (R = H_2O).[223] The labilization is a kinetic effect since the equilibrium constants for formation of all three species are essentially identical. With alkyl groups carrying β-OH or halogen groups treatment with H_3O^+ leads to β elimination giving $[Cr(H_2O)_6]^{3+}$ and the corresponding alkene.[222]

3.4.8.3. R = π-Arene and π-Alkene. The presence of the η^5-Cp* ($=\eta^5$-C_5Me_5) group in the half sandwich "piano-stool" complex $[\eta^5\text{-Cp*M}(H_2O)_3]^{2+}$ (M = Rh and Ir), Figure 20a, significantly labilizes the waters with respect to their hexaaqua trivalent counterparts by an astonishing factor of 10^{14}! The effect is believed to be due to a significant weakening in the M−O(H_2O) bonds promoting a dissociative process ($\Delta V^{\ddagger}$ +0.6 (Rh) and +2.4 (Ir) cm^3 mol^{-1}; $\Delta S^{\ddagger}$ +75.3 J K^{-1} mol^{-1} (Rh) and +23.6 (Ir) J K^{-1} mol^{-1} respectively).[224] The strongly dissociative nature of substitution reactions here is corroborated by invariant formation rate constants for 1:1 anation by Cl^-, Br^-, I^-, SCN^-, pyridine, 4-cyanopyridine, nicotinamide, thiourea, and dimethyl sulfide that are close to the values for water exchange on both complexes leading to the suggestion that despite the small $\Delta V^{\ddagger}$ values an extreme **D** process might not be excludable.[225] The considerable rate acceleration vs the respective hexaaqua ions correlates with a 70−80 kJ mol^{-1} lowering in $\Delta H^{\ddagger}$. The π-arene complexes $[\eta^6\text{-}C_6H_6M(H_2O)_3]^{2+}$, Figure 20b, have been characterized for M = Ru and Os[226] offering a rare comparison down group 8. As with η^5-Cp* of group 9, the presence of the π-C_6H_6 ligand significantly labilizes the water ligands (factor of 10^3) versus those on $[Ru(H_2O)_6]^{2+}$. Virtually identical kinetic parameters are obtained for the Ru^{2+} and Os^{2+} species, Table 17, showing that the effects of the π-arene ligand outweigh the differences here between the two group 8 metals. An $\mathbf{I_D}$ mechanism has been proposed in each case without excluding extreme **D** as for the Cp* complexes of group 9. For M = Ru, the $10^3\times$ labilizing effect from the η^6-C_6H_6 moiety is not manifest in a significant lengthening of the Ru−O bonds cf. vs $[Ru(H_2O)_6]^{2+}$.

Table 18. Kinetic Parameters for 1:1 Water Ligand Substitution on the Hybrid Carbonyl-aqua Ion *Fac*-$[Re(H_2O)_3(CO)_3]^{+}$ [233]

incoming ligand	$10^3 k_f/M^{-1} s^{-1}$	$\Delta V^{\ddagger}/cm^3 mol^{-1}$	$10^5 k_b/s^{-1}$	$\Delta V^{\ddagger}/cm^3 mol^{-1}$
hard				
$CF_3CO_2^-$	0.81 ± 0.01	99 ± 2		
Br^-	1.6 ± 0.3	230 ± 100		
CH_3CN	0.76 ± 0.04	16 ± 2		
pyrazine	1.06 ± 0.05	+5.4 ± 1.5	0.45 ± 0.04	+7.9 ± 1.2
soft				
tetrahydrothiophen	1.28 ± 0.07	−6.6 ± 1	3.05 ± 0.09	−6.2 ± 1
dimethyl sulfide	1.52 ± 0.06	−10 ± 2	14.2 ± 0.8	−6 ± 2
thiourea	2.49 ± 0.09		1.6 ± 0.2	

This is not the case however within the complex $[(\eta^4\text{-COD})Ru(H_2O)_4]^{2+}$ (COD = 1,5-cyclooctadiene), Figure 20c. Here a significant lengthening in the Ru−O(H_2O) bonds trans to the double bonds reflects a significant labilizing at these water sites toward water exchange and ligand substitution reactions.[224,227] Thus, formation of $[(\eta^4\text{-COD})Ru(H_2O)_3(CO)]^{2+}$ involves CO substitution at one of the labile trans waters. Furthermore the cis waters appear to be orientated so as to facilitate some degree of π-donation from O to Ru^{2+} as opposed to the labile trans waters which are more "tetrahedral" at the O atom reflecting only σ donation to Ru^{2+}. It appears that removal of the electron density on Ru toward the π acid COD in this complex results in more π acidity at Ru^{2+} in the cis direction as opposed to the trans direction. Thus, both cis and trans compensating effects may be involved. The presence of these compensating effects within the 3-fold symmetric $[\eta^6\text{-}C_6H_6Ru(H_2O)_3]^{2+}$ may be the reason the observed labilization at the water ligands here is not reflected by changes in the bond lengths.

$[Ru(H_2O)_6]^{2+}$ is an active catalyst for a number of alkene isomerizations[228] and dimerizations,[229] the active intermediates likely to be π-alkene and π-allyl complexes.[228] In the catalytic dimerization of ethene, the selectivity toward the formation of *E*-but-2-ene suggests the involvement of *cis*-$[Ru(\eta^2\text{-}CH_2{=}CH_2)_2(H_2O)_4]^{2+}$ [230] as an intermediate. Water ligand exchange and substitution on $[Ru(\eta^2\text{-}CH_2{=}CH_2)(H_2O)_5]^{2+}$ have been studied. The cis and trans water sites are dissociatively activated ($\Delta V^{\ddagger}$ = +6.5 $cm^3 mol^{-1}$ (cis), +6.1 $cm^3 mol^{-1}$ (trans). For a range of $[RuR(H_2O)_5]^{2+}$ complexes, the cis retardation effect is in the order R = $F_2C{=}CH_2$ ~ CO > Me_2SO > N_2 > $CH_2{=}CH_2$ > MeCN > H_2O. The effect is however not manifest in relative *cis*-Ru−O(H_2O) bond lengths unlike the case of the trans effect from R; order $N_2 \ll$ MeCN < H_2O < CO < Me_2SO < $CH_2{=}CH_2$ < $F_2C{=}CH_2$, in which a direct correlation of lability with the Ru−O(H_2O) bond length is seen. The increase in trans water lability correlates with an increase in the π-accepting ability of R.

3.4.8.4. R = CO. The family of carbonylaqua ions $[Ru(CO)_n(H_2O)_{6-n}]^{2+}$ (n = 1−3) has been characterized and the water exchange dynamics studied. Here the lability of the water ligands compared to those on $[Ru(H_2O)_6]^{2+}$ depends strongly on whether they are cis or trans to the CO group.[231] The water trans to the CO in $[Ru(CO)(H_2O)_5]^{2+}$ exchange with a rate constant ($k^t_{H_2O}$(25 °C) = 3.54 ± 0.02 × 10^{-2} s^{-1}) similar in magnitude to those on $[Ru(H_2O)_6]^{2+}$ (Table 14), whereas those cis are much more inert ($k^c_{H_2O}$(25 °C) = 2.54 ± 0.05 × 10^{-6} s^{-1}). In *cis*-$[Ru(CO)_2(H_2O)_4]^{2+}$, however, the trend is reversed with the waters trans to the two cis CO ligands more inert than those cis to CO. The mechanism is believed to be dissociative in each case with the rates directly reflecting the respective Ru−O(H_2O) bond lengths in crystal structures. The behavior of $[Ru(CO)(H_2O)_5]^{2+}$ shows that CO exerts a clear cis retardation effect, whereas in *cis*-$[Ru(CO)_2(H_2O)_4]^{2+}$, the relative cis effects somewhat nullify each other. The waters of *fac*-$[Ru(CO)_3(H_2O)_3]^{2+}$ are highly acidic (K_a = 1.37 ± 0.36M) with exchange promoted through the conjugate base *fac*-$[Ru(CO)_3(H_2O)_2OH]^{+}$ (k_{OH}(25 °C) = 0.053 s^{-1}). The spontaneous exchange (k_{H_2O}) is estimated to be between 10^{-4} and 10^{-3} s^{-1} at 25 °C based on the Ru−O bond distance in the triaqua species being similar to that for the waters cis to CO in *cis*-$[Ru(CO)_2(H_2O)_4]^{2+}$. This is another example where a cis conjugate base effect must be involved.

The *fac*-tricarbonyl triaqua M^I cations $[M(H_2O)_3(CO)_3]^{+}$ are known for all three group seven members (Mn, Tc, and Re) and offer a rare comparison in properties.[232−234] In the preparation of the Re derivative, the Ag^+ catalyzed aquation of the tribromo compound makes use of the lability of the Br^- ligands induced by a trans effect from CO. Despite the lower charge, the Mn^I compound is considerably more inert (k_{H_2O}(25 °C) = 19 ± 4 s^{-1}) than $[Mn(H_2O)_6]^{2+}$ reflecting the t_{2g}^6 configuration.[232] Interestingly, the activation volume for the Mn^I exchange is −4.5 $cm^3 mol^{-1}$ indicative of the same $\mathbf{I_A}$ mechanism as for the t_{2g}^6 group 9 species: $[Rh(H_2O)_6]^{3+}$ and $[Ir(H_2O)_6]^{3+}$. Here it appears the π-withdrawing CO groups effectively expand the "size" of the 3d Mn center making it behave like a 4d or 5d metal leading to significant penetration of the entering group as with the group 9 species above. The substitution behavior of the corresponding Re^I ion is however intriguing in that though it is more inert as expected (k_{H_2O}(25 °C) = 6.3 ± 0.1 × 10^{-3} s^{-1}) than the Mn^I species the mechanism, at least for hard incoming ligands, is dissociative ($\mathbf{I_D}$) with little discrimination between water and the entering ligand. This is in contrast to the normal trend of increasing associativeness as a group is descended and highlights the often unique properties of hybrid aqua metal centers. With soft entering ligands however a changeover in mechanism occurs to associative activation, Table 18, explained by a strong soft−soft interaction.[233] Consistent with the changeover, there is a stronger discrimination, reflected by k_b, when the leaving ligand is hard but

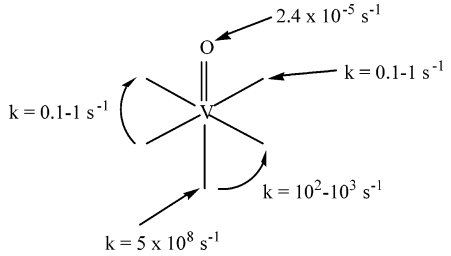

Figure 21. Oxygen exchange rate constants for different sites on $[VO(H_2O)_5]^{2+}$.[236]

very little discrimination when the departing ligand is soft. Because of their relative inertness and water solubility, the ^{188}Re and ^{99m}Tc tricarbonyl species are under investigation as possible radiotherapeutic and radioimaging agents, respectively.[234]

3.4.8.5. R = O^{2-} (Terminal oxo). The vanadyl ion VO^{2+}_{aq} is the architypal text book example of oxo group trans labilization. The influence of the V=O group in the vanadyl ion can be seen on the relative labilities of the two types of water ligands as measured by ^{17}O NMR, Figure 21.[235] The weakly bonded axial water is extremely labile ($k_{H_2O} > 5 \times 10^8$ s^{-1}) with those in the equatorial positions somewhat more inert ($k_{H_2O} = 5 \times 10^2$ s^{-1}), the exchange rate constants correlating with the respective V−O bond lengths. An intramolecular exchange process may be relevant wherein initial rapid substitution at the axial site precedes interchange with the equatorial site.[236] Rate constants ~0.1−1.0 s^{-1} obtained when direct equatorial substitution on VO^{2+} is defined in complexes implies a $>10^8\times$ difference in lability between axial and equatorial sites.[236] A similar axial−equatorial mechanism operates in equatorial ligand substitution reactions on other multiple bonded compounds such as terminal nitrido species **25** (cf. in $[TcNCl_5]^{2-}$ and $[(TcN)_2(\mu\text{-}O)_2(H_2O)_6]^{2+}$) and quadruple M−M bonded dimers **26**, e.g., in $[Mo_2(O_2CCH_3)_4]$ and $[Mo_2(H_2O)_8]^{4+}$.[237] The V=O group itself is extremely inert, a feature retained in other VO^{2+} complexes, e.g., various Schiff-base species[238] wherein rate constants for exchange with $H_2{}^{18}O$ vary from 6×10^{-7} to 6×10^{-5} s^{-1}.

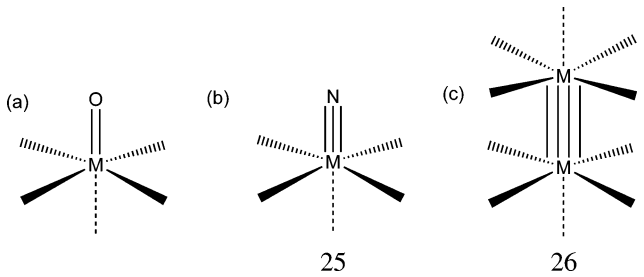

25 26

3.4.8.6. R = Planar μ_3-O^{2-} (oxo) and μ_3-N^{3-} (nitrido). Strong trans labilization at the terminal ligands L from planar μ_3-O and μ_3-N groups is well documented in the case of triangular basic carboxylates and sulfates of formula $[M_3O(\mu\text{-}O_2CCR_3)_6L_3]^{n+}$ (e.g., M = Cr and Ru, $n = 0, 1$) and $[M_3N(\mu\text{-}SO_4)_6L_3]^{n-}$ (M = Ir, $n = 4$). The labilization seems largely to promote dissociative loss of L as illustrated by a recent study of pyridine exchange on a series of alkyl and chloroalkyl oxotrichromium carboxylates which revealed distinctly positive values for $\Delta V^{\ddagger}$ of between +9.6 and +14.3 cm^3 mol^{-1}.[239] Similar findings have been reached in regard to other trimetal carboxylates on the basis of rate constants, $\Delta H^{\ddagger}$, and $\Delta S^{\ddagger}$ values. Dissociative water exchange on trivalent $[Ru_3O(\mu\text{-}O_2CCH_3)_6(H_2O)_3]^+$ occurs ca. $10^3\times$ faster than on $[Ru(H_2O)_6]^{3+}$, a feature correlating with a 9 pm longer Ru−O(H_2O) bond within the former.[240] Second-order rate constants (50 °C) for substitution at the terminal waters of $[Ir_3N(\mu\text{-}SO_4)_6(H_2O)_3]^{4-}$ by Cl^-, Br^-, and N_3^- fall in a narrow range ca. 10^{-4} M^{-1} s^{-1} indicating dissociative trans labilization from the e$^-$ rich planar μ_3-N^{3-} ligand.[241]

3.4.9. Ligand "Substitution" Not Involving Interchange

A class of substitution reactions is known which although involving apparent replacement of a ligand on the metal does not involve breakage of a bond to any of the resident ligands. One such reaction is the apparent replacement of water (or OH^-) on inert metal centers usually trivalent Co, Rh, or Ir with low spin $t_{2g}{}^6$ configurations. The reacting "ligands" each possess electrophilic carbon centers: examples being carboxylates, CO_2, SO_2, β-diketonates, oximes, nucleosides, and even CN^- bound to another metal. The reaction of $[Ir(H_2O)_6]^{3+}$ with oxalic acid is particularly noteworthy in that it provides thus far the only successfully monitored "anation" reaction on this inert center, complete within a few days at 25 °C,[144b] whereas a water exchange event on $[Ir(H_2O)_6]^{3+}$ occurs every 50 years.[41] For this reason the reaction cannot be a simple interchange but must involve either a "concerted" or direct attack by coordinated water or OH^- on the electrophilic carbon of the oxalic acid, Figure 22. Here the M−$H_2O(OH^-)$ bond is not broken but retained as an O donor of the "ligand" in the final complex, confirmed in a number of key cases by oxygen labeling studies.[242] In this regard, the incoming ligand is better termed a "substrate". As a consequence of the C−X (X = O or N) bond breaking process, it is no surprise that for a given ligand "substrate", e.g., oxalic acid in Table 19, the rate constant and activation parameters fall in a very narrow range for different group 9 complexes and are as expected far removed from those for water exchange and moreover independent of the metal Co−Rh−Ir. The highly negative $\Delta S^{\ddagger}$ values reflect the highly compacted transition state in Figure 22. Other reactions falling into this category include the CO_2 and SO_2 addition reactions to $[M(NH_3)_5(H_2O)]^{3+}$ complexes (M = Co or Rh) to give the corresponding monodentate carbonate and sulfite complexes, respectively.[243]

From group 9 trivalent Alum crystal structures it is known that the $t_{2g}{}^6$ metal centers suppress Op_π to Md_π overlap resulting in pyramidal-O water coordination to M^{3+} which in turn increases significantly its nucleophilicity. Metal bound OH^- is of course an even stronger nucleophile. Effective Lewis acid catalytic hydrolysis of amides, peptides and esters promoted by such nucleophilic OH^- ligands on a range of low spin inert d^6 Co^{III} aquahydroxo amine complexes have been widely studied and reviewed[244] because of the conveniently slow rates. Understand-

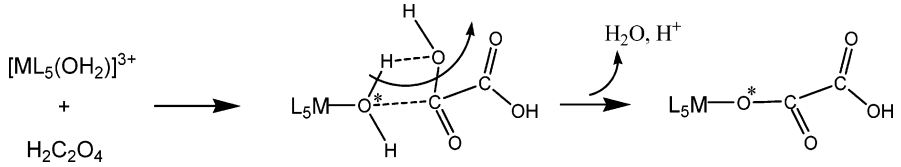

Figure 22. Complexation of oxalic acid to inert low spin d^6 aqua metal centers without involving M−O bond breakage.

Table 19. Kinetic Data for Oxalic Acid Complexation on Inert d^6 Trivalent Metal Aqua Ions and Comparison with Water Exchange.

	k_f(25 °C)/ M^{-1} s^{-1}	$\Delta H^{\ddagger}$/ kJ mol^{-1}	$\Delta S^{\ddagger}$/ J K^{-1} mol^{-1}	k_{H_2O}(25 °C)/ s^{-1}	$\Delta H^{\ddagger}$/ kJ mol^{-1}	$\Delta S^{\ddagger}$/ J K^{-1} mol^{-1}
M−H_2O attack at L						
$[Co(NH_3)_5(H_2O)]^{3+}$	20×10^{-5} [a]	57.3	-150.6	5.7×10^{-6}	111	+28
$[Rh(NH_3)_5(H_2O)]^{3+}$	13×10^{-5} [b]	35	-213	8.4×10^{-6}	103	+3
$[Co(en)_2(NH_3)(H_2O)]^{3+}$	5.4×10^{-5} [a]	95.8	-37.6			
$[Rh(H_2O)_6]^{3+}$	1.2×10^{-5}	76.7	-81.7	2.2×10^{-9}	131	+29.3
$[Ir(H_2O)_6]^{3+}$	1.3×10^{-5}	73.1	-94.1	1.1×10^{-10}	131	+2.1
M-OH attack at L						
$[Rh(H_2O)_5OH]^{2+}$	1.7×10^{-2} [a]	57.9	-85.7	4.2×10^{-5}	103	
$[Ir(H_2O)_5OH]^{2+}$	1.4×10^{-2} [a]	n.a.	n.a.	4.0×10^{-7}	n.a.	n.a.

[a] At 40 °C. [b] At 60 °C.

Table 20. Kinetic Data for Reaction of $[Rh(H_2O)_5OH]^{2+}$ with Various "Ligand" Substrates

ligand	k_f(25 °C)/ M^{-1} s^{-1}	$\Delta H^{\ddagger}$/ kJ mol^{-1}	$\Delta S^{\ddagger}$/ J K-1 mol^{-1}	ref
H_2O (true interchange)	4.2×10^{-5} [a]	103		140
adenosine		93.0	−49.0	246
pyridine-2-aldoxime		87.5	−52.3	247
DL-methionene		75.0	−81.3	248
L-cysteine		72.6	−91.0	249
Hacac	7.4×10^{-3}	64.3	−70	250
cytidine		62.7	−129.0	251
L-aspartic acid		62.0	−120.8	252
$H_2C_2O_4$	1.7×10^{-2}	57.9	−85.7	144a
salicylaldoxime		54.4	−77	253
$[Fe(CN)_6]^{3-}$		36.5	−191.0	245
picolinic acid	2.3×10^{-5}			254

[a] Units of s^{-1}.

ing these reactions has provided many indicators to the mechanisms underpinning the action of powerful biological Lewis acid metal centers such as Ni^{II}, Cu^{II}, and Zn^{II}, which also possess filled t_{2g}^6 sets.

Finally, the reported mechanism underpinning a growing series of examples of ligand "complexation" to $[Rh(H_2O)_5OH]^{2+}$ [245] needs some discussion. These reactions, listed in Table 20 along with the data for oxalate, have been assigned to an $\mathbf{I_A}$ interchange process at the Rh^{III} center largely on the basis of their activation parameters. However, it is also conceivable that they represent further examples of the above process with the "ligand" acting as a substrate upon which a Rh-bound OH^- ligand attacks at an electrophilic carbon. Each of the ligands have such a center available. The conclusions reached in many of the studies in Table 2 are moreover accompanied by little or no characterization of the final Rh^{III} product.

Although the rates are in several cases comparable to aqua ligand exchange on $[Rh(H_2O)_5OH]^{2+}$, both the rates and $\Delta H^{\ddagger}$ values are sufficiently ligand dependent to reflect the different electrophilic carbon centers involved and a rate determining step involving C−X bond breakage and not breakage of a Rh−O(H_2O) bond. Moreover, the large and negative $\Delta S^{\ddagger}$ values obtained reflect a highly compacted "concerted" transition state. The saturation kinetics often observed[254] probably reflects considerable reactant preassociation via H-bonding before concerted attack by Rh-bound OH^- at the electrophilic carbon. Oxygen labeling studies on these reactions are awaited with interest.

3.4.10. Low Symmetry Metal Centers: Polynuclear Metal Clusters

These can be divided into two categories: those that contain what are in essence metal−metal bonds and those that do not. Two further categories can be defined: (i) those which are homometal clusters wherein reaction at the terminal ligands are considered and (ii) those which are heteronuclear in which some special reactivity is imparted to the terminal ligands on the heterometal. We consider the heterometal species first.

3.4.10.1. Heteronuclear $[M'M_3X_4(H_2O)_{9+n}]^{m+}$ Clusters (n = 1 or 3, M = Mo or W, and X = S or Se). These species can be thought of as complexes of M'^{n+} with $[M_3X_4(H_2O)_9]^{4+}$ acting as a tripodal ligand via donation of three bridging X^{2-} ligands. The range of species is shown in Figure 23 with the heterometal

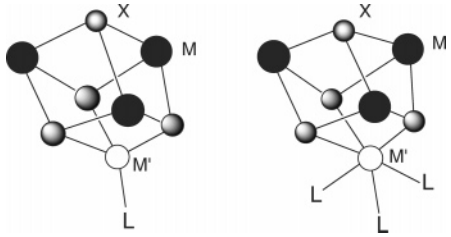

Figure 23. Heteronuclear $[M'M_3X_4(H_2O)_{9+n}]^{m+}$ clusters with pseudo-tetrahedral and octahedral geometry involving replaceable L ligands around M′.

M′ relevant to ligand substitution reactions being Cr, Fe, Co, Ni, Cu, Sn, and In.[255] The all Mo and W species are also known.[256] The most extensive studies have been carried out with M = Mo and X = S. The rates of replacement at the L ligands are often quite different than on simple complexes of M'^{n+}. For M′ = Cr the cluster $[CrMo_3S_4(H_2O)_{12}]^{4+}$ (L = H_2O) has been characterized containing formally Cr^{III} and 3 Mo^{III}.[257] Substitution at the three H_2O ligands on Cr^{III} occurs much faster than substitution on $[Cr(H_2O)_6]^{3+}$

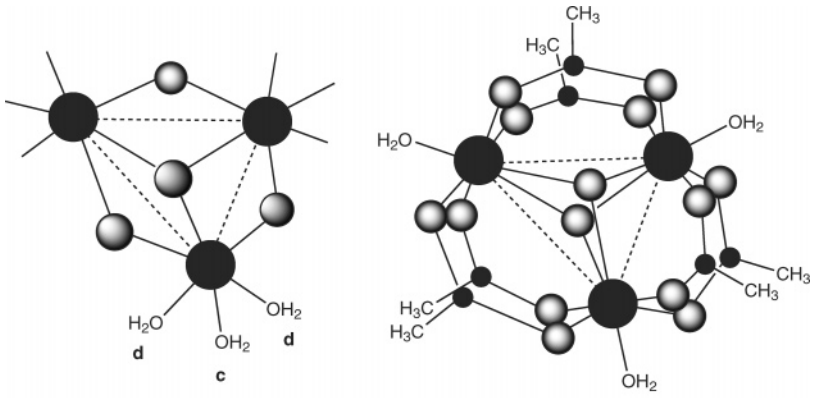

Figure 24. (a) Incomplete cuboidal homometal $[M_3(\mu_3\text{-}X)(\mu\text{-}X)_3(c\text{-}H_2O)_3(d\text{-}H_2O)_6]^{4+}$ cluster showing the two distinct terminal water sites c and d. (b) Trinuclear μ-acetate cluster $[M_3(\mu_3\text{-}O)_2(\mu\text{-}O_2CCH_3)_6(H_2O)_3]^{2+}$ showing the single water site.

and is due to labilization from the electron-rich bridging S^{2-} groups (cf. the labilization by SH^- and H_2S ligands on Cr^{3+}_{aq} discussed earlier). A conjugate-base labilizing effect from a deprotonated adjacent H_2O ligand is relevant and reminiscent of the corresponding labilization by $CrOH^{2+}_{aq}$ on substitution at $[Cr(H_2O)_6]^{3+}$. Here though it can be defined as a clear cis effect due to the imposed *fac*-ML_3 arrangement (see below). For M′ = Fe, a similar $[FeMo_3S_4(H_2O)_{10}]^{4+}$ cluster (L = H_2O) has been characterized although here the geometry at Fe is approximately tetrahedral. Mossbauer spectroscopy fits for a spin couple Fe^{III} center.[258] The second-order rate constant for Cl^- substitution at the single water site ($\geq 2 \times 10^4$ M^{-1} s^{-1}) is $\sim 10^4$ faster than for reactions at $[Fe(H_2O)_6]^{3+}$ and comparable to reactions on $FeOH^{2+}_{aq}$. This is a rare example of a substitution rate measured at a tetrahedral Fe^{III} center. For M′ = Ni, the cluster $[NiMo_3S_4(H_2O)_{10}]^{4+}$ (L = H_2O) has been characterized with again a tetrahedral Ni^{II} site. Substitution of the water is unusually slow for a tetrahedral Ni^{II} center with k_f (25 °C) values respectively 9.4 (Cl^-), 45 (NCS^-), 14.6 (Br^-), 32.3 (I^-), 119 (1,3,5-triaza-7-phosphaadamantane; PTA), and 58 M^{-1} s^{-1} (tris(3-sulfonatophenyl)phosphine; $TPPTS^{3-}$).[258] The narrow range of values suggests a dissociative (**I_D**) mechanism akin to reactions on $[Ni(H_2O)_6]^{2+}$ although rates here are significantly slower by a factor of 10^3−10^4. Although few tetrahedral Ni^{II} complexes have received detailed study, typical complexes are more labile that those of octahedral Ni^{II}. Somewhat even slower substitution by CO is relevant ($k_f = 0.66$ M^{-1} s^{-1}) and questions the presence of Ni^{II} in the cluster. The rate constant for CO exchange on $[Ni(CO)_4]$ in toluene (0.02 M^{-1} s^{-1}) and the measured ν_{CO} for $[Ni(CO)Mo_3S_4(H_2O)_9]^{4+}$ (2060 cm^{-1}) being somewhat less than that for free CO (2143 cm^{-1}) both point to a lower oxidation state approaching Ni^0.[259] The concensus is for a Ni^0 center somewhat labilized by the three electron-rich S^{2-} ligands as with Cr^{III} above. For M′ = Pd, the cluster $[PdMo_3S_4(H_2O)_{10}]^{4+}$ (L = H_2O) is characterized with a tetrahedral Pd center. Here again it is likely that the Pd is in a lower oxidation state than 2+. Rate constants have been reported for the replacement of the water at the Pd center by CO and compared to the rates above for Ni.[260] The reaction with CO here is only 9× and 20× slower respectively than for reaction with the two water soluble phosphines PTA and $TPPTS^{3-}$. Similar conclusions to those for M′ = Ni have been reached. For M′ = Cu, two air-sensitive clusters $[CuMo_3S_4(H_2O)_{10}]^{4+/5+}$ (L = H_2O) have been characterized each with a tetrahedral Cu site. The 5+ cluster is the most stable.[261] Rapid 1:1 complexation with Cl^- ($t_{1/2}$ < 3ms) is observed at Cu (K = 3500 M^{-1}) in the 5+ cluster although substitution is still some 10^6× slower than on $[Cu(H_2O)_{5(6)}]^{2+}$. It is believed that the 4+ cluster contains formally Cu^+ and the 5+ cluster Cu^{2+}. Reduction of Cu^{2+} to Cu^+ is believed to be the reason behind the ready displacement of the heterometal by Cu in the case of the 4+ Fe and Ni clusters.

In each of these clusters, considerable electron delocalization is relevant around the puckered Mo_3S_3 ring so assignment of rigid formal oxidation state (e.g., Ni^{II} or Ni^0) to the heterometal might not be strictly relevant in many cases. The result is the creation of a highly distinctive metal center with its own unique ordering of rate constants for different ligands.

3.4.10.2. Homotrinuclear $[M_3(\mu_3\text{-}X)(\mu\text{-}X)_3(H_2O)_9]^{4+}$ Clusters (M = Mo, W, or Nb and X = O, S, Cl, or Se). For M = Mo, a range of triangular incomplete cuboidal M−M clusters with X = O, S, or Se has been prepared and some reactivity trends have emerged. Because of the two kinds of bridging X ligand now present, two distinct substitution sites c and d are defined, Figure 24a, with distinctly differing reactivity. When the apical μ_3-X ligand is S or Se with μ-X = O, substitution rates at the more labile d site are slower by a factor of 6 (X = S) and by 10 (X = Se) versus when μ_3-X is O.[262] However, a significant rate acceleration is seen when the bridging μ-O ligands are replaced by X = S (factor of ~600); X = Se (factor of ~2500). Table 21 shows values for NCS^- substitution. The labilization from the heavier bridging μ-chalcogenides is believed to stem from their e^- rich nature coupled with strong e^- delocalization within the puckered $Mo_3(\mu\text{-}X)_3$ ring.[263] As mentioned earlier (section 3.2) these clusters express a strong cis conjugate base labilization at the d-H_2O site from a deprotonated adjacent water, a rare demonstrated example. Interestingly no such labilization is apparent at the c-H_2O site and as a result the two sites differ in lability by a factor of $\sim 10^5$.[147,264] Rate constants (k_f, M^{-1} s^{-1}) for Cl^- and

Table 21. Comparisons of Rate Constants (25 °C) for Equilibration of NCS^- with the d-H_2O Sites on $[M_3(\mu_3\text{-}X)(\mu\text{-}X)_3(H_2O)_9]^{4+}$ (X = S or Se) in 2.00 M $HClO_4$[261]

	X = S			X = Se		
cluster core	$k_f/M^{-1}\,s^{-1}$	k_f/s^{-1}	K/M^{-1}	$k_f/M^{-1}\,s^{-1}$	k_f/s^{-1}	K/M^{-1}
$Mo_3(\mu_3\text{-}O)(\mu\text{-}O)_3^{4+}$	2.13	2.2×10^{-3}	970	2.13	2.2×10^{-3}	970
$Mo_3(\mu_3\text{-}X)(\mu\text{-}O)_3^{4+}$	0.37	1.6×10^{-4}	2310	0.19	1.25×10^{-4}	1520
$Mo_3(\mu_3\text{-}X)(\mu\text{-}X)_3^{4+}$	212.0	9.2×10^{-2}	2300	480.0	2.0×10^{-1}	2400

NCS^- complexation and water exchange along with activation parameters ($\Delta H^{\ddagger} = +83 \pm 4$ kJ mol^{-1}, $\Delta S^{\ddagger} = +107 \pm 15$ J K^{-1} mol^{-1}) for the latter on the all μ-S system[147] indicate a dissociative activation mechanism at the more labile d sites as expected for reaction on the conjugate base, $[Mo_3(\mu_3\text{-}S)(\mu\text{-}S)_3(H_2O)_8OH]^{3+}$. Reactions on the corresponding homotungsten clusters show similar reactivity trends to the molybdenum species above but with slower rates (factor of 10).[265] With characterization of $[Nb_3(\mu_3\text{-}S)(\mu\text{-}O)_3(NCS)_9]^{6-}$ [266] and $[Nb_3(\mu_3\text{-}Cl)(\mu\text{-}O)_3(H_2O)_9]^{4+}$,[267−269] examples of such trimetal clusters extend into group 5. $[Nb_3(\mu_3\text{-}Cl)(\mu\text{-}O)_3(H_2O)_9]^{4+}$ is moreover interesting in that no conjugate base labilizing effect is apparent for exchange at the d-H_2O's[267] although they remain much more labile (factor of 10^4) than the c-H_2O's. Activation parameters for d-H_2O exchange ($\Delta H^{\ddagger} = +37 \pm 2$ kJ mol^{-1}, $\Delta S^{\ddagger} = -72 \pm 7$ J K^{-1} mol^{-1}) indicate associative activation. One can therefore speculate as to whether the same trend in increasing dissociativeness along the period from left to right, here Nb → Mo continuing along to Ru (see below), is being seen in polynuclear μ-X bridged aqua clusters as is apparent from left to right along the first row homoleptic transition metal hexaaqua ions.[28,29,52a] Here the behavior of the early ions $[Ti(H_2O)_6]^{3+}$ and $[V(H_2O)_6]^{3+}$ (strongly associative, no conjugate base activation to water exchange) can be compared with later elements, e.g., $[Fe(H_2O)_6]^{3+}$ (less associative and a dominant conjugate base assisted dissociative pathway). The lability of the d-H_2O's on the $[M_3(\mu_3\text{-}X)(\mu\text{-}X)_3(H_2O)_9]^{4+}$ (M = Mo or W)[147,262,264] (k_{H_2O}(25 °C) ~ 10^2 s^{-1}) contrasts with the extreme inertness of the single water ligands on the trinuclear μ-acetate clusters; $[M_3(\mu_3\text{-}O)_2(\mu\text{-}O_2CCH_3)_6(H_2O)_3]^{2+}$, Figure 24b, $k_{H_2O}(25\ °C) = 10^{-6}$ s^{-1} (M = Mo) and (M = W).[149] The rate constants for NCS^- substitution and water exchange along with activation parameters for the latter (M = Mo) ($\Delta H^{\ddagger} = 140 \pm 0.9$ kJ mol^{-1}, $\Delta S^{\ddagger} = +130 \pm 2.7$ J K^{-1} mol^{-1}) support an extreme dissociative process. The extreme steric crowding at the metal center (coordination number = 9 if M−M bonds are included, Figure 24b) would be expected to disfavor associative approach of the exchanging/replacing ligand.

The special reactivity at the terminal sites of the above clusters imparted by the presence of the other resident ligands, M−M bonding and, more crucially, by the low symmetry coordination geometry, can be seen in the context of more simple 'regular geometry' systems in a plot of log k_{H_2O} versus the $\Delta H^{\ddagger}$ value, Figure 25, for a range of measurable aqua ions and aquapentammine species around the periodic table. As expected, most of the simple mononuclear ions with regular geometries fall roughly on a straight line shown from $Cu^{2+}{}_{aq}$ through the $Ln^{3+/2+}{}_{aq}$ ions at the top down to the highly inert trivalent hexaaqua species $Rh^{3+}{}_{aq}$ and $Ir^{3+}{}_{aq}$ at the bottom showing that as expected the rate of water exchange is largely governed by the energetics of M−H_2O bond breaking. The rates cover 20 orders of magnitude reflecting an increase in $\Delta H^{\ddagger}$ from top to bottom of ~115 kJ mol^{-1}. The region to the right of the line could be regarded as a region of extreme dissociativeness (**D**) as governed by an unusually small rate constant for water exchange or an unusual large $\Delta H^{\ddagger}$ value indicating little or no incoming ligand assistance to the M−O(H_2O) bond breakage process. It is noticed that those hexaaqua ions having distinctly positive values of both $\Delta V^{\ddagger}$ and $\Delta S^{\ddagger}$ namely $[Fe(H_2O)_6]^{2+}$, $[Co(H_2O)_6]^{2+}$, $[Mg(H_2O)_6]^{2+}$, $[Ni(H_2O)_6]^{2+}$, $[Ga(H_2O)_6]^{3+}$, and $[Al(H_2O)_6]^{3+}$ (open squares) all lie distinctly off to the right of the defined line of correlation consistent with dissociative activation. The region to the left of the line is where the water exchange rate constant is unusually small given the value of $\Delta H^{\ddagger}$ or vice versa the value of $\Delta H^{\ddagger}$ is unusually small given the value of log k_{H_2O} implying a significant degree of incoming ligand assistance. Such values might be expected to be accompanied by a significantly negative value of $\Delta S^{\ddagger}$ and could be regarded as in a region of extreme associativeness (**A**). Here the situation for the homoleptic species is less clear even for those with distinctly negative activation volumes such as Be^{2+}, Ti^{3+}, and Eu^{2+}. The only hexaaqua ion positioned distinctly to the left of the line into this region is $[Ru(H_2O)_6]^{3+}$ (open triangle) which, although not possessing the most negative activation volume ($\Delta V^{\ddagger} = -8.3$ cm^3 mol^{-1}), does possess the most negative value of $\Delta S^{\ddagger}$ (-48 ± 14 J K^{-1} mol^{-1}) measured on a

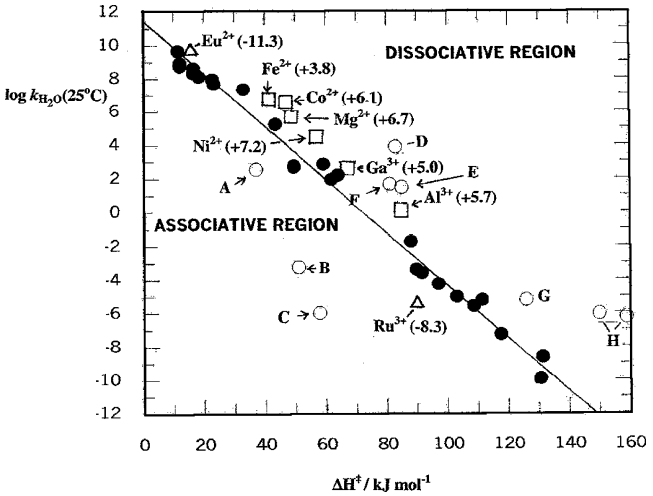

Figure 25. Plot of log k_{H_2O} (25 °C) versus the $\Delta H^{\ddagger}$ value for water exchange on measurable mononuclear aqua ion and aquapentammine species around the periodic table (filled circles). The positions of various polynuclear aqua clusters is denoted by open circles and labeled A−H (see text). (Activation volumes (cm^3 mol^{-1}) for selected homoleptic species are shown in parentheses.)

homoleptic aqua ion species. Each of the other species discussed above in terms of associative activation such as $[Be(H_2O)_4]^{2+}$, $[Ti(H_2O)_6]^{3+}$, $[Eu(H_2O)_7]^{2+}$, $[V(H_2O)_6]^{3+}$, $[Cr(H_2O)_6]^{3+}$, $[Rh(Ir)(H_2O)_6]^{3+}$, and $[Pt(Pd)(H_2O)_4]^{2+}$ interestingly lie pretty well on the line of correlation (black circles) and all have $\Delta S^{\ddagger}$ values significantly more positive than $[Ru(H_2O)_6]^{3+}$.[21] Can it be concluded therefore that $[Ru(H_2O)_6]^{3+}$ is the only homoleptic metal aqua ion with a rate of exchange reflecting significant incoming H_2O ligand assistance indicated by its relatively small $\Delta H^{\ddagger}$ value and significantly negative $\Delta S^{\ddagger}$ and $\Delta V^{\ddagger}$ values? In this regard, the absence of water exchange kinetic data for $[Mo(H_2O)_6]^{3+}$ and $[Co(H_2O)_6]^{3+}$ is a particular shame given the indications of significant associative activation as discussed in section 3.3.2.3.

What is also apparent from Figure 25 is that the points representing water exchange on the various homometal aqua clusters (open circles) mentioned in this review lie distinctly away from the correlation line either significantly to the left, e.g., $[Nb_3(\mu_3\text{-}Cl)(\mu\text{-}O)_3(H_2O)_9]^{4+}$ **A**,[267] $[W_3(\mu_3\text{-}O)(\mu\text{-}O_2CCH_3)_6(H_2O)_3]^{2+}$ **B**,[149] and $[W_3(\mu_3\text{-}O)_2(\mu\text{-}O_2CCH_3)_6(H_2O)_3]^{2+}$ **C**[149], or significantly to the right, e.g., $[Mo_3(\mu_3\text{-}S)(\mu\text{-}S)_3(H_2O)_8OH]^{3+}$ **D**,[147] $[Mo_3(\mu_3\text{-}S)(\mu\text{-}O)_3(H_2O)_8OH]^{3+}$ **E**,[262a] $[Ru_4(\mu\text{-}O)_6(H_2O)_{12}]^{4+}$ **F**,[270] $[Mo_3(\mu_3\text{-}O)_2(\mu\text{-}O_2CCH_3)_6(H_2O)_3]^{2+}$ **G**,[149] and $[Ru_2(\mu\text{-}OH)_2(H_2O)_8]^{4+}$ **H**.[75] Given the arguments presented above, it is interesting to speculate as to whether Figure 25 indicates extreme dissociative **D** mechanisms for water exchange on clusters **D** ($\Delta S^{\ddagger} = +107 \pm 15$ J K^{-1} mol^{-1}), **E** ($\Delta S^{\ddagger} = +57 \pm 14$), **F** ($\Delta S^{\ddagger} = +69 \pm 47$), **G** ($\Delta S^{\ddagger} = +77 \pm 30$), and **H** ($\Delta S^{\ddagger} = +141$ (cis to OH) and $+168$ (trans to OH)),[75] while indicating extreme associative **A** mechanisms for water exchange on clusters **A** ($\Delta S^{\ddagger} = -72 \pm 7$ J K^{-1} mol^{-1}), **B** ($\Delta S^{\ddagger} = -131 \pm 11$), and **C** ($\Delta S^{\ddagger} = -164 \pm 25$).

A number of conclusions are apparent from the above findings:

(i) A correlation in the sign and magnitude of both activation parameters $\Delta V^{\ddagger}$ and $\Delta S^{\ddagger}$ is desirable if extreme mechanisms that approach the **D** or **A** limiting situations are to be inferred.

(ii) Values of $\Delta V^{\ddagger}$ around $+9$ to $+10$ cm^3 mol^{-1} may be representative of a limiting **D** water exchange process (close packed limit) whereas values of up to -13 cm^3 mol^{-1} (close to Swaddle's upper limit) may underestimate the case of limiting **A** and most importantly;

(iii) The use of as many different mechanistic indicators as are available (including the use of increasingly powerful computational methods) should be encouraged before meaningful deductions of the mechanism of ligand replacement processes can be reached.

It is clear that further work (both experimentally and accompanied by theoretical approaches) is needed to substantiate the conclusions reached thus far regarding the intimate mechanisms of ligand substitution processes around the elements of the periodic table and indeed many of the tables of data presented here and elsewhere would benefit from the inclusion of many more case examples. Despite the clear short OLINIT-term advantages of concentrating further studies on those systems of direct relevance to industrial applications, much more research is still needed in fundamental areas if progress is to be made toward a more intimate understanding of the underpinning mechanisms surrounding a given inorganic center.

It is clear that very small, often quite subtle, distortions to local coordination geometry can exert considerable effects on the rates and mechanism of ligand replacement processes, and in this regard, I would encourage further studies to understand fully the behavour of centers having irregular (low symmetry) coordination geometries especially if we are to understand fully the rates and mechanisms of reactions relevant to biological centers since this is the common situation. Some of the studies mentioned here in regard to metal clusters, 5 coordinated species, and Ln^{3+} complexes highlight some progress in this direction.

4. References

(1) Lincoln, S. F.; Richens, D. T.; Sykes, A. G. In *Comprehensive Coordination Chemistry II*; McCleverty, J. A., Meyer, T. J., Eds.; Elsevier: Amsterdam, 2003; Vol. 1.25, p 515.
(2) (a) Burgess, J.; Hubbard, C. D. *Adv. Inorg. Chem.* **2002**, *54*, 71. (b) Lincoln, S. F.; Merbach, A. E. *Adv. Inorg. Chem.* **1995**, *42*, 1. (c) Lincoln, S. F.; Merbach, A. E. *Adv. Inorg. Bioinorg. Mech.* **1983**, *2*, 95.
(3) Basolo, F.; Pearson, R. G. *The Mechanisms of Inorganic Reactions*; Wiley: New York, 1958.
(4) Basolo, F.; Pearson, R. G. *The Mechanisms of Inorganic Reactions*; *A Study of Metal Complexes in Solution*, 2nd ed.; Wiley: New York, 1967.
(5) Langford, C. H.; Gray, H. B. *Ligand Substitution Processes*; Benjamin: New York, 1965.
(6) (a) Eigen, M. *Z. Electrochem.* **1960**, *64,* 115; *Pure. Appl. Chem.* **1963**, *6*, 97. (b) Eigen, M.; Wilkins, R. G. *Adv. Chem. Ser.* **1965**, *49*, 55.
(7) Pearson, R. G. *Inorg. Chem.* **1988**, *27*, 734.
(8) Pearson, R. G. *J. Chem. Educ.* **1968**, *45*, 64.
(9) Tobe, M. L. *Inorganic Reaction Mechanisms*; Nelson: London, 1972.
(10) Sykes, A. G. *Kinetics of Inorganic Reactions*, Pergamon: Oxford, 1966.
(11) Margerum, D. W.; Cayley, G. R.; Weatherburn, D. C.; Pagenkopf, G. K. Kinetics and Mechanism of Complex Formation and Ligand Exchange. In *Coordination Chemistry*; Martell, A. E., Ed.; ACS Monograph 174; American Chemical Society: Washington, DC, 1978; Vol 2.
(12) Benson, D. *Mechanisms of Inorganic Reactions in Solution*; McGraw-Hill: London, 1968.
(13) Tobe, M. L., Ed.; *Reaction Mechanisms in Inorganic Chemistry. MTP Int. Rev. Sci., Inorg. Chem.*; Butterworth: London 1971; Ser. 1, Vol. 9; 1973, Ser. 2.
(14) Sykes, A. G., Ed.; *Advances in Inorganic and Bioinorganic Mechanisms*; Academic: London, 1982; Vol. 1; 1983, Vol. 2; 1985, Vol. 3; 1986, Vol. 4.
(15) Twigg, M. V., Ed.; *Mechanisms of Inorganic and Organometallic Reactions*; Plenum: New York, 1983, Vol. 1; onwards to 1994.
(16) Katakis, D.; Gordon, G. *Mechanisms of Inorganic Reactions*; Wiley: New York, 1987.
(17) Wilkins, R. G. *The Study of the Kinetics and Mechanism of Reactions of Transition Metal Complexes*, 2nd ed.; VCH: New York, 1991; 1st ed., Allyn and Bacon: New York, 1974.
(18) Jordan, R. B. *Reaction Mechanisms of Inorganic and Organometallic Systems*; OUP: Oxford, 1991.
(19) Atwood, J. D. *Inorganic and Organometallic Reaction Mechanisms*; VCH: New York, 1997; 1st ed., Brooks/Cole: Monterey, CA, 1985.
(20) Henderson, R. A. *The Mechanisms of Reactions at Transition Metal Sites*; OUP: Oxford, 1993.
(21) Richens, D. T. *The Chemistry of Aqua Ions*, Wiley: Chichester, 1997.
(22) Hay, R. W. *Reaction Mechanisms of Metal Complexes*; Horwood: Chichester, U.K., 2000.
(23) Burgess. J.; Tobe, M. L. *Inorganic Reaction Mechanisms*, Addison-Wesley-Longmans: Harlow, Essex, 1999.
(24) See, e.g.: (a) Winterton, N. *RSC London, Ann. Rep. Sect. A* **1994**, *89,* 475; **1995**, *90,* 515; **1996**, *92,* 481; **1997**, *93,* 541; **1998**, *94,* 537; **1999**, *95*, 535. Winterton, N. *RSC London, Ann. Rep. Prog. Chem. Sect. A* **2000**, *96*, 557. (b) Davies, M. B. *RSC London,*

Annu. Rep. Prog. Chem. Sect. A **2001**, *97*, 501; **2002**, *98*, 531 and previous articles in this series.
(25) van Eldik, R. *Inorganic High-Pressure Chemistry, Kinetics and Mechanism*; Elsevier: Amsterdam, 1986.
(26) (a) van Eldik, R., Klärner, F.-G., Eds.; *High-Pressure Chemistry—Synthetic, Mechanistic and Supercritical Applications*; Wiley-VCH: Weinheim, Germany, 2002. (b) van Eldik, R. In *High-Pressure Molecular Science*; Winter, R., Jonas, J., Eds.; Klüwer: Dordrecht, The Netherlands, 1999; p 267. (c) van Eldik, R., Hubbard, C. D., Eds.; *Chemistry under Extreme or non-Classical Conditions*; Wiley: New York, 1997.
(27) (a) van Eldik, R. *Coord. Chem. Rev.* **1999**, *182*, 373. (b) Stöchel, G.; van Eldik, R. *Coord. Chem. Rev.* **1999**, *187*, 329; **1997**, *159*, 153. (c) van Eldik, R. in Williams, A. F., Floriani, C., Merbach, A. E., Eds.; *Perspectives in Coordination Chemistry*; VCH: Basel, 1992; p 52.
(28) (a) Merbach, A. E.; Helm, L. *J. Chem. Soc., Dalton Trans*. **2002**, 633; *Coord. Chem. Rev.* **1999**, *187*, 151. (b) van Eldik, R.; Merbach, A. E. *Comm. Inorg. Chem.* **1992**, *12*, 341.
(29) Dunand, F. A.; Helm, L.; Merbach, A. E. *Adv. Inorg. Chem.* **2003**, *54*, 1.
(30) (a) Helm, L.; Powell, D. H.; Merbach, A. E. In *High-Pressure Techniques in Chemistry and Physics: A Practical Approach*; Holzapfel, W., Isaacs, N., Eds.; OUP: Oxford, 1997; (b) Frey, U.; Powell, D. H.; Merbach, A. E. in *Dynamics of Solution and Fluid Mixtures by NMR*; Delpuech, J.-J., Ed.; Wiley: Chichester, U.K., 1995; p 263.
(31) deVito, D.; Weber, J.; Merbach, A. E. *Inorg. Chem.* **2004**, *43*, 858.
(32) Deeth, R. J.; Elding, L. *Inorg. Chem*. **1996**, *35*, 5019
(33) Hartmann, M.; Clark, T.; van Eldik, R. *J. Am. Chem. Soc*. **1997**, *119*, 5867.
(34) See, e.g.: Orvig, C., Abrams, M. J., Eds.; *Chem. Rev.* **1999**, *99*, 2201 (bioinorganic).
(35) (a) Martell, A. E.; Mötekaitis, R. J. *Determination and Use of Stability Constants*; VCH: Weinheim, Germany, 1988. (b) Rossotti, F. J. C.; Rossotti, H. *The Determination of Stability Constants*; McGraw-Hill: New York, 1961.
(36) (a) Perrin, D. *Stability Constants of Metal Ion Complexes, Part B, Organic Ligands*; IUPAC Chemical Data Series; Pergamon: Oxford, 1982. (b) Martell, A. E.; Smith, R. M. *Critical Stability Constants, vols. 1−6*; Plenum: New York, 1974, 1975, 1976, 1977, 1982, and 1985. (c) Rossotti, H. *The Study of Ionic Equilibria*; Longman: New York, 1978. (d) Cram, D. J. *Angew. Chem., Intl. Ed. Eng.* **1986**, *25*, 1039.
(37) (a) Anderegg, G. *Pure. Appl. Chem.* **1982**, *54*, 2693. (b) Harris, W. R.; Martell, A. E. *Inorg. Chem.* **1976**, *15*, 713. (c) Harris, W. R.; Motekaitis, R. J.; Martell, A. E. *Inorg. Chem.* **1975**, *14*, 974.
(38) Irving, H., Williams, R. J. P. *J. Chem. Soc.* **1953**, 3192.
(39) Eigen, M. *Pure Appl. Chem*. **1963**, *6*, 97.
(40) Lincoln, S. F.; Merbach, A. E. *Adv. Inorg. Chem.* **1995**, *42*, 1.
(41) Cusanelli, A.; Frey, U.; Richens, D. T.; Merbach, A. E. *J. Am. Chem. Soc*. **1996**, *118*, 5265.
(42) Taube, H. *Chem. Revs.* **1952**, *50*, 69.
(43) Shannon, R. D. *Acta Crystallogr*., *Sect. A*: *Cryst*. *Phys*., *Diffr*., *Theor*. *Gen*. *Crystallogr*. **1976**, *A32*, 751.
(44) (a) Moreau, G.; Helm, L.; Purans, J.; Merbach, A. E. *J. Phys. Chem. A* **2002**, *106*, 3034. (b) Caravan, P.; Töth, E.; Rockenbauer, A.; Merbach, A. E. *J. Am. Chem. Soc*. **1999**, *121*, 10403.
(45) Bleuzen, A.; Föglia, F.; Furet, E.; Helm, L.; Merbach, A. E.; Weber, J. *J. Am. Chem. Soc*. **1996**, *118*, 12777.
(46) Kowall, T.; Föglia, F.; Helm, L.; Merbach, A. E. *Eur. Chem. J*. **1996**, *2*, 285.
(47) Hunt, J. P.; Taube, H. *J. Chem. Phys.* **1950**, *18*, 757; **1951**, *19*, 602. (b) Plane, R. A.; Taube, H. *J. Chem. Phys.* **1952**, *56*, 33. (c) Hunt, J. P.; Plane, R. A. *J. Am. Chem. Soc.* **1954**, *76*, 5960. (d) Plane, R. A.; Hunt, J. P. *J. Am. Chem. Soc.* **1957**, *79*, 3343.
(48) Gamsjager, H.; Murmann, R. K. *Adv. Inorg. Bioinorg. Mech.* **1983**, *2*, 317 and references therein.
(49) See ref 21, p 66.
(50) Stranks, D. R.; Swaddle, T. W. *J. Am. Chem. Soc.* **1971**, *93*, 2783.
(51) Xu, F.-C.; Krouse, H. R.; Swaddle, T. W. *Inorg. Chem.* **1985**, *24*, 267.
(52) (a) Merbach, A. E.; Akitt, J. W. High-Resolution Variable Pressure NMR for Chemical Kinetics. In *NMR Basic Principles and Progress*; Springler-Verlag: Berlin, 1990; Vol. 24, p 189 (and refs. therein). (b) Lincoln, S. F. *Prog. React. Kinet.* **1977**, *9*, 1.
(53) Swift, T. J.; Connick, R. E. *J. Chem. Phys.* **1962**, *37*, 307; **1964**, *41*, 2553.
(54) See ref 21, p 69.
(55) Richens, D. T.; Pittet, P.-A.; Merbach, A. E.; Humanes, M.; Lamprecht, G. J.; Ooi, B.-L.; Sykes, A. G. *J. Chem. Soc., Dalton Trans.* **1993**, 2305.
(56) Wilkins, R. G. *Trans. Met. Chem.* **1998**, *23*, 735.
(57) Wilkins, R. G. *Adv. Inorg. Bioinorg. Mech*. **1983**, *2*, 139.
(58) Fuöss, R. M. *J. Am. Chem. Soc.* **1958**, *80*, 5059.
(59) (a) Cross, R. J. *Adv. Inorg. Chem*. **1989**, *34*, 219. (b) Cross, R. J. *Chem. Soc. Rev*. **1985**, *14*, 197.
(60) See, e.g.: Garrison, J. M.; Crumbliss, A. L. *Inorg. Chem.* **1987**, *26*, 3660.
(61) Pearson, R. G. *Coord. Chem. Rev.* **1990**, *100*, 403; *J. Am. Chem. Soc.* **1963**, *85*, 3533.
(62) Swaddle, T. W. *Coord. Chem. Rev.* **1974**, *14*, 217.
(63) Swaddle, T. W. *Adv. Inorg. Bioinorg. Mech.* **1983**, *2*, 95.
(64) Swaddle, T. W. *Comm. Inorg. Chem.* **1991**, *12*, 237.
(65) Lay, P. A. *Comm. Inorg. Chem.* **1991**, *9*, 235.
(66) Swaddle, T. W. *Rev. Phys. Chem. Japan*. **1980**, *50*, 230.
(67) (a) Drljaca, A.; Hubbard, C. D.; van Eldik, R.; Asano, T.; Basilevsky, M. V.; leNoble, W. J. *Chem. Rev.* **1998**, *98,* 2167. (b) van Eldik, R.; Asano, T.; leNoble, W. J. *Chem. Rev.* **1989**, *89*, 549.
(68) Stranks, D. R. *Pure Appl. Chem.* **1974**, *38*, 303.
(69) Rötzinger, F. P. *J. Am. Chem. Soc.* **1997**, *119*, 5230.
(70) Rötzinger, F. P. *J. Am. Chem. Soc.* **1996**, *118*, 6760.
(71) Richens, D. T.; Ducommun, Y.; Merbach, A. E. *J. Am. Chem. Soc.* **1987**, *109*, 603.
(72) (a) Ducommun, Y.; Laurenczy, G.; Merbach, A. E. *Inorg. Chem.* **1989**, *27*, 1148. (b) Möhr, R.; van Eldik, R. *Inorg. Chem.* **1985**, *24*, 3396. (c) Doss, R.; van Eldik, R. *Inorg. Chem*. **1982**, *21*, 4108.
(73) (a) Swaddle, T. W. *Inorg. Chem.* **1983**, *22*, 2663. (b) Swaddle, T. W.; Mak, M. K. S. *Can. J. Chem.* **1983**, *61,* 473.
(74) (a) Swaddle, T. W. In *Mechanistic Aspects of Inorganic Reactions*; Rorabacher, D. B., Endicott, J. F., Eds.; ACS Sym. Ser.; American Chemical Society: Washington, DC, 1982; Vol. 198; p 39. (b) Swaddle, T. W. *Inorg. Chem.* **1980**, *19*, 3203.
(75) Drljaca, A.; Zahl, R.; van Eldik, R. *Inorg. Chem.* **1998**, *37*, 3948.
(76) Eve, D. A. *Inorg. Chim. Acta* **1990**, *174*, 205.
(77) Sasaki, Y.; Sykes, A. G. *J. Chem. Soc., Dalton Trans.* **1975**, 1048.
(78) See, e.g.: Grant, M. W.; Jordan, R. B. *Inorg. Chem.* **1981**, *20*, 55 for a good compilation of examples.
(79) Swaddle, T. W.; Guastalla, G. *Inorg. Chem.* **1969**, *8*, 1604.
(80) (a) Elding, L. I.; Arhland, S. *Coord. Chem. Rev.* **1996**, *153*, 1. (b) Ahrland, S.; Chatt, J.; Davies, N. R. *Q. Rev. Chem. Soc.* **1958**, *12*, 265.
(81) (a) Bechtler, A.; Breitschwerdt, K. G.; Tamm, K. *J. Chem. Phys.* **1970**, *52*, 2975. (b) Eigen, M.; Tamm, K. *Z. Elektrochem.* **1962**, *66*, 93, 107.
(82) Frahm, J.; Fuldner, H. H. *Ber. Bunsen-Ges. Phys. Chem.* **1980**, *84*, 173.
(83) Connick, R. E.; Fiat, D. N. *J. Chem. Phys.* **1963**, *39*, 1349.
(84) Pittet, P.-A.; Elbaze, G.; Helm, L.; Merbach, A. E. *Inorg. Chem.* **1990**, *29*, 1936.
(85) Swaddle, T. W. *Inorg. Chem.* **1983**, *22*, 2663.
(86) Baldwin, W. G.; Stranks, D. R. *Aust. J. Chem.* **1968**, *21*, 2161.
(87) Inamo, M.; Ishihara, K.; Funahashi, S.; Ducummon, Y.; Merbach, A. E.; Tanaka, M. *Inorg. Chem.* **1991**, *30*, 1580.
(88) Lee, M. A.; Winter, N. W. and Casey, W. H. *J. Phys. Chem.* **1994**, *98*, 8641.
(89) Bock, C. W.; Glüsker, J. P. *Inorg. Chem.* **1993**, *32*, 1242.
(90) Crea, J.; Lincoln, S. F. *J. Chem. Soc., Dalton Trans.* **1973**, 2075.
(91) Ruhlandtsenge, K.; Bartlett, R. A.; Olmstead, M. M.; Power, P. P. *Inorg. Chem.* **1993**, *32*, 1724.
(92) Farrow, M. M.; Purdie, N.; Eyring, E. M. *Inorg. Chem.* **1975**, *14*, 1584.
(93) (a) Chuit, C.; Corriu, R. J. P.; Reye, C.; Young, J. C. *Chem. Rev*. **1993**, *93*, 1371. (b) Boudin, A.; Cerveau, G.; Chuit, C.; Corriu, R. J. P.; Reye, C. *Angew. Chem., Int. Ed. Engl.* **1986**, *25*, 473.
(94) Monlien, F. J.; Helm, L.; Abou-Hamdan, A.; Merbach, A. E. *Inorg. Chem.* **2002**, *41*, 1717.
(95) Monlien, F. J.; Helm, L.; Abou-Hamdan, A.; Merbach, A. E. *Inorg. Chim. Acta* **2002**, *331*, 257.
(96) Cheeseman, T. P.; Odell, A. L.; Raethel, H. A. *J. Chem. Soc. Chem Commun.* **1968**, 1496.
(97) Helm, L.; Elding, L. I.; Merbach, A. E. *Helv. Chim. Acta* **1984**, *67*, 1453.
(98) Helm, L.; Elding, L I.; Merbach, A. E. *Inorg. Chem.* **1985**, *24*, 1719.
(99) Gröning, O.; Elding, L. I. *Inorg. Chem.* **1989**, *28*, 3366.
(100) Elding, L. I. *Inorg. Chim. Acta*. **1972**, *6*, 683.
(101) Elding, L. I. *Inorg. Chim. Acta*. **1978**, *28*, 255.
(102) Elding, L. I.; Olsson, L. F. *Inorg. Chim. Acta* **1986**, *117*, 9.
(103) Bugaræiæ, Z. Ph.D. Thesis, Kragujevac University: Kragujevac, Yugoslavia, 1989.
(104) Ducummon, Y.; Merbach, A. E.; Hellquist, B.; Elding, L. I. *Inorg. Chem.* **1987**, *26*, 1759.
(105) Elding, L. I.; Gröning, A.-B. *Inorg. Chim. Acta*. **1978**, *31*, 243.
(106) Hellquist, B.; Elding, L. I.; Ducummon, Y. *Inorg. Chem.* **1988**, *27*, 3620.
(107) Elmroth, S.; Bugarćić, Z.; Elding, L. I. *Inorg. Chem.* **1992**, *31*, 3551.
(108) Frey, U.; Helm. L.; Merbach, A. E.; Romeo, R. *J. Am. Chem. Soc*. **1989**, *111*, 8161.
(109) Alibrandi, G.; Minniti, D.; Scolaro, L. M.; Romeo, R. *Inorg. Chem*. **1989**, *28*, 1939.
(110) Romeo, R.; Grassi, A.; Scolaro, L. M. *Inorg. Chem.* **1992**, *31*, 4383.
(111) Berger, J.; Kotowski, M.; Van Eldik, R.; Frey, U.; Helm, L.; Merbach, A. E. *Inorg. Chem.* **1989**, *28*, 3759.

(112) Schmülling, M.; van Eldik, R. *Chem. Ber. Receuil.* **1997**, *130*, 1791.
(113) Hall, A. J.; Satchell, D. P. N. *J. Chem. Soc., Dalton Trans*. **1977**, 1403.
(114) Elding, L. I.; Olsson, L. F. *Inorg. Chem.* **1982**, *21*, 779.
(115) Churlaud, R.; Frey, U.; Metz, F.; Merbach, A. E. *Inorg. Chem.* **2000**, *39*, 304.
(116) Helm, L.; Lincoln, S. F.; Merbach, A. E. *Inorg. Chem.* **1986**, *25*, 2550.
(117) Powell, D. H.; Helm, L.; Merbach, A. E. *J. Chem. Phys.* **1991**, *95*, 9258.
(118) Powell, D. H.; Furrer. P.; Pittet, P.-A.; Merbach, A. E. *J. Phys. Chem.* **1995**, *99*, 16622.
(119) Pasquarello, A.; Petri, I.; Salmon, P. S.; Parisel, O.; Car, R.; Toth, E.; Powell, D. H.; Fischer, H. E.; Helm, L.; Merbach A. E. *Science* **2001**, *291*, 856.
(120) Powell, D. H.; Merbach, A. E.; Fabian, I.; Schindler, S.; van Eldik, R. *Inorg. Chem.* **1994**, *33*, 4468.
(121) Priimov, G. U.; Moore, P.; Helm, L.; Merbach, A. E. *Inorg. React. Mech*. **2001**, *3*, 1.
(122) Lee, C.-D.; Chung, C.-S. *Inorg. Chem.* **1984**, *23*, 4162.
(123) McConnell, A.; Lightfoot, P.; Richens, D. T. *Inorg. Chim. Acta* **2002**, *331*, 143.
(124) Dittler-Klingemann, A. M.; Orvig, C.; Hahn, F. E.; Thäler, F.; Hubbard, C. D.; van Eldik, R. *Inorg. Chem.* **1996**, *35*, 7798.
(125) Thäler, F.; Hubbard, C. D.; Heinemann, F. W.; van Eldik, R. Schindler, S.; Fabian, I. Dittler-Klingemann, A. M.; Hahn, F. E.; Orvig, C. *Inorg. Chem.* **1998**, *37*, 4022.
(126) Spees, S. T.; Perumareddi, J. R.; Adamson, A. W. *J. Phys. Chem.* **1968**, *72*, 1822.
(127) Companion, A. L. *J. Phys. Chem.* **1969**, *73*, 739.
(128) Meyer, F. K.; Newman, K. E.; Merbach, A. E. *J. Am. Chem. Soc*. **1979**, *101*, 5588.
(129) Rode, B. M.; Reibnegger, G. J.; Fujiwara, S. *J. Chem. Soc*., *Faraday Trans. 2* **1980**, *76*, 1268.
(130) Hartmann, M.; Clark, T.; van Eldik, R. *J. Am. Chem. Soc*. **1997**, *119*, 7843.
(131) Rötzinger, F. P. *Chimia* **1997**, *51*, 97.
(132) (a) Doine, H.; Ishihara, K.; Krouse, H. R.; Swaddle, T. W. *Inorg. Chem.* **1987**, *26*, 3240. (b) Swaddle, T. W. *J. Chem. Soc. Chem. Commun.* **1982**, 832.
(133) (a) Haim, A.; Wilmarth, W. K. *Inorg. Chem.* **1962**, *1*, 573, 583. (b) Haim, A.; Grassi, R. J.; Wilmarth, W. K. *Adv. Chem. Ser.* **1965**, *49*, 61.
(134) (a) Bradley, S. M.; Doine, H.; Krouse, H.; Sisley, M. J.; Swaddle, T. W. *Aust. J. Chem.* **1988**, *41*, 1323. (b) Abouelwafa, M. H. M.; Burnett, M. G.; McCullagh, J. F. *J. Chem. Soc., Dalton Trans.* **1987**, 2311. (c) Abouelwafa, M. H. M.; Burnett, M. G. *J. Chem. Soc. Chem. Commun.* **1983**, 833.
(135) (a) Ashley, K. R.; Leipoldt, J. G. *Inorg. Chem.* **1981**, *20*, 2326. (b) Ashley, K. R.; Berggren, M.; Cheng, M. *J. Am. Chem. Soc*. **1975**, *97*, 1422.
(136) Funahashi, S.; Inamo, M.; Ishihara, K.; Tanaka, M. *Inorg. Chem.* **1982**, *21*, 447.
(137) Schneppensieper, T.; Zahl, A.; van Eldik, R. *Angew. Chem., Int. Ed. Engl*. **2001**, *40*, 1678.
(138) Maciejowska, I.; van Eldik, R.; Stöchel, G.; Stasicka, Z. *Inorg. Chem.* **1997**, *36*, 5409.
(139) (a) Plumb, W.; Harris, G. M. *Inorg. Chem.* **1964**, *3*, 542. (b) Buchaćek, R. J.; Harris, G. M. *Inorg. Chem.* **1976**, *15*, 926. (c) Swaminathan, K.; Harris, G. M. *J. Am. Chem. Soc.* **1966**, *88*, 4411.
(140) Laurenczy, G.; Rapaport, I.; Zbinden, D.; Merbach, A. E. *Magn. Reson. Chem.* **1991**, *29*, S45.
(141) Galbraith, S. C.; Robson, C. R.; Richens, D. T. *J. Chem. Soc., Dalton Trans.* **2002**, 4335.
(142) deVito, D.; Sidorenkova, H.; Rötzinger, F. P.; Weber, J.; Merbach, A. E. *Inorg. Chem*. **2000**, *39*, 5547.
(143) Castillo-Blum, S. E.; Richens, D. T. Sykes, A. G. *Inorg. Chem.* **1989**, *28*, 954.
(144) (a) Patel, A.; Leitch, P.; Richens, D. T. *J. Chem. Soc., Dalton Trans.* **1991**, 1029. (b) McMahon, M. R.; McKenzie, A.; Richens, D. T. *J. Chem. Soc., Dalton Trans.* **1988**, 711.
(145) Hyde, K. E.; Kelm, H.; Palmer, D. A. *Inorg. Chem.* **1978**, *17*, 1647.
(146) Gamsjäger, H.; Murmann, R. K. *Inorg. Chem*. **1989**, *28*, 379.
(147) Richens, D. T.; Pittet, P.-A.; Merbach, A. E.; Humanes, M.; Lamprecht, G. J.; Ooi, B.-L.; Sykes, A. G. *J. Chem. Soc., Dalton Trans.* **1993**, 2305.
(148) Bracken, D. E.; Baldwin, H. W. *Inorg. Chem*. **1974**, *13*, 1325.
(149) Powell, G.; Richens, D. T. *Inorg. Chem.* **1993**, *32*, 4021.
(150) (a) Langford, C. H. *Inorg. Chem.* **1965**, *4*, 265. (b) Haim, A. *Inorg. Chem.* **1970**, *9*, 426.
(151) Tobe, M. L. *Adv. Inorg. Bioinorg. Mech.* **1983**, *2*, 1. McCleverty, J. A., Wilkinson, G., Gillard, R. D., Eds.; *Comprehensive Coordination, Chemistry*; Pergamon: New York, 1987; Vol. 1, p 281.
(152) Jackson, W. G. *Inorg. React. Mech.* **2002**, *4*, 1.
(153) (a) Jackson, W. G.; McGregor, B. C.; Jurisson, S. S. *Inorg. Chem.* **1987**, *26*, 1286. (b) Brasch, N. E.; Buckingham, D. A.; Clark, C. R.; Finnie, K. S. *Inorg. Chem.* **1989**, *28*, 4567.
(154) Ahmed, E.; Tobe, M. L. *Inorg. Chem.* **1976**, *15*, 2635. (b) Buckingham, D. A.; Olsen, I. I.; Sargeson, A. M. *J. Am. Chem. Soc.* **1966**, *88*, 5443. (c) Jackson, W. G.; Begbie, C. M.; Randall, M. L. *Inorg. Chim. Acta* **1983**, *70*, 7.
(155) Garrick, F. J. *Nature (London)* **1937**, *139*, 507.
(156) Basolo, F. *Coord. Chem. Rev*. **1990**, *100*, 47.
(157) Green M.; Taube, H. *Inorg. Chem.* **1963**, *2*, 948.
(158) (a) Buckingham, D. A.; Clark, C. R.; Lewis, T. W. *Inorg. Chem.* **1979**, *18*, 2041. (b) Chan, S. C. *J. Chem. Soc. A* **1966**, 1124.
(159) Benzo, F.; Gonzalez, G.; Martinez, M.; Sienra, B. *Inorg. React. Mech*. **2001**, *3*, 25.
(160) Henderson, R. A.; Tobe, M. L. *Inorg. Chem.* **1977**, *16*, 2576.
(161) Nordmeyer, F. R. *Inorg. Chem*. **1969**, *8*, 2780.
(162) Dong, L. S.; House, D. A. *Inorg. Chim. Acta* **1976**, *19*, 23.
(163) Comba, P.; Jackson, W. G.; Marty, W.; Stoeckli-Evans, H.; Zipper, L. *Helv. Chim. Acta* **1992**, *75*, 1147.
(164) Comba, P.; Jackson, W. G.; Marty, W.; Zipper, L. *Helv. Chim. Acta* **1992**, *75*, 1147, 1172.
(165) Newitt, P.; Jackson, W. G. unpublished work mentioned in ref 152.
(166) Baran Y.; Comba, P.; Lawrance, G. *Inorg. React. Mech.* **2002**, *4*, 31.
(167) Brasch, N. E.; Buckingham, D. A.; Clark, C. R.; Finnie, K. S. *Inorg. Chem.* **1989**, *8*, 4567.
(168) Jackson, W. G. In *Rearrangements in Ground and Excited States*; de Mayo, P., Ed.; Academic: New York, 1980; Vol. 2, p 273.
(169) Jackson, W. G.; Spencer, B. P.; Walsh, R. J. *Inorg. Chim. Acta*. **1989**, *284*, 37.
(170) Madej, E.; Mönsted, O.; Kita, P. *J. Chem. Soc., Dalton. Trans.* **2002**, 2361.
(171) Reference 22 p 81.
(172) Cox, B. G.; Garcia-Rosa, J.; Schneider, H. *J. Am. Chem. Soc.* **1981**, *103*, 1054.
(173) Vallet, V.; Wählgren, U.; Grenthe, I. *J. Am. Chem. Soc*. **2003**, *125*, 14941.
(174) Elias, H. *Coord. Chem. Rev.* **1999**, *187*, 37.
(175) Stuzhin, P.; Khelevina, O. G. *Coord. Chem. Rev.* **1996**, *147*, 41.
(176) Drumhiller, J. A.; Montavon, F.; Lehn, J.-M.; Taylor, R. W. *Inorg. Chem.* **1986**, *25*, 3751.
(177) Hassan, M. M.; Hay, R. W. *Inorg. React. Mech.* **2000**, *2*, 361.
(178) Josceanu, A. M.; Moore, P. *Rev. Roum. Chim.* **1999**, *44*, 31.
(179) Eigen, M.; Winkler-Oswatitsch, R. in *The Neurosciences: Second Study Program*; Schmitt, F. O., Ed.; Rockefeller University Press: New York, 1975; p 685. (b) Burgemeister, W.; Winkler-Oswatitsch, R. *Top. Curr. Chem.* **1977**, *69*, 91.
(180) Serratrice, G.; Biaso, F.; Thomas, F.; Beguin, C. *Eur. J. Inorg. Chem*. **2004**, 1552.
(181) Jung, W.-S.; Harada, M.; Tomiyasu, H.; Fukutomi, H. *Bull. Chem. Soc. Jpn.* **1988**, *61*, 3895; **1987**, *60*, 489; **1986**, *59*, 3761; **1985**, *58*, 938; **1984**, *57*, 2317.
(182) Navaza, A.; Villain, F.; Charpin, P. *Polyhedron* **1984**, *3,* 143.
(183) (a) Matsumoto, F.; Ohki, Y.; Suzuki, Y.; Ouchi, A. *Bull. Chem. Soc. Jpn.* **1989**, *62*, 2081. (b) Cl salt.
(184) Geier, G. *Ber. Bunsen.-Ges. Phys. Chem.* **1965**, *69*, 617.
(185) (a) Yarasov, V. P.; Kirakosyan, G. A.; Trots, S. V.; Buslaev, Yu. A.; Panyushin, V. T. *Koord. Khim.* **1983**, *9*, 205. (b) Kirakosyan, G. A.; Tarasov, V. P. *Koord. Khim.* **1982**, *8,* 261.
(186) Pisaniello, D. L.; Nichols, P. J.; Ducommun, Y.; Merbach, A. E. *Helv. Chim. Acta* **1982**, *65*, 1025.
(187) Hatakeyama, Y.; Kido, H.; Harada, M.; Tomiyasu, H.; Fukutomi, H. *Inorg. Chem.* **1988**, *27*, 992.
(188) Kagan, H. B., Ed.; *Chem. Rev.* **2002**, *102*, 1805, 2476.
(189) Parker, D.; Dickins, R. S.; Püschmann, H.; Crossland, C.; Howard, J. A. K. *Chem. Rev*. **2002**, *102*, 1977.
(190) Cossy, C.; Helm, L.; Powell, D. H.; Merbach, A. E. *New J. Chem.* **1995**, *19*, 27.
(191) Kowal, T.; Föglia, F.; Helm, L.; Merbach, A. E. *J. Am. Chem. Soc.* **1995**, *117*, 3790.
(192) Cossy, C.; Merbach, A. E. *Pure Appl. Chem*. **1988**, *60*, 1785.
(193) Pisaniello, D. L.; Helm, L.; Meier, P.; Merbach, A. E. *J. Am. Chem. Soc*. **1983**, *105*, 4528.
(194) Fay, D.; Litchinski, D.; Purdie, N. *J. Phys. Chem.* **1969**, *73*, 544.
(195) Bjerrum, N. *K. Dan. Vidensk. Selsk. Skr. Naturvidensk. Math. Afd.* **1926**, *7*, 9.
(196) Chen, Z.; Detellier, C. *J. Solution Chem.* **1992**, *21*, 941.
(197) Mićskei, K.; Powell, D. H.; Helm, L.; Brücher, E.; Merbach, A. E. *Magn. Reson. Chem*. **1993**, *31*, 1011.
(198) Cossy, C.; Helm, L.; Merbach, A. E. *Inorg. Chem.* **1989**, *28*, 2699.
(199) Cossy, C.; Helm, L.; Merbach, A. E. *Inorg. Chem.* **1988**, *27*, 1973.
(200) Powell, D. H.; Merbach, A. E. *Magn. Reson. Chem.* **1994**, *32*, 739.
(201) Galera, S.; Lluch, J. M.; Oliva, A.; Bertran, J.; Foglia, F.; Helm, L.; Merbach, A. E. *New J. Chem.* **1993**, *17*, 773.
(202) Kowall, T.; Foglia, F., Helm, L.; Merbach, A. E. *Chem. Eur. J.* **1996**, *2*, 285.

(203) Ducummon, Y.; Helm, L.; Laurenczy, G.; Merbach, A. E. *Magn. Reson. Chem.* **1988**, *26*, 1023.
(204) Birus, M.; van Eldik, R.; Gabricvic, M.; Zahl, A. *Eur. J. Inorg. Chem*. **2002**, 819.
(205) Graeppi, N.; Powell, D. H.; Laurenzy, G.; Zekany, L.; Merbach, A. E. *Inorg. Chim. Acta* **1995**, *235*, 311.
(206) Töth, E.; Connac, F.; Helm, L.; Adzamli, K.; Merbach, A. E. *Eur. J. Inorg. Chem.* **1998**, 2017.
(207) Töth, E.; Connac, F.; Helm, L.; Adzamli, K.; Merbach, A. E. *J. Biol. Inorg. Chem.* **1998**, *3*, 606.
(208) Szilagyi, E.; Brücher, E. *J. Chem. Soc., Dalton Trans.* **2000**, 2229.
(209) Szilagyi, E.; Töth, E.; Kovacs, Z.; Platzek, J.; Raduchel, B.; Brücher, E. *Inorg. Chim. Acta* **2000**, *298*, 226.
(210) Burai, L.; Kiraly, R.; Lazar, I.; Brücher, E. *Eur. J. Inorg. Chem*. **2001**, 813.
(211) Comblin, V.; Gilsoul, D.; Hermann, M.; Humblet, V.; Jacques, V.; Mesbahi, M.; Sauvage, C.; Desreuz, J. F. *Coord. Chem. Rev*. **1999**, *185, 186*, 451.
(212) Micskei, K.; Helm, L.; Brücher, E.; Merbach, A. E. *Inorg. Chem.* **1993**, *32*, 3844.
(213) Ruloff, R.; Töth, E.; Scopelliti, R.; Tripier, R.; Handel, H.; Merbach, A. E. *J. Chem. Soc. Chem. Commun*. **2002**, 2630.
(214) Laus, S.; Ruloff, R.; Töth, E.; Merbach, A. E. *Chem. Eur. J*. **2003**, *9*, 3555.
(215) (a) Aime, S.; Botta, M.; Fasano, M.; Terreno, E. *Acc. Chem. Res.* **1999**, *32*, 941. (b) Aime, S.; Barge, A.; Bruce, J. I.; Botta, M.; Howard, J. A. K.; Moloney, D.; Parker, D.; DeSousa, A. D.; Woods, M. *J. Am. Chem. Soc.* **1999**, *121*, 5762. (c) Dünand, F. A.; Aime, S.; Merbach. A. E. *J. Am. Chem. Soc.* **2000**, *122*, 1506. (d) Aime, S.; Barge, A.; Balsanov, A. S.; Botta, M.; Delli-Castelli, D.; Fedeli, F.; Montillano, A.; Parker, D.; Puschmann, H. *J. Chem. Soc. Chem. Commun.* **2002**, 1120.
(216) Zhang, S.; Wu, K. Sherry, A. D. *J. Am. Chem. Soc.* **2002**, *124*, 4226.
(217) Coe, B. J.; Glenwright, S. J. *Coord. Chem. Rev.* **2000**, *203*, 5.
(218) Ardon, M.; Taube, H. *J. Am. Chem. Soc.* **1967**, *89*, 3661.
(219) Ramasami, T.; Sykes, A. G. *Inorg. Chem.* **1976**, *15*, 1010.
(220) Ramasami, T.; Taylor, R. S.; Sykes, A. G. *J. Chem. Soc. Chem. Commun.* **1976**, 383; *Inorg. Chem.* **1977**, *16*, 1931.
(221) Asher, L. E.; Deutsch, E. *Inorg. Chem.* **1976**, *15*, 1531; **1973**, *12*, 1774; **1972**, *11*, 2927.
(222) Espenson, J. H. *Acc. Chem. Res.* **1992**, *25*, 222; *Prog. Inorg. Chem.* **1983**, *30*, 189; *Adv. Inorg. Bioinorg. Mech.* **1982**, *1*, 1.
(223) Bakac, A.; Espenson, J. H.; Miller, L. *Inorg. Chem.* **1982**, *21*, 1557.
(224) (a) Dadci, L.; Elias, H.; Frey, U.; Hornig, A.; Kölle, U.; Merbach, A. E.; Paulus, H.; Schneider, J. S. *Inorg. Chem.* **1995**, *34*, 306. (b) Kölle, U. *Coord. Chem. Rev*. **1994**, *135*, 623.
(225) Cayemittes, S.; Poth, T.; Ferdandez, M. J.; Lye, P. G.; Becker, M.; Elias, H.; Merbach, A. E. *Inorg. Chem.* **1999**, *38*, 4309.
(226) Stebler-Rothlisberger, M.; Hummel, W.; Pittet, P.-A.; Burgi, H.-B.; Ludi, A.; Merbach, A. E. *Inorg. Chem.* **1988**, *27*, 1358.
(227) Kölle, U.; Flunkert, G.; Gorissen, R.; Schmidt, M. U.; Englert, U. *Angew. Chem., Int. Ed. Engl.* **1992**, *31*, 440.
(228) Karlen, T.; Ludi, A. *Helv. Chim. Acta* **1992**, *75*, 1604.
(229) Novak, B. M.; Grubbs, R. H. *J. Am. Chem. Soc.* **1988**, *110*, 960, 7542.
(230) Laurenczy, G.; Merbach, A. E. *J. Chem. Soc., Chem. Commun.* **1993**, 187.
(231) Meier, U. C.; Scopelliti, R.; Solari, E.; Merbach, A. E. *Inorg. Chem.* **2000**, *39*, 3816.
(232) Prinz, U.; Kölle, U.; Ulrich, S.; Merbach, A. E.; Maas, O.; Hegetschweiler, K. *Inorg. Chem.* **2004**, *43*, 2387.
(233) Grundler, P. V.; Salignac, B.; Cayemittes, S.; Alberto, R.; Merbach, A. E. *Inorg. Chem.* **2004**, *43*, 865.
(234) Alberto, R.; Schibli, R.; Waibel, R.; Abram, U.; Schubiger, A. P. *Coord. Chem. Rev.* **1999**, *192*, 901.
(235) (a) Kuroiwa, Y.; Harada, M.; Tomiyasu, M.; Fukotomi, H. *Inorg. Chim. Acta* **1988**, *146*, 7. (b) Reuben, J.; Fiat, D. *Inorg. Chem.* **1967**, *6*, 579. (c) Wuthrich, K.; Connick, R. E. *Inorg. Chem.* **1968**, *7*, 1377.
(236) Saito, K.; Sasaki, Y. *Adv. Inorg. Bioinorg. Mech.* **1982**, *1*, 186.
(237) Reference 21, p 354.
(238) Tsuchimoto, M.; Hoshina, G.; Uemura, R.; Nakajima, K.; Kojima, M. *Bull. Chem. Soc. Jpn.* **2000**, *73,* 2317.
(239) Fujihara, T.; Yasui, M.; Ochikoshi, J.; Terasaki, Y.; Nagasawa, A. *Inorg. React. Mech.* **2000**, *2*, 119.
(240) Powell, G.; Richens, D. T.; Powell, A. K. *Inorg. Chim. Acta* **1993**, *213*, 147.
(241) Hills, E. F.; Richens, D. T.; Sykes, A. G. *Inorg. Chem.* **1986**, *25*, 3144.
(242) Miskelly, G. M.; Buckingham, D. A. *Comm. Inorg. Chem.* **1985**, *4*, 163.
(243) Chaffee, E.; Dasgupta, T. P.; Harris, G. M. *J. Am. Chem. Soc.* **1973**, *95*, 4169.
(244) See, e.g.: Hay, R. W. In *Comprehensive Coordination Chemistry*; McCleverty, J. A., Wilkinson, G., Gillard, R. D., Eds.; Pergamon: New York, 1987; Vol. 6, p 411.
(245) Brahma, G. S.; Mohanty, P. *Inorg. React. Mech.* **2001**, *3*, 233.
(246) Ghosh, A. K. *Trans. Met. Chem.* **1998**, *23*, 649.
(247) Ghosh, A. K.; Ghosh, S.; De, G. S. *Transition Met. Chem.* **1996**, *21*, 358.
(248) Ghosh, A. K.; Ghosh, S.; De, G. S. *Ind. J. Chem.* **1996**, *35A*, 342.
(249) Ghosh, A. K.; Sengupta, P. S.; De, G. S. *Ind. J. Chem.* **1997**, *36A*, 611.
(250) Ghosh, A. K.; De, G. S. *Ind. J. Chem.* **1994**, *33A*.
(251) Mukhopadhyay, S. K.; De, G. S.; Ghosh, A. K. *Ind. J. Chem.* **1999**, *38A*, 895.
(252) Mohanty, S.; Anand. S.; Mohanty, P. *Ind. J. Chem.* **2002**, *41A*, 1191.
(253) Ghosh, A. K.; De, G. S. *Ind. J. Chem.* **1994**, *33A*, 929.
(254) Mohanty, S.; Anand, S.; Mohanty, P. *J. Ind. Chem. Soc.* **2003**, *80*, 82.
(255) (a) Hernandez-Molina, R.; Sokolov, M. N.; Sykes, A. G. *Acc. Chem. Res.* **2001**, *34*, 223. (b) Hernandez-Molina, R.; Sykes, A. G. *Coord. Chem. Rev.* **1999**, *187*, 291. (c) Shibahara, T. *Coord. Chem. Rev*. **1993**, *123*, 73. (d) Shibahara, T. *Adv. Inorg. Chem.* **1991**, *37*, 143.
(256) (a) Brorson, M.; Hyldtoft, J.; Jacobsen, C. J. M.; Olesen, K. G. *Inorg. Chim. Acta* **1995**, *232*, 171. (b) Nasreldin, M.; Hënkel, G.; Kampmann, G.; Krebs, B.; Lamprecht, G. J.; Routledge, C. A.; Sykes, A. G. *J. Chem. Soc., Dalton Trans.* **1993**, 737. (c) Hong, M. C.; Li, Y.-J.; Lu, J.-X.; Nasreldin, M.; Sykes, A. G. *J. Chem. Soc., Dalton Trans.* **1993**, 2613. (d) Akashi, H.; Shibahara, T.; Narabara, T.; Tsuru, H.; Kuroya, H. *Chem. Lett.* **1989**, *129*.
(257) Routledge, C. A.; Humanes, M.; Li, Y.-J.; Sykes, A. G. *J. Chem. Soc., Dalton Trans*. **1994**, *1275*, 2023.
(258) (a) Shibahara, T.; Akashi, H.; Kuroya, H. *J. Am. Chem. Soc.* **1986**, *108*, 8, 1342. (b) Dimmock, P. W.; Dickson, D. P. E.; Sykes, A. G. *Inorg. Chem.* **1990**, *29*, 5920.
(259) Saysell, D. M.; Borman, C. D.; Kwak, C. H.; Sykes, A. G. *Inorg. Chem*. **1996**, *35*, 173.
(260) Saysell, D. M.; Lamprecht, G. J.; Darkwa, J.; Sykes, A. *Inorg. Chem*. **1996**, *35*, 5531.
(261) (a) Nasreldin, M.; Li. Y.-J.; Mabbs, F. E.; Sykes, A. G. *Inorg. Chem.* **1994**, *33*, 4283. (b) Shibahara, T.; Akashi, H.; Kuroya, H. *J. Am. Chem. Soc.* **1988**, *110*, 3314.
(262) (a) Lente, G.; Dobbing, A. M.; Richens, D. T. *Inorg. React. Mech.* **1998**, *1*, 3. (b) Lamprecht, G. J.; Martinez, M.; Nasreldin, M.; Routledge, C. A.; Sykes, A. G. *J. Chem. Soc., Dalton Trans.* **1993**, 747.
(263) (a) Wendan, C.; Qianer, Z.; Jinshun, H.; Jia-xi, L. *Polyhedron* **1989**, *8*, 2785. (b) Li, J., Liu, C.-W.; Jia-xi, L. *Polyhedron* **1994**, *13*, 1841.
(264) Richens, D. T.; Helm, L.; Pittet, P.-A.; Merbach, A. E.; Nicolo, F.; Chapuis, G. *Inorg. Chem.* **1989**, *28*, 1394.
(265) (a) Li, Y.-J.; Routledge, C. A.; Sykes, A. G. *Inorg. Chem*. **1991**, *30*, 5043. (b) Ooi, B.-L.; Petrou, A.; Sykes. A. G. *Inorg. Chem.* **1988**, *27*, 3626. (c) Nasreldin, M.; Olatunji, A.; Dimmock, P. W.; Sykes, A. G. *J. Chem. Soc., Dalton Trans.* **1990**, 1765.
(266) Cotton, F. A.; Diebold, M. P.; Llüsar, R.; Röth, W. J. *J. Chem. Soc. Chem. Commun.* **1986**, 1276.
(267) Minhas, S.; Richens, D. T. *J. Chem. Soc., Dalton Trans.* **1996**, 703.
(268) Richens, D. T.; Shannon, I. J. *J. Chem. Soc., Dalton Trans.* **1998**, 2611.
(269) Ooi, B.-L.; Shibahara, T.; Sakane, G.; Mok, K. F. *Inorg. Chim. Acta* **1997**, *266*, 103.
(270) (a) Patel, A.; Richens, D. T. *Inorg. Chem.* **1991**, *30*, 3789. (b) Osman, J. A.; Richens, D. T.; Crayston, J. A. *Inorg. Chem.* **1998**, *37*, 1665.

CR030705U